Decoding the biosynthesis and transport of α-glucans in *Mycobacterium tuberculosis*

Inaugural dissertation

for the attainment of the title of doctor in the

Faculty of Mathematics and Natural Sciences,

Heinrich Heine University Düsseldorf.

presented by

Mohammed Rizwan Babu Sait

from Chennai, India

Düsseldorf, November 2020

from the Institute of Pharmaceutical Biology and Biotechnology

at the Heinrich Heine University Düsseldorf

Published by permission of the

Faculty of Mathematics and Natural Sciences at

Heinrich Heine University Düsseldorf

Supervisor: Prof. Dr. Rainer Kalscheuer

Co-supervisor: Prof. Dr. Marc Jacobsen

Date of the oral examination: 11-11-2020

The most beautiful experience we can have is the mysterious. It is the fundamental emotion that stands at the cradle of true art and true science.

To raise new questions, new possibilities, to regard old problems from a new angle, requires creative imagination and marks real advance in science.

Albert Einstein

Acknowledgements

My first and foremost thanks to Prof. Dr. Rainer Kalscheuer for accepting me as a PhD candidate in his lab. I'm grateful to him for giving me the opportunity to work and I have cherished my time working in the lab under his leadership. I would like to thank Manchot Graduate School - Molecules of Infection III for the funding. The graduate school provided an exceptional curriculum that encourages students to succeed not only with research skills but also with strong interpersonal skills. I would like to thank every member of the MOI graduate school especially Prof. Dr. Johannes Hegemann, Prof. Dr. med. Klaus Pfeffer, Dr. Inge Krümpelbeck, Dr. Stephanie Spelberg and Dr. Sabrina Zander for their support and guidance throughout my time at HHU. I would also like to thank Prof. Dr. Marc Jacobsen, my second supervisor, who has been extremely helpful with my projects and other official formalities.

My biggest thanks goes to our laboratory technician, Heike Goldbach-Gecke, who had given enormous support throughout my time as a PhD student. Her encouragement, support and remarks gave me full confidence to work hard and be successful with my doctoral degree. I would like to thank M.Sc. Steffen Schindler, Dr. rer. nat. Lasse van Geelen, M.Sc. Anna-Lene Kiffe-Delf, M. Sc. Emmanuel Tola Adeniyi, M.Sc. Wang Lin, Apotheker Viktor Simons, Apotheker Tino Seidemann, M. Sc. Kristin Schwechel, Dr. rer. nat. Jan Korte for the wonderful time all these years.

My next set of thanks goes to my family and friends. I am grateful to my parents for their unconditional love and support. Special thanks to my closest friends, Sucharitha Parthasarathy and Jaganath Ramachandran for their immense support and they had always helped me to get through the tough times and hold my hands in the time of despair.

Thanks to the almighty.

Mohammed Rizwan Babu Sait
November 2020, Düsseldorf.

INDEX

Decoding the biosynthesis and transport of α-glucans in *Mycobacterium tuberculosis*

Summary

Tuberculosis(TB) is one of the leading causes of death in the world caused by a single infectious organism, *Mycobacterium tuberculosis* (*Mtb*), affecting millions of people every year. There have been no other reservoirs for *Mtb* except humans. Hence, this pathogen evolved adapting its' metabolism and virulence system to grow and multiply in human macrophages. The unique cell envelope of *Mtb* consist of different glycoconjugates that are either essential structural components and virulence determinants. *Mtb* also produces intracellular glycoconjugates such as trehalose and methyl glucose lipopolysaccharides (MGLP) that are crucially involved in viability and virulence of the bacillus. In this thesis, we focus on the characterization of the metabolism, biosynthesis and transport of trehalose and MGLP in *Mtb*.

In **Chapter 3**, the transport of trehalose across the outer mycolic acid-containing mycomembrane was investigated. The ABC transporter *LpqY-SugA-SugB-SugC* has previously been demonstrated to mediate the specific uptake of trehalose across the cytoplasmic membrane. However, it was unknown how transport of trehalose across the mycomembrane is mediated. In this study, the anti-mycobacterial activity of 6-Azido trehalose was harnessed to select for spontaneous resistant *Mtb* mutants in a merodiploid strain harbouring two *LpqY-SugA-SugB-SugC* copies. Mutations mediating resistance to 6-Azido trehalose mapped to the proline-proline-glutamate (PPE) family member PPE51 (Rv3136), which has recently been shown to be an integral mycomembrane protein involved in uptake of several low-molecular weight compounds including some mono- and disaccharides. A site-specific ppe51 gene deletion mutant of *Mtb* was unable to grow on trehalose as the sole carbon source. Furthermore, bioorthogonal labelling of cells of the *Mtb Δppe51* mutant incubated with 6-Azido trehalose corroborated the impaired internalization. Taken together, the results indicate that the transport of trehalose and trehalose analogues across the mycomembrane of *Mtb* is exclusively mediated by PPE51.

Mtb also produces cytoplasmic complex oligomeric glycoconjugates such as 6-O-methylglucose lipopolysaccharides (MGLP) that can form 1:1 ratio stable complex with fatty acyl chains and Acyl-CoA in vitro. Thereby, MGLP have been proposed to regulate the enzymatic activity of fatty acid synthase I. However, so far the biological function of MGLP could never been validated because of the lack of *Mtb* mutant strains that exhibit a substantial reduction in MGLP formation. MGLP comprises 10-20 glucose or 6-O-methylglucose units with additional 3-O-methylglucose units at the non-reducing end and diglucosylglycerate (DGG) as a starter unit at the reducing end. The formation of DGG from glucosylglycerate is an essential step in the synthesis of MGLP. In **Chapter 4**, we hypothesize that the enzyme catalysing DGG formation is a branching enzyme

encoded by the essential Rv3031 gene. A conditional Rv3031 mutant was generated in *Mtb* H37Rv by inserting a tetracycline-regulatable synthetic promoter cassette immediately upstream of the start codon of Rv3031 employing specialized transduction. We validated the essentiality of the gene by conditional silencing. We performed proteomic profiling of the conditional mutant under both fully induced and partially silenced conditions to observe different expression levels of proteins related to mycolic acid biosynthesis and mycomembrane proteins. Mycolic acid methyl esters were extracted to monitor the mycolic acid content at different gene expression levels of Rv3031. Taken together, the results provide the basis for understanding the role of the putative branching enzyme Rv3031 in the MGLP biosynthesis in *Mtb.*

Poor diagnostic tools to detect active disease limit tuberculosis control programs and affect patient care. Accurate detection of live *Mtb* could improve tuberculosis diagnosis and patient treatment. In **Chapter 5**, we report that mycobacteria and other corynebacteria can be specifically detected with a fluorogenic trehalose analog. We designed a 4-N, N-dimethylamino-1,8-naphthalimide–conjugated trehalose (DMN-Tre) probe that undergoes >700-fold increase in fluorescence intensity when transitioned from aqueous to hydrophobic environments. This enhancement occurs upon metabolic conversion of DMN-Tre to trehalose monomycolate and incorporation into the mycomembrane of Actinobacteria. DMN-Tre labelling enabled the rapid, no-wash visualization of mycobacterial and corynebacterial species without nonspecific labelling of Gram-positive or Gram-negative bacteria. DMN-Tre labelling was detected within minutes and was inhibited by heat killing of mycobacteria. Furthermore, DMN-Tre labelling was reduced by treatment with TB drugs, unlike the clinically used Auramine stain. Lastly, DMN-Tre labelling is an operationally simple method that may be deployable for rapid diagnosis of tuberculosis.

Introduction

Tuberculosis disease

It was in 1882 that *Mycobacterium tuberculosis* (*Mtb*) was first presented as the cause of tuberculosis (TB) disease. According to the World Health Organisation, approximately 10 million people are infected with *Mtb* every year. It is the primary cause of death from a single infectious organism and also belong to worlds' top 10 causes of death. Health related risk factors include smoking, diabetes, HIV infection and other causes include unhygienic living conditions. With early diagnosis and appropriate treatment, TB infection can be cured. In spite of the recommended four-antibiotic treatment, (Rifampicin, Ethambutol, Isoniazid, Pyrazinamide), the pathogen still infects one fourths of the worlds' population which creates an urgent need for a new set of antibiotics and other treatment measures[1]. The World Health Organisation developed a special program called END TB STRATEGY to minimize the infection rate to 100 cases per 1 million people within 15 years. The strategy includes early diagnosis and treatment, screening for patients with high risk of developing active TB disease, and also deliver preventive measures [2].

TB can exist in two forms: latent state and active state. Among people who have latent TB infection, only 5-10% develop the active TB disease [3]. Also, additional stages have been proposed between these two states, namely incipient and subclinical TB. This will allow for clear understanding of the disease and effective diagnosis and treatment. Following are the definitions of the four stages of tuberculosis disease with an additional term called eliminated TB infection. A person with eliminated TB infection has a previous record of TB infection but has cured from the infection by chemotherapy or by host immune responses. Latent TB infection is a contained infection with viable *Mtb* without developing to active disease in the near time. Incipient TB infection is the next stage where the latent infection has high probability to develop in to active disease without producing any detectable symptoms. Subclinical TB infection is the infection without TB like symptoms but produces other difficulties and symptoms that could by detected by biological assays. Active TB disease is a condition with high infection rate, and the person shows TB related clinical symptoms that could be detected through various microbiological or other diagnostic assays [4].

Tuberculosis is caused by different members of the *Mtb* complex (*MTB*C). The complex includes:

- *Mtb* causes TB in humans.
- *Mycobacterium africanum* causes TB in humans only in certain regions of Africa.

- *Mycobacterium bovis* causes TB in wild and domesticated mammals.
- *Mycobacterium caprae* causes TB in wild and domesticated mammals.
- *Mycobacterium pinnipedii* causes TB in wild and domesticated mammals.
- *Mycobacterium microti* causes TB in voles.

Tuberculosis Diagnosis

Sputum Smear Microscopy

Sputum smear microscopy is used for fast and reliable detection of *Mtb* in patients with pulmonary TB. It is estimated that there are about 5000 bacilli per millilitre of sputum. The regularly used staining procedures include Ziehl-Neelsen staining and Auramine-Rhodamine staining. The sputum smear microscopy is also used to monitor the infection rate and progress of the treatment. Two sputum specimens are usually collected to ensure accuracy and reliability in TB diagnosis. However, sputum smear microscopy cannot differentiate tuberculous mycobacteria from non-tuberculous mycobacteria and also live from dead mycobacteria.

Ziehl-Neelsen Staining

Ziehl-Neelsen staining is one of the common sputum based diagnostic methods used for *Mtb* detection [5]. It was first presented by Paul Erich as haematoxylin stain but was later modified for enhanced staining and detection by Franz Ziehl and Friedrich Neelsen. This stain is used to detect acid-fast organisms. Many bacteria possess a physical property called acid-fastness, which is to develop resistances to acid decolourization during staining methods and retain the primary stain. This resistance comes from the bacteria possessing high amount of lipid contents and long chain fatty acids. One such group of bacteria are mycobacteria which exhibit acid-fastness due to the presence of a unique cell wall containing high amounts of mycolic acids. One of the primary dyes for this staining procedure is the carbol fuchsin that stains the bacilli red. The procedure includes dropping of cells on the microscope glass slides, air-drying and heat-fixing the cells followed by the application of the primary staining reagent, carbol fuchsin. After few minutes of incubation, the slides are washed and then the decolourizer is applied. The acid-fast organisms are resistant to the decolourizer and hence retain the primary red colour whereas the non-acid fast organisms lose the red colour after the application of decolourizer. Counter stains such as methylene blue or malachite green is used and the non-acid fast organisms pick up the counter stain (Figure 1E).

Auramine Rhodamine Staining

Another commonly used sputum based diagnostic method is the Auramine Rhodamine staining procedure. This staining is also called truant staining method which is used for the detection of acid-fast bacilli. Auramine-Rhodamine is a fluorochrome dye that could bind to *Mtb* cell wall and give the yellow or orange fluorescence on a green background under fluorescent microscope. The counter stain used in this staining is potassium permanganate and results in non-fluorescence.

TB Culture test

In this diagnostic method, the bacteria are grown on different substances to identify particular microorganism. Both solid medium like agar plates and liquid medium such as culture broths can be used to grow the tested bacteria. The growth medium could also contain antibiotics to test for drug susceptibility. This is crucial to detect multi-drug resistant TB (MDR-TB) or extensively drug resistant TB (XDR-TB). MDR-TB show resistance to rifampicin and isoniazid. XDR-TB also display similar resistance but in addition are also resistant to fluoroquinolones and at least one of the injectable antibiotics. The gold standard of drug susceptibility testing is the indirect drug susceptibility test, which involves growing pure culture with drug containing substances. Culturing *Mtb* on defined medium provides high accuracy detection of TB. The major disadvantage of the TB culture test is that it is more complex, time consuming and expensive to carry than the sputum smear microscopy. This test requires specific laboratory conditions and equipment. It can take up to 4 weeks to receive a test result and it can take a few additional weeks to receive results for drug susceptibility tests for MDR-TB or XDR-TB.

TB blood tests

TB blood test, otherwise better known as IGRA (Interferon Gamma Release Assay) test, is a more specific and reliable TB diagnostic method. It is based on the measurement of immune response developed by host to TB infection. This method is used to detect latent TB infection and not for active TB disease. Upon *Mtb* infection, interferon gamma (IFN-γ) molecules are released by T lymphocytes when the cells are exposed to *Mtb* antigens. IFN-γ is the cytokine belonging to type II class of the interferons. It activates macrophages and also induces the expression of class II MHC molecules. It has immunomodulatory and immunostimulatory effects and also can inhibit the viral replication. Two different IGRAs are commonly used for TB diagnosis namely, QuantiFERON TB test, T-Spot TB test.

QuantiFERON TB GOLD test involves blood collection, and the blood samples are mixed with *Mtb* antigens, namely ESAT-6 and CFP-10, that can produce an immune response. The test consists of three tubes: Nil tube which is a negative control to quantify background IFN-γ, TB antigen tube which contains the mixture of *Mtb* antigens and a Mitogen tube to quantify any minimal immune response denoting the inability to release IFN-γ. After incubation of the blood samples with *Mtb* antigens and the control tubes for 16 to 24 hours, the amount of IFN-γ released is measured. If the patient is infected with *Mtb*, high amounts of IFN-γ is released and the patient is tested TB positive. IGRAs have several advantages over TB skin test. The whole blood is extracted for TB diagnosis which makes it convenient for processing and does not require lymphocyte isolation, washing or counting. This test is also convenient for screening large amounts of blood samples [6] (Figure 1A).

T-spot TB test is a type of ELISPOT assay developed by OXFORD IMMUNOTEC. It is based on the quantification of anti-mycobacterial effector T cells and white blood cells that can produce IFN-γ. This test has the advantage that it can be used for immunocompromised patients or people vaccinated with BCG vaccine with high sensitivity and accuracy. This is the test with high specificity and sensitivity of over 95% (Figure 1D).

TB skin test

The TB skin test detects the previously induced immune response in the host when infected with *Mtb.* The immune response could also result from the BCG vaccine against TB infection. This test is called Mantoux tuberculin test or PPD test – Purified protein derivative test. This test is based on the principal that the *Mtb* infections produce hypersensitive reaction to some antigens of the mycobacterium. These antigens are extracted and form the core component of the tuberculin or purified protein derivative test. These protein derivatives are used for skin testing for *Mtb* detection. When injected in the arm, the host immune system develops induration forming a hard area around the injected area based on which the results are analysed. This test requires two visits: the first visit for injection and the second test for reading the swelling. Reading depend upon the amount of induration. The diameter of the swelling is measured in millimetres. A positive skin test exhibits an induration greater than or equal to 15 mm in a healthy individual. For few individuals, for instance, recent immigrants from highly infected areas, children under 4 years, the test is positive if induration is greater than or equal to 10 mm. For people with supressed immune system, people infected with HIV, people who had recent contacts with TB patients, people with organ transplantation, an induration of about 5 mm and above are considered positive. Also, a negative test does not necessarily mean the person is not infected with *Mtb*. Patients with chronic

medical conditions or chemotherapy can often have false negative results. People vaccinated with BCG may also test positive due to the persistence of the vaccine for a long time. People infected with other strains of mycobacteria may also have false positive results (Figure 1B).

Xpert *MTB*/RIF Assay

The Xpert *MTB*/RIF assay is one of the recently developed and more commonly used rapid diagnostic methods for TB. It is based on DNA amplification that can detect both TB and antibiotic susceptibility. During early 2000s, a collaborative effort from the Foundation for Innovative New Diagnostics (FIND), United States National Institutes of Health, Bill and Melinda Gates Foundation and Cepheid developed a diagnostic system named GeneXpert, a cartridge based nucleic acid amplification test for rapid TB diagnosis. The GeneXpert system was introduced in 2004 and it includes one-time use disposable cartridges with lyophilized reagent, buffers and washes. Additional components include the instrument, barcode scanner and a computer with preloaded software. Xpert *MTB*/RIF assay was developed for this testing platform in 2009 and was a breakthrough in TB diagnosis [7]. Major advantages of this assay include great performance with higher sensitivity and less time consumption. It also provides information about mixed infection and increased accuracy for rifampicin sensitivity. The assay detects genomic DNA sequences of *Mtb*. The Xpert *MTB*/RIF collects DNA samples from TB patients and amplifies DNA by polymerase chain reaction. The system also detects for rifampicin resistance causing mutations in the *rpoB* (RNA polymerase beta) gene in the genomic DNA of *Mtb* by using molecular beacons [5] (Figure 1C).

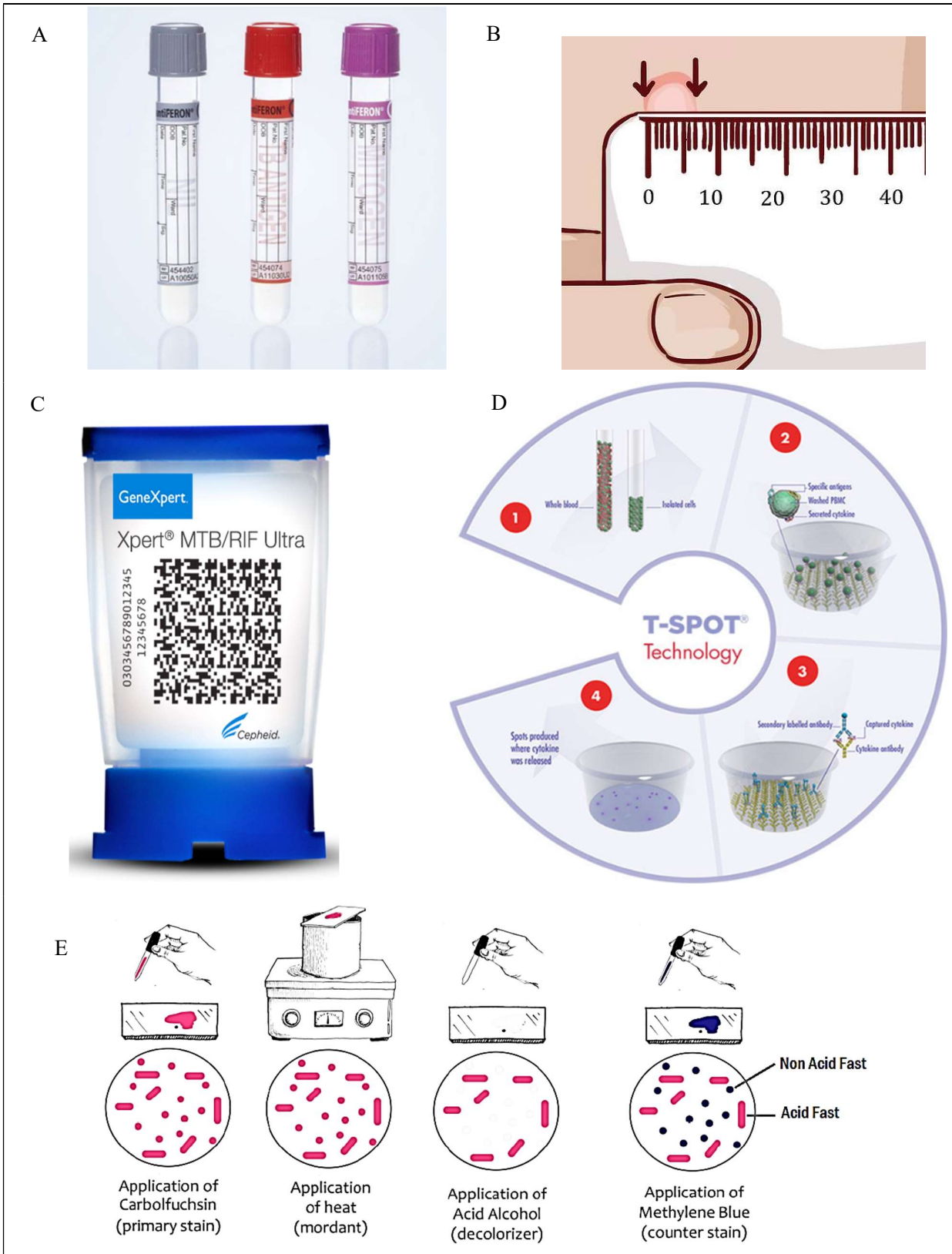

Figure 1 - Tuberculosis Diganosis tools and methods.

(A) IGRA test – Interferon Gamma Release Assay test tubes (B) Tuberculin Skin test (C) Xpert *MTB*/RIF Assay Kit (D) Schematic representation of T-spot TB test. (E) Ziehl-Neelsen Stain procedure.

For explanation of each diagnostic tool, see the text under Tuberculosis Diagnosis.

Sources:
(A) https://www.quantiferon.com/products/quantiferon-tb-gold/
(B) https://www.wikihow.com/Read-a-Tuberculosis-Skin-Test
(C) https://www.cepheid.com/en/tests/Critical-Infectious-Diseases/Xpert-*MTB*-RIF
(D)https://www.tspot.com/why-the-t-spot-tb-test/technology/
(E) https://laboratoryinfo.com/zn-stain/

TB epidemiology

According to the World Health Organization, approximately 25% of the world´s population (~1.7 billion) have been infected with *Mtb*. About 10 million people have been newly infected with TB in 2018. There were about 251,000 deaths among HIV positive patients, which is 61% less than the deaths in this cohort in 2000 (Figure 2A - 2C). TB has emerged as leading cause of death from a single bacterial pathogen since 2007 affecting all age groups in all sexes. In 2018, most TB cases were reported in South-east Asia and Africa, which accounted for 66% of total TB patients (World Health Organisation Global Tuberculosis Report 2019). Also, new cases of rifampicin resistant TB accounted to 0.5 million, out of which 3/4 of the population had MDR-TB. Figure 2D represents new Tuberculosis cases with Multidrug resistant/Rifampicin resistant TB [8].

There are different factors that influence TB epidemiology. Firstly, the socioeconomic development. Since the 18th century, the TB mortality rate in European countries was reduced by 5 to 6% primarily due to better living conditions and improved nutrition during the pre-antibiotics era. TB is regarded as the disease of the poor as 90% cases occur in low income and under developed countries. Secondly, the TB treatment. Early diagnosis and appropriate treatment are required to fight TB. Since the beginning of anti-TB treatment and preliminary diagnosis, the TB cases and risk of infection have drastically reduced in the highly developed countries. The BCG vaccination program and various TB diagnosis programs have contributed to this reduction. Thirdly, HIV infection. HIV causes immunodeficiency which enhances TB infection. HIV-positive TB patients have an annual infection risk of 10%, which is equivalent to the lifetime risk of HIV negative TB patients concluding the high infection risk for HIV patients. In Africa, 82% of HIV patients have TB infection. Other factors include BCG vaccination. There is a protection rate of 40 to 70% if BCG vaccine is administered before the primary infection.

The health-related risk factors include immunosuppression and increased exposure to infected patients. As discussed previously, HIV infection contributes more to TB progression.

Also, patients who take prednisone glucocorticoids with a daily dosage of more than 15 mg also have high chances of getting infected with TB. Diabetic patients also develop increased risk for TB progression. Patients with rheumatic disease and inflammatory bowel disease take tumour necrosis factor alpha (TNF-α) inhibitors for treatment, and these inhibitors affect the host resistance to TB infection. Patients, who had undergone liver, renal and cardiac transplantation, have increased risk for TB development. The new anti-TB drugs and regimens in the development pipeline globally as on August 2019 are listed in Figure 2E.

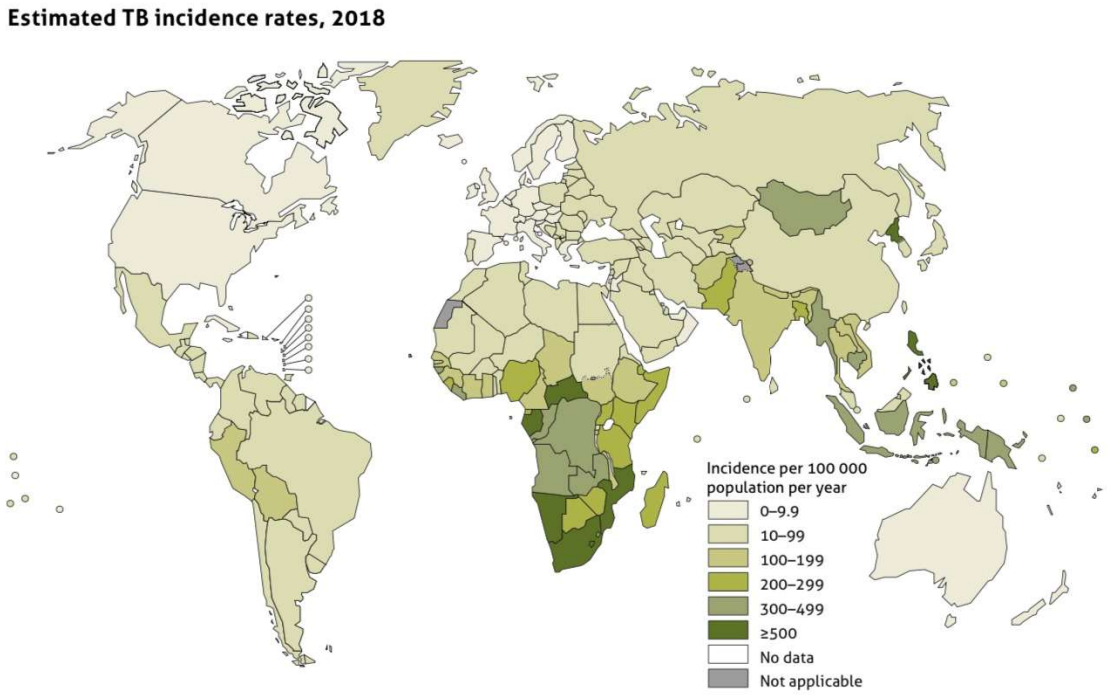

Figure 2A – Estimated Tuberculosis Incidence Rates worldwide in 2018. Source: World Health Organisation Global Tuberculosis Report 2019.

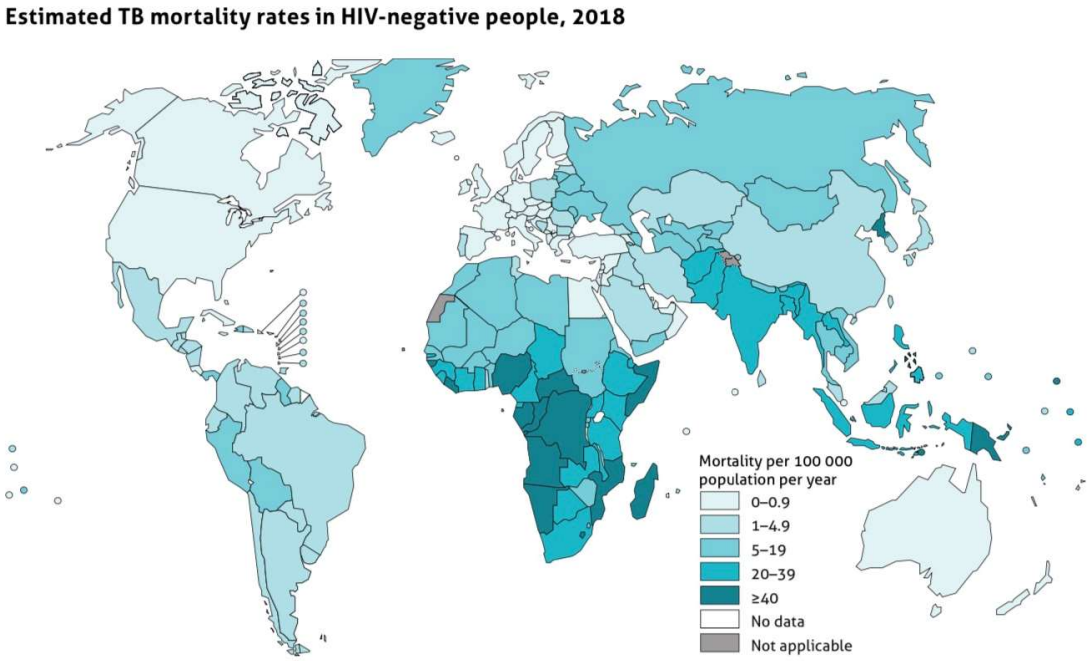

Figure 2B – Estimated Tuberculosis mortality rates in HIV negative people worldwide in 2018. Source: World Health Organisation Global Tuberculosis Report 2019.

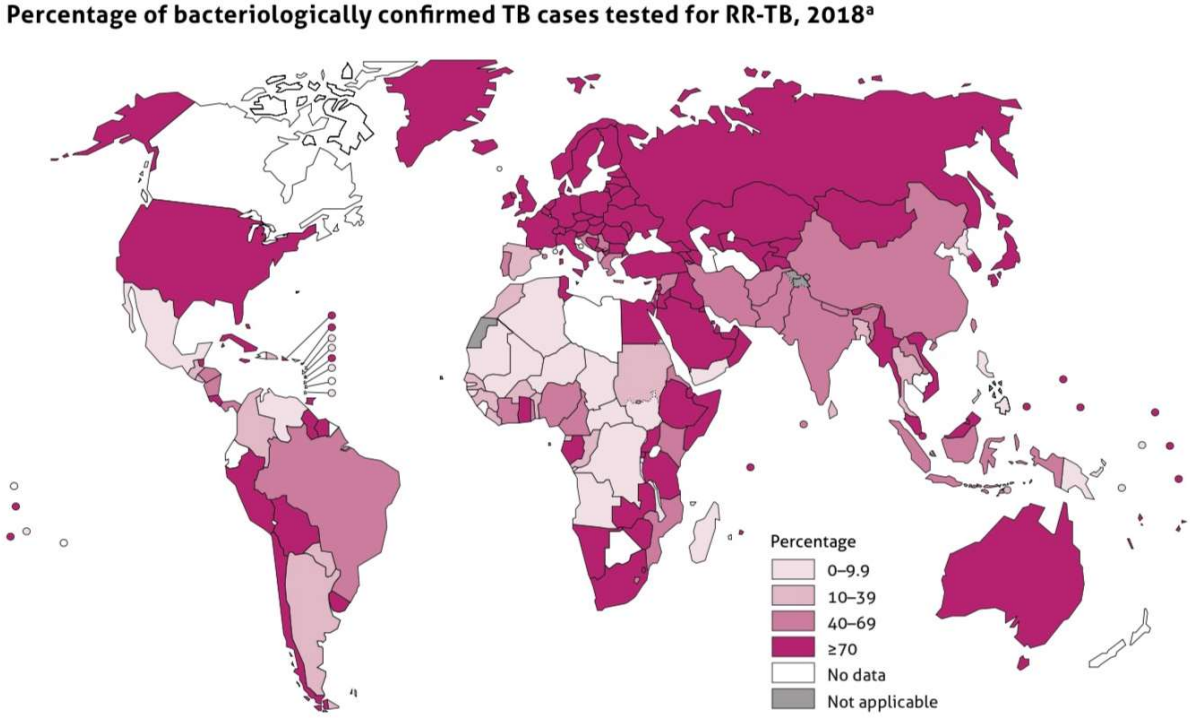

Figure 2C – Estimated percentage of confirmed Tuberculosis cases tested for Rifampicin resistantce TB in 2018. Source: World Health Organisation Global Tuberculosis Report 2019.

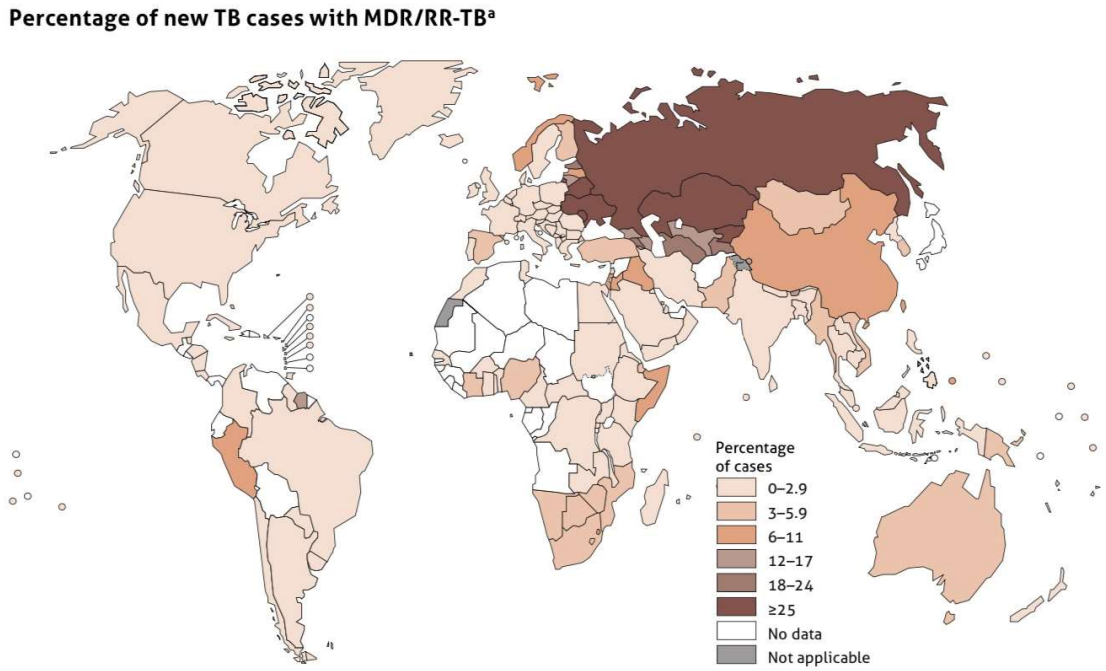

Figure 2D – Percentage of new Tuberculosis cases with Multidrug resistant/Rifampicin resistant TB. Source: World Health Organisation Global Tuberculosis Report 2019 .

The global clinical development pipeline for new anti-TB drugs and regimens, August 2019

Phase I[a]

- BTZ-043[b]
- GSK-3036656[b]
- Macozinone[b]
- OPC-167832[b]
- SPR720[b]
- TBA-7371[b]
- Contezolid (MRX-4/MRX-1)
- TBI-166
- TBI-223

Phase II[a]

- Telacebec (Q203)[b]
- Delpazolid (LCB01-0371)
- SQ109
- Sutezolid
- Linezolid dose ranging
- Nitazoxanide
- High dose rifampicin for drug-susceptible TB (PanACEA)
- Bedaquiline and delamanid (ACTG 5343 DELIBERATE trial)
- Bedaquiline and pretomanid with existing and re-purposed anti-TB drugs for MDR-TB (TB PRACTECAL Phase II/III trial)
- Delamanid, linezolid, levofloxacin, and pyrazinamide for quinolone-sensitive MDR-TB (MDR-END trial)
- Levofloxacin with OBR[c] for MDR-TB (Opti-Q)
- 4-month treatment for drug-susceptible TB (PredictTB trial)

Phase III[a]

- Bedaquiline[b]
- Delamanid[b]
- Pretomanid
- Clofazimine
- High-dose rifampicin for treatment of drug-susceptible TB
- Rifapentine for treatment of drug-susceptible TB
- Bedaquiline–delamanid–linezolid–levofloxacin–clofazimine (6 month oral for RR-TB) or Bedaquiline–delamanid–linezolid–clofazimine, 6–9 months oral for pre-XDR and XDR-TB (BEAT TB trial)
- Bedaquiline – Pretomanid – Moxifloxacin – Pyrazinamide (BPaMZ) (SimpliciTB trial)
- Bedaquiline – Pretomanid – Linezolid (NiX-TB trial)
- Bedaquiline – Pretomanid – Linezolid (ZeNix trial) – Linezolid optimization
- Bedaquiline with two OBRs[c] (all-oral, 9 months; with injectable, 6 months) (STREAM trial)
- Bedaquiline – Linezolid – Levofloxacin with OBR[c] for MDR-TB (NeXT trial)
- Bedaquiline and delamanid with various existing regimens for MDR-TB and XDR-TB (endTB trial)
- Rifapentine – Moxifloxacin for treatment of drug-susceptible TB (TB Trial Consortium Study 31/ A5349)
- Several 2-month regimens for drug-susceptible TB (TRUNCATE-TB trial)

Figure 2E – List of new anti-TB drugs and regimens in the development pipeline as on August 2019. Source: World Health Organisation Global Tuberculosis Report 2019.

Mycobacterium tuberculosis pathogenesis

Mycobacterium tuberculosis (Mtb) is a human pathogen and the cause for TB. It belongs to the family *Mycobacteriaceae* in the class of actinobacteria. It is the leading causes of death from a single infectious organism affecting millions of people every year. There have been no other reservoirs for *Mtb* except humans. Hence, it evolved with developing its metabolism and virulence system to grow and multiply in human macrophages [9] [10]. The bacterial transmission to human host occurs by aerosol inhalation. The alveolar macrophages are infected and become the growth niche for *Mtb* [2]. After the infection with *Mtb*, the pathogen remains in an asymptomatic state, which is called a latent TB infection. *Mtb* can also exist in active state, but only 5% develop the active TB disease [11] [12]. The World Health Organization defines active TB infection as "clinically symptomatic patients with microbiological or radiological evidence of *Mtb*". Following is a table (Table 1) of information on different stages of a TB disease in people.

Eliminated TB infection	A person with eliminated TB infection has a previous record of TB infection but has cured from the infection by chemotherapy or by host immune responses.
Latent TB infection	Latent TB infection is a contained infection with viable *Mtb* without developing to active disease in the near time.
Incipient TB infection	Incipient TB infection is the next stage where the latent infection have high probability to develop in to active disease without producing any detectable symptoms.
Sub clinical TB infection	Sub clinical TB infection is the infection without TB like symptoms but produces other difficulties and symptoms that could by detected by biological assays.
Active TB disease	Active TB disease is a condition with high infection rate and the person shows TB related clinical symptoms that could be detected through various microbiological or other diagnostic assays.

Table 1: Different types of TB infection

After the transmission through aerosol, the bacteria are phagocytosed by alveolar macrophages and also by dendritic cells and are sequestered in immature phagosomes, where they can perform intracellular replication. The growth inside macrophages is unaffected by phagocytosis as the fusion of phagosome and lysozyme is prevented by the action of various virulence factors of *Mtb*. During the latent infection, the infected macrophages are surrounded by different immune cells such as T-cells, B-cells, neutrophils, macrophages, and fibroblasts. This containment of the infected macrophages surrounded by immune cells is called granuloma [13][14]. During active TB infection, the granulomas undergo disruption due to excess of *Mtb* infection that occurs by intracellular replication within macrophages. Later, the infection progresses to tissue necrosis and caseation. Then infected cells then reach local draining lymph nodes and then circulate through the bloodstream. During the circulation they also infects additional host immune cells (Figure 3) [15] [16] .

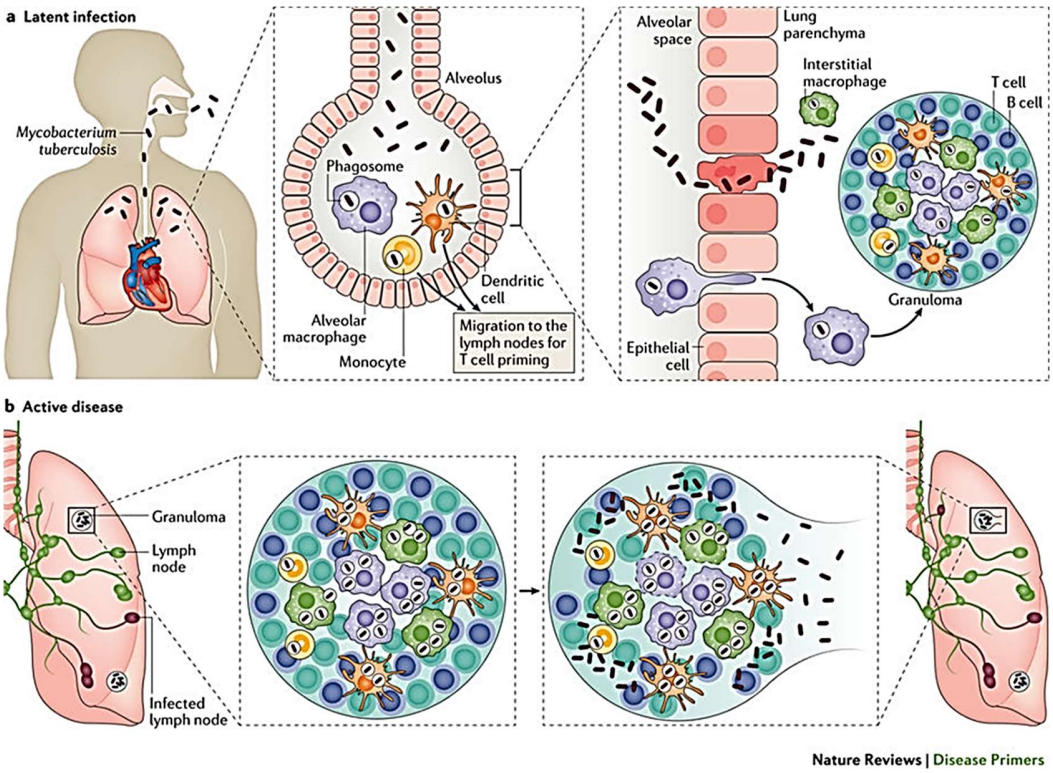

Figure 3- *Mycobacterium tuberculosis* - Infection cycle – *For explanation, see text.*
Source: Pai, M., Behr, M., Dowdy, D. et al. Tuberculosis. Nat Rev Dis Primers 2, 16076 (2016). https://doi.org/10.1038/nrdp.2016.76.

Characteristics of *Mycobacterium tuberculosis*

Mycobacterium tuberculosis (Mtb) is a rod-shaped bacillus measuring 0.1 µm - 0.5 µm (width) by 2 µm -5 µm (length) without flagellum. The bacteria are aerobic, non-motile, non–spore-forming and slow growing (typically takes 18-24 hours for each division). The cell wall contains unique mycolic acids (alpha branched long chain fatty acids). The cell wall contains high amounts of lipids which is responsible for the resistance to antibiotics, conferring resistance to lysis by acidic and alkaline compounds. They also confer resistance to osmotic lysis and lethal oxidation [17]. The cell wall consists of an inner cytoplasmic membrane, the periplasmic space, the peptidoglycan layer, the arabinogalactan linked to mycolic acids (mAGP complex) and an outer membrane or capsular layer.

Another important virulence factor is the protein secretion system in *Mtb*. *Mtb* contains five different type VII secretion system, among which ESX-1 confers high virulence and secretes ESAT-6 and CFP-10 which are used as antigens in the IGRA TB test. ESX-3 plays a vital role in the uptake of iron and zinc and is essential for *in vitro* growth. ESX-5 was found to be present only in the *Mtb* complex (*MTB*C) together with *Mycobacterium marinum* and *Mycobacterium ulcerans*. The ESX-5 secretion system is known to consist of essential genes required for the growth and several virulence factors, few of them were not yet characterized. Not a lot is known about the ESX-2 and ESX-4 secretion systems. The size of the *Mtb* H37Rv genome is 4.4 million base pairs with 3,906 protein encoding genes and 65.9 % of GC content [18]. The genome also contains about 7% - 10% of conserved Proline-Glutamic acid (PE) and Proline-Proline-Glutamic acid (PPE) motifs at N-terminal of the proteins. *Mtb*H37Rv strain consists of 99 PE and 69 PPE proteins encoding genes [19].

Regulation of various metabolism in *Mtb*

Mtb has the ability to use various compounds as the major carbon sources in order to support their growth in *in vitro* conditions. Although *Mtb* shares some identical metabolisms with some other bacteria, it possesses several different regulation mechanisms, which are either dependent or independent to each other. One common mechanism employed by many bacteria is the carbon catabolite repression. This cycle categorizes the use of carbon sources in an orderly fashion depending upon the ability to enhance the bacterial growth. Those carbon sources that can promote maximum growth are utilized first. However, this conventional cycle is absent in *Mtb*. *Mtb* has the ability to co-catabolize many carbon sources at once and can enhance its growth

efficiency by utilizing the mixture of carbon sources that from a single source. The previous studies on *Mtb* strains carrying mutations in genes responsible for the catalyzing major steps in glycolysis and gluconeogenesis have proven the carbo co-catabolism of *Mtb*. For *Mtb* to utilize the ability of co-catabolism of glucose and fatty acids, the enzyme pyruvate kinase is essential. Pyruvate kinase is responsible for the conversion of phosphoenolpyruvate to pyruvate. Deletion of the gene that codes for pyruvate kinase results in the allosteric inhibition of isocitrate dehydrogenase from the citric acid cycle. Isocitrate dehydrogenase inhibition occurs by the accumulation of phosphoenolpyruvate in the culture containing glucose and fatty acid. These sequences result in the inhibition of co-catabolism of *Mtb*. Further, previous studies have reported that the regulation of nutrient utilization in *Mtb* can occur in a cAMP- (cyclic adenosine monophosphate) dependent process. *Mtb* can also adopt metabolic recycling. It can recycle lipids from glycerophospholipids and trehalose from trehalose dimycolates synthesis [20].

Mtb cell wall

The cell wall of *Mtb* is critical for its physiology as many disease causing virulence factors are located in this compartment. These protective virulence factors help *Mtb* to survive antibiotic treatment and helps in the transport of various nutrients and proteins. 40% of the dry weight of *Mtb* cells consists of lipids, and the cell wall contains about 58% of lipids. Major lipids are the mycolic acids which are unique to the order Corynebacteriales [21]. The mycolic acids are long chain fatty acids that are either covalently bound to arabinogalactan which is linked to peptidoglycan or esterified to sugars like trehalose as trehalose monomycolates (TMM) or trehalose dimycolates (TDM). The cell envelope has five major sub compartments namely, inner cell membrane, peptidoglycan layer, arabinogalactan layer, mycomembrane and outer capsular layer [22][23] (Figure 4). The inner cytoplasmic membrane consists of glycerophospholipids, phosphatidylinositol mannosides, lipomannans and lipoarabinomannans. The peptidoglycan layer lies outside the inner cell membrane and is covalently attached to arabinogalactan layer. It is the founding layer for mAGP complex. The peptidoglycan layer offers osmotic stability to the bacterium. *Mtb* peptidoglycan consists of N-acetylglucosamine (GlcNAc) and modified muramic acid (Mur - contains mixture of N-acetyl and N-glycolyl derivatives) connected in a β(1 → 4) arrangement. The N-glycolyl muramic acid is responsible for the resistance to lysozyme [24][25]. The peptidoglycan layer bears highly concentrated (70%–80%) cross-linked peptides. The first step in the biosynthesis of peptidoglycan is the conversion of fructose-6-phosphate to UDP-N-acetylglucosamine (UDP-GlcNAc) catalyzed by Rv3436, Rv3441 and Rv1018 encoding enzymes.

The product is then forwarded to the following steps: (2) synthesis of UDP-GlcNAc enoylpyruvate, (3) synthesis of UDP-MurNAc-L-Ala-D-Glu-mADP-D-Ala-D-Ala, (4) synthesis of MurNAc-(pentapeptide)-pyrophosphorylundecaprenol, (5) synthesis of GlcNAc-MurNAc-(pentapeptide)-pyrophosphoryl-decapreno,l (6) the translocation of lipid II molecule across inner membrane, and (7) maturation of peptidoglycan by transglycosylases and transpeptidases [26]. Arabinogalactan is another unique compartment in *Mycobacterium* species and consists of arabinose and galactose monosaccharides in the furanoid ring form. It is covalently linked to muramic acid residues of peptidoglycan by phosphodiester bond. The arabinogalactan layer can be divided into three subcompartments: 1. the linker unit (LU), 2. galactan, and 3. Arabinan [27].

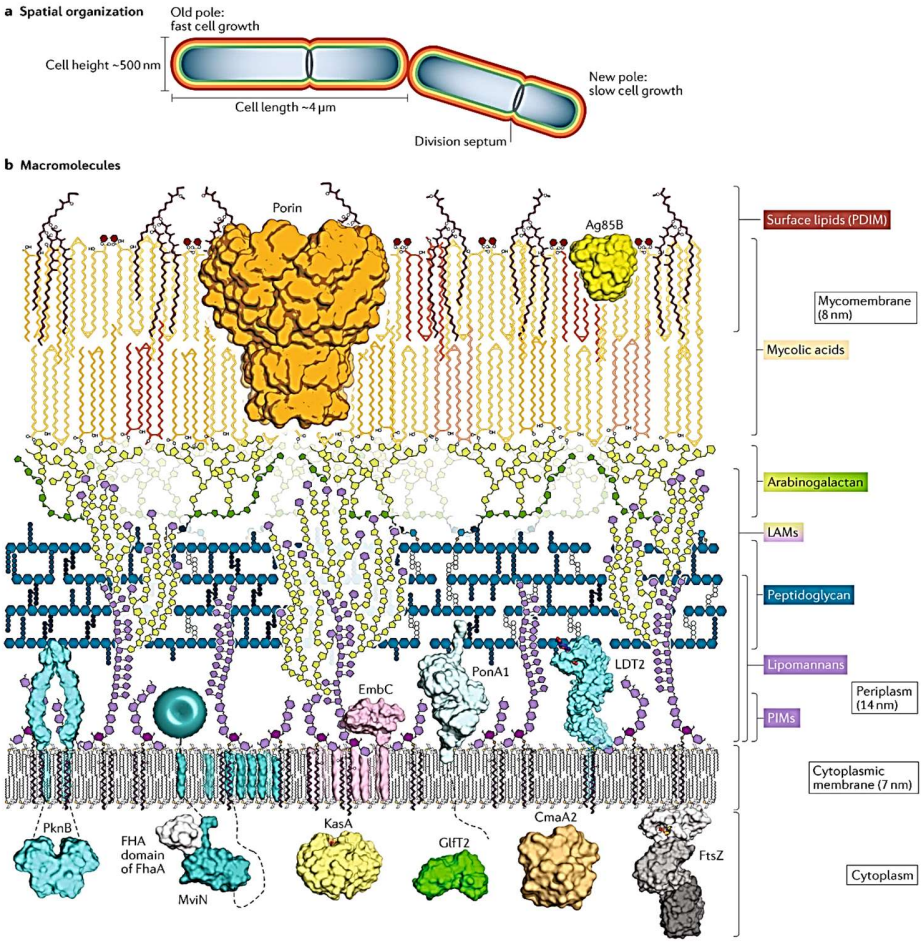

Figure 4 – Mycobacterial cell envelope (*For explanation see text)*

Source: Dulberger, C.L., Rubin, E.J. & Boutte, C.C. The mycobacterial cell envelope — a moving target. Nat Rev Microbiol 18, 47–59 (2020). https://doi.org/10.1038/s41579-019-0273-7.

Mycolic acids

Mycolic acids are long-chain fatty acids, which are present in all of the mycobacterial strains. There are three different types of mycolic acids present in virulent *Mtb,* and they are α-mycolic acids, methoxy-mycolic acids and keto-mycolic acids. α-Mycolic acids accounts to approximately 70% of the mycolic acids composition and contain about 74–80 carbon atoms [28]. Mycolic acids confer resistance to various stress conditions, antibiotic treatment and damage mechanisms. Mycolic acids also participate in the mechanism allowing *Mtb* to grow in the phagosome within macrophages and eliminate the fusion with lysozyme. Mycolic acids are synthesized from the natural mycobacterial fatty acid precursors by the action of fatty acid synthases FAS I and II. FAS-I is encoded by Rv2524c. The transfer from FAS-I to FAS-II is regulated by the action of several enzymes encoded by *fabD, acpM, fabH* genes. FAS-II is composed of β-ketoacyl-ACP synthase, β-ketoacyl-ACP reductase and β-hydroxyacyl-ACP dehydratase. This is followed by biosynthesis of *cis*,*cis*-diunsaturated meroacid precursors and α-meroacids. The final assembly of the mycolic acids is executed by the claisen-type condensation by Pks13 [29]. The TMM molecules generated from the previous step are transported to mycomembrane through mycobacterial membrane proteins large 3 (MmpL3) proteins[30]. The mycolic acid from one TMM is either transferred to another TMM forming TDM, or it is linked to arabinogalactan polysaccharides forming the mycolyl-arabinogalactan-peptidoglycan complex. These transfers are regulated by Antigen85 (Ag85A, Ag85B, and Ag85C) complex encoded by *fbpA*, *fbpB* and *fbpC2* [31][32] (Figure 5).

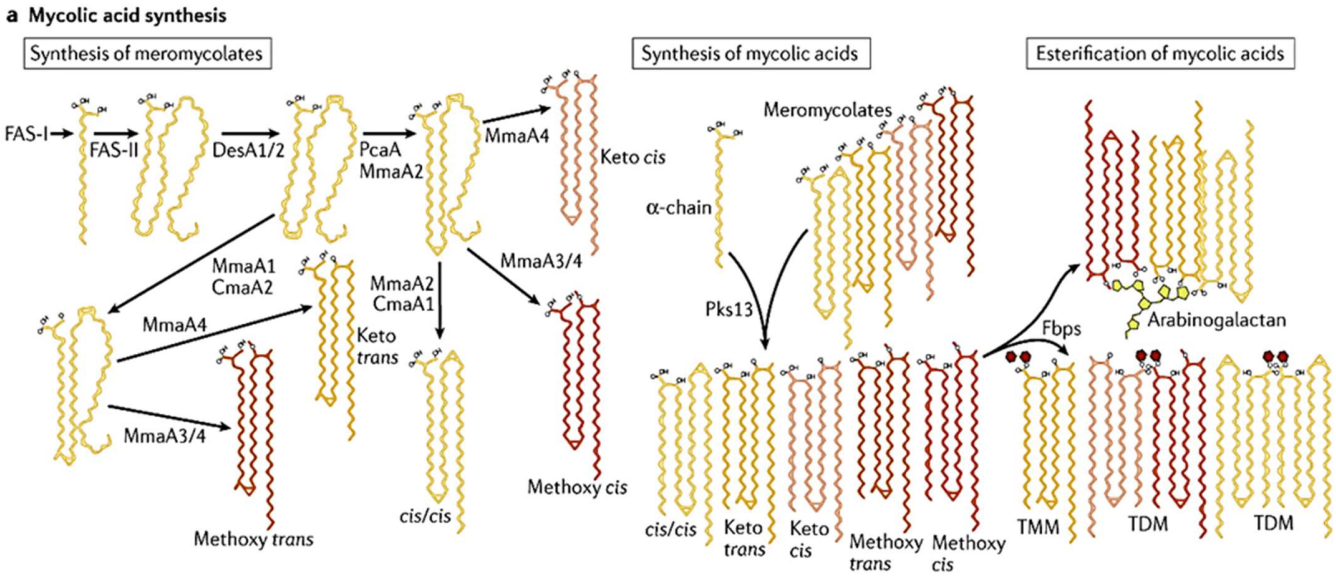

Figure 5 – Mycobacterial cell envelope Metabolism – Regulation of Mycolic acid biosynthesis. *For explanation, see text*.
Source: Dulberger, C.L., Rubin, E.J. & Boutte, C.C. The mycobacterial cell envelope — a moving target. Nat Rev Microbiol 18, 47–59 (2020). https://doi.org/10.1038/s41579-019-0273-7.

Trehalose - Importance and function (adapted from manuscript)

Trehalose is a non-reducing sugar, which is widely distributed among several eukaryotic organisms such as plants, insects, fungi, nematodes, insects and members of the prokaryotic class such as bacteria and archaea. Trehalose performs multiple function ranging from the regulation of energy metabolism to intracellular communication [33]. Trehalose is often referred to as a protector molecule due to its multiple protective function by safeguarding the bacterium from various stress conditions such as heating, freezing and other lytic conditions. Biosynthesis of trehalose has been an important factor for infection by the members of *Streptomyces*, *Pseudomonas aeruginosa* and various bacterial strains belonging to actinobacteria. Trehalose is crucial for the composition of the mycobacterial cell envelope. *De novo* biosynthesis of trehalose can occur through five different pathways in eukaryotic and prokaryotic organisms. In mycobacterium, it is synthesized mainly by the OtsA-OtsB2 or the TreY-TreZ pathway [34][35]. TMM is synthesized in the cytoplasm by the 6-O-mycoloylation of trehalose catalyzed by Pks13 and is then transported to the mycomembrane through Mycobacterial membrane proteins Large3 (MmpL3) proteins. In the mycomembrane, the mycolic acid from one TMM is either transferred to another TMM molecule forming TDM, or it is transferred to arabinogalactan polysaccharides forming arabinogalactan linked mycolates. Both reaction lead to the concomitant release of free trehalose. These transfers are catalyzed by the antigen 85 (Ag85A, Ag85B, and Ag85C) complex. The free trehalose molecules are then recycled back to the cytoplasm through the LpqY-SugABC transporter located in the cytoplasmic membrane. Large amount of TDM contributes to increased virulence of *Mtb* and *vice versa*. The following is a table (Table 2) with different trehalose based glycolipids and oligosaccharides and their respective function [36].

Trehalose based compounds	Organism	Function
Diacyltrehalose	*Mycobacterium tuberculosis*	Regulation in virulence mechanisms.
Triacyltrehalose	*Mycobacterium tuberculosis*	
Pentaacyltrehalose	*Mycobacterium tuberculosis*	
Sulfolipid-1	*Mycobacterium tuberculosis*	Major Virulence factor
Trehalose 6,6'-dimannosyl-phosphate	*Mycobacterium smegmatis*	Uncharacterized
Trehalose monomycolates	Mycobacterial strains	Vital in synthesis of mycolic acid membrane and assembly. *Mtb*growth in macrophages.
Trehalose dimycolates	Mycobacterial strains	
Lipooligosaccharides - 0	*M. mucogenicum, M. smegmatis, M. szulgai, M. gastri*, *M. gordonae, M. kansasii, M. marinum*	Plays an important role in biofilm formation, Virulence mechanisms and colony morphology.
Lipooligosaccharides - I		
Lipooligosaccharides - II		
Lipooligosaccharides - III		
Lipooligosaccharides – IV		
Lipooligosaccharides - V		

Table 2: Trehalose based glycolipids and oligosaccharides (adapted from Nobre A, Alarico S, Maranha A, Mendes V, Empadinhas N. The molecular biology of mycobacterial trehalose in the quest for advanced tuberculosis therapies. Microbiology (Reading). 2014 Aug;160(Pt 8):1547-1570. doi: 10.1099/mic.0.075895-0. Epub 2014 May 23. PMID: 24858083).

Methyl glucose lipopolysaccharides

There are few other unbound polysaccharides in the capsular layer that play a role in the host-pathogen interactions. *Mtb* also synthesizes intracellular polysaccharides, one among which are polymethylated polysaccharides. These polysaccharides are known to be present in closely related mycobacterial species and other bacteria such as *Streptomyces griseus*, *Nocardia farcinica* and *Nocardia brasiliensis*. They contain multiple units of glucose or mannose molecules and have ability to form a complex with long chain fatty acids in 1:1 ratio. Two classes of polymethylated polysaccharides have been identified so far in mycobacterial species: Methyl mannose polysaccharides (MMP) and methyl glucose lipopolysaccharides (MGLP). They have been known to regulate the *in vitro* enzymatic activity of FAS-I and are also believed to play a vital

role in the biosynthesis and maturation of mycolic acids in *Mtb* [37]. MMP are composed of a α-(1-4) branched chain containing ten to fourteen 3-O-methylmannoses and are found to exist in only fast growing organisms such as *Mycobacterium smegmatis* and *Streptomyces griseus* [38]. The slow growing mycobacteria such as *Mtb, Mycobacterium bovis* and *Mycobacterium xenopi* contain only MGLP. MGLP have sixteen to twenty units of glucoses and 6-O-methyl glucoses linked in an α-(1-4) linear chain with α-(1-6) branched diglucosylglycerate at the reducing end [39][40]. It is to the first glucose of the diglucosylglycerate that the MGLP main chain of methyl glucoses is attached. Diglucosylglycerate is the initial precursor for the synthesis of long chain MGLPs [41][42]. There are two additional glucoses linked to the first and third glucoses of the main chain in a β-(1-3) branching fashion. MGLP contain propionate, acetate and isobutyrate linked to the methyl glucose units close to the non-reducing end and an octanoate moiety linked to the glyceric acid at the reducing end [43][44]. MGLP are proposed to act as carriers of newly synthesized fatty acid chains and protect them from interacting with lytic enzymes. MGLP are also known to contribute to the temperature adaptability of *Mtb* and also protect them from environmental stress. Taken together, MGLP are considered to be one of the important components of the *Mtb*. However, the biosynthesis and the function of MGLP have not fully characterized yet. MGLP are critical for the viability of *Mtb* as strict essentiality of some genes involved in their biosynthesis has been suggested from genome-wide transposon mutant studies. The formation of diglucosylglycerate (DGG) from glucosylglycerate (GG) is an essential step in the synthesis of MGLP (Figure 6). In this study, we will characterize the branching enzyme Rv3031, potentially catalyzing the DGG synthesis by employing molecular genetics to reveal insights into the essential role of MGLPs for viability of *Mtb*.

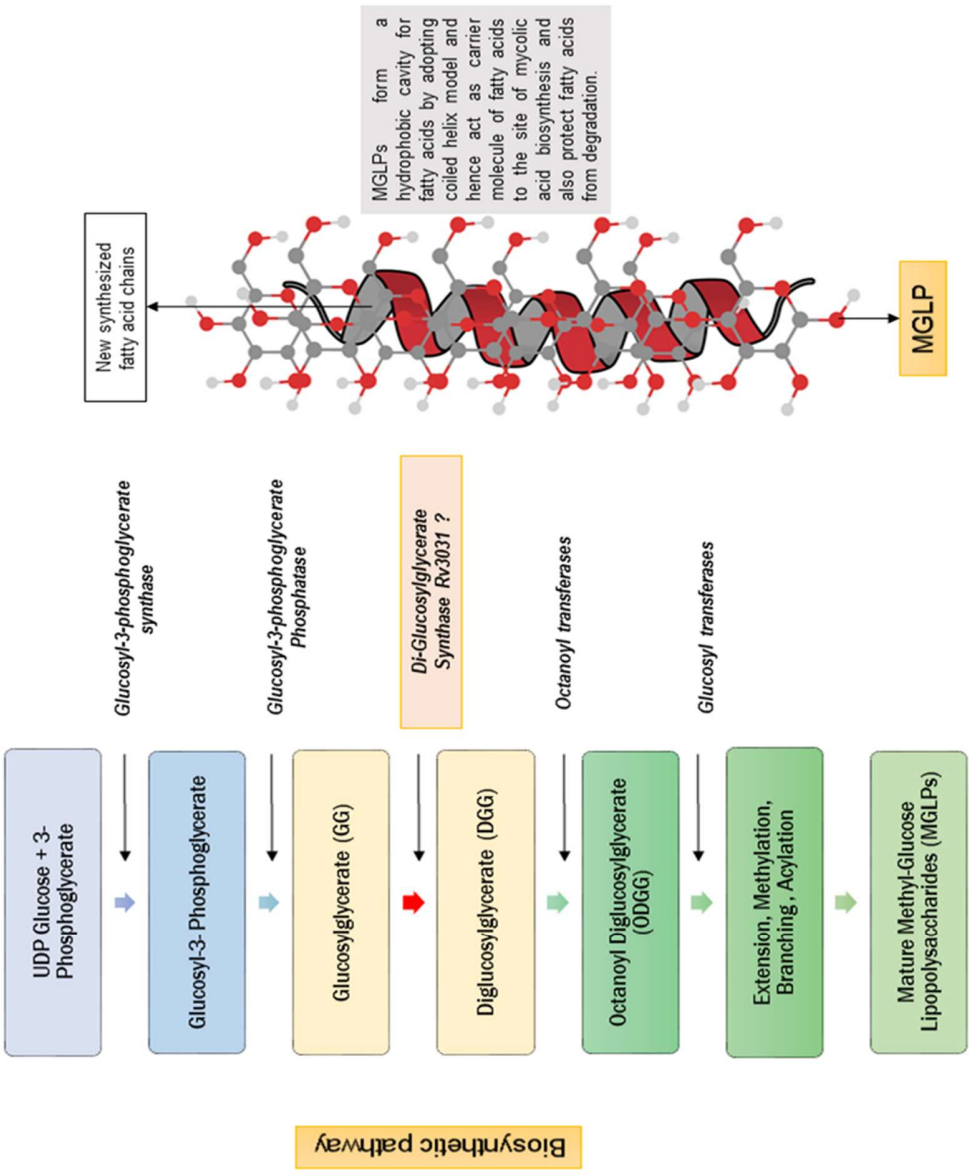

Figure 6.

Schematic representation of MGLP Biosynthetic pathway and the predicted function of MGLP to preserve fatty acids from degradation by lytic enzymes

Chapter 2 - Materials and Methods

1. ***List of abbreviations***

AES	Allelic exchange substrate
AF	Alexa Fluor
Ag85	Antigen 85 complex
Amp	Ampicillin
Apra	Apramycin
ATC	Anyhydrotetracycline
ATP	Adenosine triphosphate
ADP	Adenosine diphosphate
BCG	Bacille Calmette Guerin
BSA	Bovine Serum Albumin
CO_2	Carbon dioxide
CFU	Colony forming units
CTAB	Cetrimide – hexadecyltrimethylammonium bromide
DNA	Deoxyribonucleic acid
DMN-Glc	4-N,N-dimethylamino-1,8-naphthalimide Glucose
DMN-Tre	4-N,N-dimethylamino-1,8-naphthalimide Trehalose
DMSO	Dimethyl Sulfoxide
DGG	Diglucosylglycerate
DGGs	Diglucosylglycerate-synthase
DPBS	Dulbecco's phosphate-buffered saline
EMB	Ethambutol
E. coli	*Escherichia coli*
FACS	Fluorescence Activated Cell Sorting
FAS- I	Fatty acid synthase - I
FAS- II	Fatty acid synthase - II
FBS	Fetal Bovine Serum
FITC	Fluorescein IsoThioCyanate
G3P	Glycerol-3-phosphate
GDP	Guanosine diphosphate

GT	Glycosyltransferase
GpgS	Glycosylphosphoglycerate-Synthase
GFP	Green Fluorescent Protein
HIV	Human Immunodeficiency Virus
Hyg	Hygromycin
IFN	Interferon
IL	Interleukin
Kan	Kanamycin
Kbp	Kilo base pairs
LAM	Lipoarabinomannan
LM	Lipomannan
LC-MS/MS	Liquid chromatography tandem mass spectroscopy
MA	Mycolic acids
mAGP	mycolyl-Arabinogalactan-Peptidoglycan
MAME	Mycolic acid methyl ester
Man	Mannose
Man-LAM	Mannosylated lipoarabinomannan
mRNA	Messenger ribonucleic acid
MIC	Minimal Inhibitory Concentration
Mtb	*Mycobacterium tuberculosis*
M. bovis	*Mycobacterium bovis*
M. marinum	*Mycobacterium marinum*
M. smegmatis	*Mycobacterium smegmatis*
Msmeg/MSMEG	*Mycobacterium smegmatis*
MGLP	Methyl Glucose Lipopolysaccharide
MMP	Methyl Mannose Polysaccharides
NalC	N-acetyl-l-cysteine
NaCl	Sodium chloride
NaOH	Sodium hydroxide
OADC	Oleate-Albumin-Dextrose-Catalase
PDIM	Phthioceroldimycocerosate
PFU	Plaque forming unit
PMP	Polymethylated Polysaccharides

RNA	Ribonucleic acid
RR	Rifampicin-Resistant
RBS	Ribosomal binding sites
RevTetR	Reverse Tet Repressor
SDS-PAGE	Sodium Dodecyl Sulfate-Polyacrylamide Gel Electrophoresis
TAE	Tris-acetate-EDTA
TetO	Tet-Operator
TetR	Tet-Repressor
TLC	Thin layer chromatography
TLR	Toll-like receptor
TNF	Tumor necrosis factor
TRIS	Tri(hydromethyl)aminomethane
UDP	Uracil-diphosphate
UV	Ultraviolet
XDR-TB	Extensively drug-resistant *Mtb*
WHO	World Health Organization
WT	Wild type
TB	Tuberculosis
ZN	Ziehl-Neelsen test
°C	Degree Celsius
%	Percent
% (v/v)	Volume percent
% (w/v)	Mass percent
µF	Microfarad
µg	Microgram
µL	Microliter
µM	Micromolar
µm	Micrometer
nm	nanometer
3-PGA	3-Phosphoglycerate
6-FlTre	6-Fluorescein-trehalose
6-TreAz	6-Azido-trehalose
2-TreAz	2-Azido-trehalose

2. List of Instruments and devices

Bio-Rad Gene Pulser Xcell™	BIO-RAD
Tecan infinite F200 Pro	Tecan
Heating block	VWR International GmbH
NanoDrop 1000	Thermo Fisher Scientifc
TissueLyser LT	Qiagen
UVP Gel Studio	Analytik Jena AG
Thermal cycler FlexCycler²	Analytik Jena AG
Precellys® 24 Homogenizer	BERTIN
Mx3005P QPCR System	Agilent Technologies

3. List of kits and consumables

AccuClear® Ultra High Sensitivity dsDNA Quantitation Kit with DNA Standards	Biotium
NucleoSpin® Plasmid Mini Kit	Macherey-Nagel
NucleoSpin® Gel and PCR Clean-up Kit	Macherey-Nagel
RNeasy Mini Kit	Qiagen
RNase-Free DNase Set	Qiagen
SuperScript™ III First-Strand Synthesis SuperMix	Invitrogen
GoTaq® qPCR Master Mix	Promega
BCA Protein Assay Kit	Merck Millipore
ZeroBlunt® TOPO® PCR Cloning Kits	Invitrogen
MaxPlax™ Lambda Packaging Extracts	Epicentre

4. List of *Mtb* Strains and antibiotics conditions

No	RKSC No.	*Mtb* strains	Antibiotic Resistance	Source /Reference
1	1	*Mtb* H37Rv WT	-	Parent strain
2	62	*Mtb* ΔLpqY - Rv1235	Hygromycin (50 µg/ml)	Kalscheuer et al., 2010
3	63	*Mtb* ΔSugC - Rv1238	Hygromycin (50 µg/ml)	Kalscheuer et al., 2010
4	64	*Mtb* ΔLpqY-SugC - Rv1235-1238	Hygromycin (50 µg/ml)	Kalscheuer et al., 2010
5	65	*Mtb* ΔLpqY - pMV306::1235-1238	Hygromycin (50 µg/ml) Kanamycin (40 µg/ml)	Kalscheuer et al., 2010
6	66	*Mtb* ΔSugC - pMV306::1235-1238	Hygromycin (50 µg/ml) Kanamycin (40 µg/ml)	Kalscheuer et al., 2010
8	100	*Mtb* H37Rv WT - pMV306::Rv1235-1238	Kanamycin (40 µg/ml)	This study
9	101	*Mtb* H37Rv WT 6-TreAz resistant - pMV306::Rv1235-1238 C2	Kanamycin (40 µg/ml)	This study
10	101	*Mtb* H37Rv WT 6-TreAz resistant - pMV306::Rv1235-1238 C5	Kanamycin (40 µg/ml)	This study
11	101	*Mtb* H37Rv WT 6-TreAz resistant - pMV306::Rv1235-1238 C6	Kanamycin (40 µg/ml)	This study
12	101	*Mtb* H37Rv WT 6-TreAz resistant - pMV306::Rv1235-1238 C9	Kanamycin (40 µg/ml)	This study
13	101	*Mtb* H37Rv WT 6-TreAz resistant - pMV306::Rv1235-1238 C9	Kanamycin (40 µg/ml)	This study
14	328	*Mtb* 6-TreAz-res. C2 pMV361::Rv1783-84	Apramycin (40 µg/ml)	This study
15	329	*Mtb* 6-TreAz-res. C5 pMV361::ppe51	Apramycin (40 µg/ml)	This study
16	330	*Mtb* 6-TreAz-res. C6 pMV361::ppe51	Apramycin (40 µg/ml)	This study
17	331	*Mtb* 6-TreAz-res. C9 pMV361::ppe51	Apramycin (40 µg/ml)	This study
18	332	*Mtb* 6-TreAz-res. C9 pMV361::Rv1230	Apramycin (40 µg/ml)	This study
19	417	*Mtb* ΔRv3136c (PPE51)	Hygromycin (50 µg/ml)	This study
20	418	*Mtb* ΔRv3136c (PPE51) pMV361::ppe51	Hygromycin (50 µg/ml) Apramycin (40 µg/ml)	This study

21	405	*Mtb* Rv3031 - 1 Knockin (4xtetO)	Hygromycin (50 µg/ml)	This study
22	406	*Mtb* Rv3031 - 2 Knockin (4xtetO)	Hygromycin (50 µg/ml)	This study
23	407	*Mtb* CM TetON Rv3031-1 D ::pMV261::tetR_RBS-Mut. D	Hygromycin (50 µg/ml) Kanamycin (40 µg/ml)	This study
24	408	*Mtb* CM TetON Rv3031-1 E ::pMV261::tetR_RBS-Mut. E	Hygromycin (50 µg/ml) Kanamycin (40 µg/ml)	This study
25	409	*Mtb* CM TetON Rv3031-2 D ::pMV261::tetR_RBS-Mut. D	Hygromycin (50 µg/ml) Kanamycin (40 µg/ml)	This study
26	410	*Mtb* CM TetON Rv3031-2 E ::pMV261::tetR_RBS-Mut. E	Hygromycin (50 µg/ml) Kanamycin (40 µg/ml)	This study
27	411	*Mtb* CM TetOFF Rv3031-1 D ::pMV261::RevtetR_RBS-Mut. D	Hygromycin (50 µg/ml) Kanamycin (40 µg/ml)	This study
28	412	*Mtb* CM TetOFF Rv3031-1 E ::pMV261::RevtetR_RBS-Mut. E	Hygromycin (50 µg/ml) Kanamycin (40 µg/ml)	This study
29	413	*Mtb* CM TetOFF Rv3031-2 D ::pMV261::RevtetR_RBS-Mut. D	Hygromycin (50 µg/ml) Kanamycin (40 µg/ml)	This study
30	414	*Mtb* CM TetOFF Rv3031-2 E ::pMV261::RevtetR_RBS-Mut. E	Hygromycin (50 µg/ml) Kanamycin (40 µg/ml)	This study

5. List of *Mycobacterium smegmatis* Strains and antibiotics conditions

No	**RKSC no**	***Mycobacterium smegmatis* (MSMEG) strains**	**Antibiotic Resistance**	**Source /Reference**
1	1	*M. smegmatis* mc²155	-	Parent strain
2	184	ΔMSMEG 6396-99	Hygromycin (50 µg/ml)	This study
3	258	ΔMSMEG 6396-99::6396-6399	Hygromycin (50 µg/ml) Kanamycin (40 µg/ml)	This study

6. List of *E. coli* and *Rosetta* Strains and antibiotics conditions

No	*E. coli* and *Rosetta* Strains	Antibiotic Resistance	Reference	RKSC no
1	NEB 5-alpha F´Iq : Rv3031-1 4xtetO Knockin Plasmid	Hygromycin (150 µg/ml)	This study	646
2	NEB 5-alpha F´Iq : Rv3031-2 4xtetO Knockin Plasmid	Hygromycin (150 µg/ml)	This study	647
3	NEB 5-alpha F´Iq : MSmeg 2349 4xtetO Knockin Plasmid	Hygromycin (150 µg/ml)	This study	650
4	NEB 5-alpha F´Iq : Rv3031-1 4xtetO Knockin shuttle Phasmid	Hygromycin (150 µg/ml)	This study	648
5	NEB 5-alpha F´Iq : Rv3031-2 4xtetO Knockin shuttle Phasmid	Hygromycin (150 µg/ml)	This study	649
6	NEB 5-alpha F´Iq : MSmeg 2349 4xtetO Knockin shuttle Phasmid	Hygromycin (150 µg/ml)	This study	651
7	Rosetta(DE3)pLysS - pET28a::Rv3031-1-6xHis (N-Terminal)	Kanamycin (40 µg/ml) Chloramphenicol(40 µg/ml)	This study	652
8	Rosetta(DE3)pLysS - pET28a::Rv3031-2-6xHis (N-Terminal)	Kanamycin (40 µg/ml) Chloramphenicol(40 µg/ml)	This study	653
9	Rosetta(DE3)pLysS - pET28a::Rv0225-6xHis (N-Terminal)	Kanamycin (40 µg/ml) Chloramphenicol(40 µg/ml)	This study	654
10	Rosetta(DE3)pLysS – pET30a::Rv3031-1-6xHis (C-Terminal)	Kanamycin (40 µg/ml) Chloramphenicol(40 µg/ml)	This study	655
11	Rosetta(DE3)pLysS – pET30a::Rv0225-6xHis (C-Terminal)	Kanamycin (40 µg/ml) Chloramphenicol(40 µg/ml)	This study	656
12	NEB 5-alpha F´Iq : pMV306 -6396-99 complement	Kanamycin (40 µg/ml)	This study	657
13	NEB 5-alpha F´Iq : pMV261::tetR_RBS-Mut. D	Kanamycin (40 µg/ml)	This study	201
14	NEB 5-alpha F´Iq : pMV261::tetR_RBS-Mut. E	Kanamycin (40 µg/ml)	This study	202
15	NEB 5-alpha F´Iq : pMV261::revtetR_RBS-Mut.D	Kanamycin (40 µg/ml)	This study	414
16	NEB 5-alpha F´Iq : pMV261::revtetR_RBS-Mut.D	Kanamycin (40 µg/ml)	This study	415

7. List of Primers used

No	Primer Name	Primer Sequence	Reference /Source
1	Rv3136-LL-Van91I	5' TTTTTCCATAAATTGGACCCGTCAGGGCGAGAATGAATC 3'	This study
2	Rv3136-LR-Van91I	5' TTTTTCCATTTCTTGGCGGAGTTGACTTCCGGTGGTAAC AG 3'	This study
3	Rv3136-RL-Van91I	5' TTTTTCCATAGATTGGAGTTGGTTTCCGCGACCAGTCCC 3'	This study
4	Rv3136-RR-Van91I	5' TTTTTCCATCTTTTGGGCCAGAGCCAGCGCAAGCATTAG 3'	This study
5	PCRCheckPPE51-Fwd	5' ATGGACTACGCGTTCTTACC 3'	This study
6	PCRCheckPPE51-Rev	5' CTCATACTGATCGCGGTCCTAGC 3'	This study
7	MSMEG_6396-3´-ClaI	5' TTTTTATCGATCTACTTGATGGTGGCGACCAGCTC 3'	This study
8	MSMEG_6396-5´-PacI	5' TTTTTTTAATTAATGAGACGTGGGTTGAGTCTGG 3'	This study
9	MSMEG6396-99 3´-ClaI	5' TTTTTATCGATTCTCGACGCGGTGTGCTACTTG 3'	This study
10	MSMEG6396-99 5´-EcoRI	5' TTTTTGAATTCCCTGTCGAACATCGTGCACTCCTAC 3'	This study
11	MSMEG_6396-99_3-ClaI	5' TTTTTATCGATTCGATTCTCGACGCGGTGTGCTAC 3'	This study
12	cRv3031-RR-BstAPI	5' TTTTTGCATCTTTTGC-GGCCGTCGACCATGAAGTGACTG 3'	This study
13	cRv3031-RL-BstAPI	5' TTTTTGCATAGATTGCATGAACACGTCCGCAAGCCCGGT G 3'	This study
14	cRv3031-RL2-BstAPI	5' TTTTTGCATAGATTGC-GTGCCCGGCCTGTTCACGCTTGT 3'	This study

15	cRv3031-LR-BstAPI	5' TTTTTGCATTTCTTGC-TCAAGGCCGCACCGCGATCGCGATC 3'	This study
16	cRv3031-LR2-BstAPI	5' TTTTTGCATTTCTTGC-CGGGCTTGCGGACGTGTTCAAGG 3'	This study
17	cRv3031-LL	5' TTTTTGCATAAATTGC-CGGGTTAGCCTGCCTTAACAATG 3'	This study
18	MSmeg2349-LL	5' GGTTTCACAAAGTG-ATGAGCGCAATCGTGGGCGATCC 3'	This study
19	MSmeg2349-LR	5' GGTTTCACTTCGTGTCA-CCGCACTGCTATCGCCACGAG 3'	This study
20	MSmeg2349-RL	5' CCTTTCACAGAGTG-ATGACGGACGCGAGCGCAGAAC 3'	This study
21	MSmeg2349-RR	5' GGTTTCACCTTGTG-TCATCGCGGGAGCC 3'	This study
22	MSMEG_6396-99_int1-EcoNI	5' GACGGGTTCAACGTGCCCGAAAG 3'	This study
23	MSMEG_6396-99_int2-EcoNI	5' TGGTTCCTCAACTCGGGCATCTCC 3'	This study
24	MSMEG_6396-99-ext-5-EcoRI	5' TTTTTGAATTCCTTCGCCTGACGCGGTCGATAGAAG 3'	This study
25	N Terminal His Tag Rv3031- 1 Forward	5' TATCCATATGAACACGTCCGCAAGCCC 3’	This study
26	N Terminal His Tag Rv3031- 2 Forward	5' TATCCATATGCCCGGCCTGTTCACGCTTGTTC 3'	This study
27	N Terminal His Tag Rv3031 Reverse	5' TATCCTCGAGTCACTTGGGCAGCCTCC 3'	This study
28	C Terminal His Tag Rv3031- 1 Forward	5' TATCCATATGAACACGTCCGCAAGCCC 3’	This study
29	C Terminal His Tag Rv3031- 2 Forward	5' TATCCATATGCCCGGCCTGTTCACGCTTGTTC 3'	This study
30	C Terminal His Tag Rv3031 Reverse	5' TATCCTCGAGCTTGGGCAGCCTCCGAGCGTCCAG 3'	This study

MATERIALS AND METHODS

(Adapted from manuscripts)

Bacterial strains and growth conditions

All Mycobacterial strains were grown at 37˚C either in Middlebrook 7H9 complete medium supplemented with ADS (Bovine albumin serum fraction, glucose, NaCl), 0.5% (w/v) glycerol and 0.05% Tyloxapol or on 7H10 agar medium supplemented with ADS and 0.5% (w/v) glycerol unless otherwise stated. Antibiotics for selection were used in specific concentrations: Hygromycin (50 mg/l), Apramycin (40 mg/l) and Kanamycin (40 mg/l). *Mtb* strains were also grown in minimal medium containing 0.15 g L-Asparagine.H_2O, 0.5 g $(NaH_4)_2SO_4$, 1 g KH_2PO_4, 2.5 g Na_2HPO_4, 50 mg Ferric ammonium citrate, 0.5 g $MgSO_4$.7 H_2O, 0.5 mg $CaCl_2$, 0.05% (v/v) Tyloxapol and 0.1 mg $ZnSO_4$, dissolved in 1L H_2O (pH 7.0). The 7H9 minimal medium contains only Middlebrook 7H9 and 0.05% Tyloxapol. For proteomic profiling, *Mtb* strains were grown in Middlebrook 7H9 medium supplemented with 0.5% glycerol, 0.2% glucose, 0.085% sodium chloride, and 0.05% Tyloxapol. *E. coli* strains were grown in LB broth containing tryptone, yeast extract and sodium chloride.

Generation of targeted gene deletion in *Mtb*

***Polymerase chain reaction*:**

The primers for allelic exchange substrate plasmid are designed as described in [45] and [46]. The upstream and downstream flanking regions were amplified by Polymerase Chain Reaction. The same conditions can be utilized to amplify any region of genomic DNA, plasmid DNA or a previously amplified PCR product.

Reagents	**Amount**	**PCR Conditions**	**Temperature**	**Time**	
Premix J/H (Lucigen)	25 µl	*Initial denaturation*	98 ºC	5 minutes	
DNA	5 µl	*Denaturation*	98 ºC	30 seconds	**25-30 CYCLES**
Forward Primer	0.5 µl	*Annealing*	52-70 ºC	30-60 seconds	
Reverse Primer	0.5 µl	*Extension*	72 ºC	15-30 seconds per kb	
Water	18.5 µl	*Final Extension*	72 ºC	10 minutes	

Polymerase enzyme	0.5 µl	*Final temperature* 4 ºC ∞	
Total Volume	**50 µl**		

***Purification of PCR products*:**

The PCR samples are mixed with Buffer NTI in the ratio of 1:2 i.e. for every 100 µL PCR reaction add 200 µL Buffer NTI. NucleoSpin® PCR Clean-up Column was placed into a collection Tube and a volume of up to 700 µL of the mixed sample was added to the column. The collection tube containing column was then centrifuged for 1 minute at 14000 rpm and the flow-through was discarded. if there are any remaining samples left, they are added to the column and centrifugation is repeated. To the NucleoSpin® Gel and PCR Clean-up Column, Buffer NT3 (wash buffer containing ethanol) of 700 µL was added followed by centrifugation for 1 minute at 14000 rpm. The flow-through was discarded and the column was placed back into the collection tube. In order to dry the silica membrane, the empty column with the collection tube was centrifuged for 10 minutes at 14000 rpm. The column was then placed into a 1.5 mL microcentrifuge tube and 50 – 70 µL of elution Buffer NE was added and incubated at room temperature for 1 - 2 minutes. The tubes were then centrifuged for 2 minutes at 14000 rpm. The flow through was collected into the microcentrifuge tube and the concentration of the DNA was measured by using Nano drop instrument.

Agarose gel electrophoresis and purification of products from gel:

0.7-1 % agarose gels are made and in order to check for amplification 10 µl of the PCR product mixed with 2 µl of loading dye is delivered to the wells. Gels are run at 100-120 constant voltage. In order to extract specific products of given size, the total volume of the reaction is delivered to the well and the gels are run. After viewing, using a gel cutter, the specific products are cut and stored in a microcentrifuge tube which is then mixed with NTI buffer. For every 100 mg of agarose gel, 200 µL Buffer NTI was mixed and heated until all the gel particles are dissolved in the buffer (typically 5–10 minutes at 50 °C). NucleoSpin® Gel Clean-up Column was placed into a 2 ml collection Tube and a volume of up to 700 µL of the dissolved sample was added to the column. The collection tube was then centrifuged for 1 minute at 12000 rpm and the flow-through was discarded. If there are any remaining volumes left, they are added to the column and centrifugation is repeated. To the column, Buffer NT3 (wash buffer containing ethanol) of 700 µL

was added followed by centrifugation for 1 minute at 14000 rpm. The flow-through was discarded and the column was placed back into the collection tube. In order to dry the silica membrane, the empty column with the collection tube was centrifuged for 10 minutes at 14000 rpm. The column was then placed into a 1.5 mL microcentrifuge tube and 50 –70 µL of elution Buffer NE was added and incubated at room temperature for 1 - 2 minutes. The tubes were then centrifuged for 2 minutes at 14000 rpm. The flow through was collected into the microcentrifuge tube and the concentration of the DNA was measured by using Nano drop instrument.

Digestion of the DNA fragments:

5 - 10 µl of the purified PCR product or a purified plasmid DNA was digested with appropriate restriction enzyme overnight at recommended temperature in a total volume of 50 µl (usually 1 µl - restriction enzyme, 5 µl - restriction buffer and remaining volume with water). The vector differs for every plasmid designed and depends upon whether a Knockin or Knock out is required. For knockout, the gene to be deleted is replaced with the Hygromycin cassette and for a knock in, a Tet operon is placed in the front for the gene to regulate its expression [47]. The digested products were run on an agarose gel and the expected products are cut and purified from the gel. The vector fragment contains “hygromycin/SacB fragment - OriE fragment” or “tet operators - hygromycin/SacB fragment-OriE fragment” which is then ligated with the digested PCR products to generate a Knockout or a Knockin plasmid respectively.

Ligation of the DNA fragments and Transformation of the plasmid into E. coli:

The digested vector fragment and PCR products are ligated using T4 DNA ligase in a total volume of 20 µl (2.5 µl 10X ligation buffer, 1.5 µl T4 DNA ligase, 10 µl insert PCR product, 6 µl vector) for overnight incubation at room temperature. The NEB 5-alpha Competent *E. coli* cells were incubated on ice for 10 minutes. 2-10 µl of plasmid DNA was added to the competent cell mixture and the tube is flicked 5-6 times so that the cells and DNA are mixed well. The competent cells with plasmid DNA are incubated on ice for 40 minutes. After then, the cells are given heat shock at 42°C for 40 seconds and immediately kept on ice for 5 - 10 minutes. 200 µl of SOC medium was then added to the mixture and incubated at 37°C for 60 minutes. The cells were then plated on warmed selection plates and incubated overnight at 37°C.

Construction of phasmids:

After verifying the AES plasmids by sequencing and diagnostic PCR, the plasmid DNA was digested with PacI restriction enzyme at 37ºC overnight. The shuttle vector phAE159 (10-20 µg) was also digested with PacI. Following PacI digestion, 0.5µl of SAP was added for 30 minutes at 37ºC followed by heat inactivation. The digested products are run on the agarose gel and the required fragments are cut and purified using the Gel Clean up Kit. The ligation reaction included 4 – 8 µl phAE159, 8-12 µl plasmid DNA, 2 µl 10X T4 ligase buffer and 2 µl T4 DNA Ligase enzyme incubated overnight at room temperature.

Packaging of phasmids:

5 – 10 µl of the ligation mixture was added to the 25 µl MaxPlax packaging extract and mixed gently. The mixture is incubated at room temperature for 2 hours. Later, the reaction was stopped with 400µl MP (Mycobacteriophage) buffer and incubated for 30 minutes at room temperature. To this mixture, 1 ml HB101 host cells was added and incubated for 1 hour at 37ºC. The cell mixture was then centrifuged at 13000 rpm for 1 minute. The supernatant was discarded and the pellet was re-suspended in 200 µl fresh LB media. The cells were then plated on LB plates containing Hygromycin and incubated overnight at 37ºC. 5-10 colonies were picked and grown on LB medium and the phasmids are verified by sequencing and diagnostic PCR.

Preparation of E. coli HB101 for phasmid packaging:

E. coli HB101 cells were cultivated overnight at 37°C in LB medium supplemented with 10 mM $MgSO_4$, and 0.2% maltose. Next day, 500 µl of cultivated wells were added to 25 ml of fresh LB medium and incubated at 200 rpm at 37°C until OD_{600} reaches 0.8-1.0. The cells were then centrifuged at 4000 rpm at 4°C for 15 minutes. The supernatant is discarded and the pellet is resuspended in 12.5 ml ice-cold 10 mM $MgSO_4$.

Generating Phages by electroporation:

25 - 50 ml culture of *M. smegmatis* mc^2155 were cultivated in Middlebrook 7H9 medium until the OD at 600nm reaches 0.5 to 1.0. The cells were incubated on ice for 30 minutes and then washed twice with ice-cold 10% glycerol by centrifugation for 10 minutes at 4000 rpm at 4˚C. The supernatant was discarded and cell pellet was finally resuspended in ice-cold 10% glycerol $1/10^{th}$ culture volume. Phasmid DNA (5 to 10 µl) to be electroporated was transferred into an electroporation cuvette which contains 400 µl of the cell suspension. The cells were pulsed once with a GenePulser electroporator with conditions of 2500V, resistance 1000 Ω, and capacitance

25 µFD. After the electroporation, cell mixture was transferred to microcentrifuge tube containing 1 ml 7H9 medium and incubated for 1-2 hours at 37°C. The cells were either plated on 7H10 plates containing appropriate antibiotics or diluted in following ways. Dilution 1: 300µl transformed mc^2155 cells are added to 300 µl actively growing mc^2155 cells. Dilution 2: 200µl transformed mc^2155 cells are added to 1ml actively growing mc^2155 cells. 400µl of previous dilutions 1 and 2 were mixed with separately 7ml top agar, mixed and plated onto pre-warmed 7H10 plates. The plates were incubated at 30ºC for 3 days.

Preparation of high titer phages:

The plaques were cut into 200 µl MP buffer to recover phages and incubated at 37°C for 4 hours then store at 4ºC. After recovering phages, they are mixed with mc^2155 cells in following dilutions. Dilution 1: 10 µl of phages from above were added to 300µl mc^2155 culture cells resuspended in MP buffer. Dilution 2: 5 µl of phages from above were added to 300µl mc^2155 culture cells resuspended in MP buffer. Dilution 3: 1 µl of phages from above were added to 300µl mc^2155 culture cells resuspended in MP buffer. 400µl of previous dilutions were mixed with separately 7ml top agar, mixed and plated onto pre-warmed 7H10 plates. The plates were incubated at 30ºC for 3-4 days. The plates with the higher number of phages are selected and 5ml MP buffer were added onto the plates. The plates with MP buffer were incubated overnight at 4º C and the phage lysate was harvested. The phage lysates were purified twice using 0.2 µm filters.

Phage transduction:

Before transduction, a 10 ml culture of *Mtb* strain were cultivated to an OD 0.8 to 1.0 at 600nm. The culture was centrifuged for 15 minutes at 4000 rpm at 4˚C. The supernatant was discarded and the pellet was resuspended with 10 ml Mycobacteriophage wash medium. This is followed by centrifugation for 15 minutes at 4000 rpm and the supernatant is discarded. The washing step was repeated again. The pellet was resuspended in 1 ml MP buffer. 1 ml of phages was warmed at 37˚C and mixed with 1 ml cells in MP buffer. The cells and phages are mixed gently and incubated overnight at 37˚C. Next day, the cells were centrifuged for 15 minutes at 4000 rpm at 4˚C and the pellet was resuspended in 200 µl 7H9 medium. The cells were plated on selection plates and incubated for 3 to 4 weeks at 37˚C.

Construction of Merodipolid strain

A Merodipolid strain with an additional copy of trehalose recycling transporter, LpqY-SugC (Rv1235-1238) in *Mtb* genome was generated by electroporating Pmv306(Kan)Rv1235-1238 integrating plasmid (1000Ω, 25μF, 2500V) into *Mtb* H37Rv wild type strain. This additional copy of the gene compensates for any inhibited or suppressed Rv1235-1238 gene functions in spontaneous resistant mutants.

***Mtb* Genomic DNA extraction and Whole genome sequencing**

Mtb strains and spontaneous resistant mutants were cultured in 7H9 complete medium and the genomic DNA was extracted using CTAB-lysozyme method. Briefly, the cultures were pelleted and incubated with 9:1 mixture of GTE (50 mM Glucose, 25 mM Tris.Cl, 10 mM EDTA) and lysozyme solution (10mg/ml) overnight at 37˚C. Next day, 150 μl of 2:1 solution of 10% SDS and 10mg/ml proteinase K was added and incubated for 30 minutes at 55˚C. Then, 200 μl of 5M NaCl was added and mixed gently. 160 μl of preheated CTAB (cetrimide – hexadecyltrimethylammonium bromide in water) was added and mixed gently followed by incubation for 10 minutes at 65˚C. Then equal volume of 24:1 (v/v) chloroform/isoamyl alcohol was added and mixed vigorously and then centrifuged for 5 min. Aqueous layer was then transferred to fresh microcentrifuge tube and the previous step is repeated again to get rid of residual organic phase. 560 μl of 70% isopropanol was then added to the aqueous layer for precipitating the genomic DNA. This step is followed by incubation for 5 minutes and then centrifugation for 10 minutes. The pellet is then washed with 70% ethanol, air dried and resuspended in water. The concentration of the genomic DNA was measured using AccuClear® Ultra High Sensitivity dsDNA Quantitation kit. 50 ng of genomic DNA was used for whole genome sequencing. Whole genome sequencing was performed using Illumina MiSeq Next Generation Sequencer. The DNA was sequenced with genome coverage of approximately 60 – 80-fold with a read length of 2 x 250 bp using MiSeq Reagent kit v2 (500 cycles) from Illumina.

Resazurin microplate assay (REMA) for growth quantification

Trehalose and Glucose dependent growth of *Mtb* strains were quantified using a phenoxazine dye, Resazurin. Cells were grown in the minimal medium containing 8 different concentrations, from 0 mM to 5 mM, of Trehalose and glucose in a total volume of 100 μl and incubated at 37˚C for 5 days. After 5 days, Resazurin solution (10 μl/well from 100 μg/ml, Sigma-Aldrich) was added to the cells and incubated overnight at room temperature for reduction of resazurin to resorufin by aerobic respiration of metabolically active cells. Next day, *Mtb* cells were inactivated by

incubating with 10% formalin for 30 minutes at room temperature. The fluorescence (excitation 560 nm, emission 590 nm) was measured using a microplate reader (TECAN). The antibiotic susceptibility test for various mycobacterial strains and the ATC dependent growth of the conditional mutants were also determined using Resazurin assay.

Metabolic labelling of Mycobacteria

All *Mtb* strains were grown in Middlebrook 7H9 complete medium supplemented with ADS (Albumin fraction, glucose, NaCl), 0.5% (w/v) glycerol and 0.05% Tyloxapol in a square bottle until the OD600 reaches ~0.8. 50 µl from the stock culture was added to 950 µl Middlebrook 7H9 complete medium containing 100 µM 6-TreAz in a 1.5 ml screw cap tube and incubated for 3 days at 37˚C. After 3 days, the cells were centrifuged at 13000 rpm for 5 minutes and the supernatant was discarded. The cells were then washed twice with 1x PBS containing 0.5% bovine serum albumin (PBSB) by centrifugation. After the washing step, the cells were incubated with 1 ml from 1:500 dilution of 1 mM Alexa Fluor 488 DIBO Alkyne stock solution in DMSO (ThermoFisher Scientific) at room temperature for 45 minutes in dark. Then, cells were washed again with PBSB twice and inactivated with 4% paraformaldehyde for 60 minutes at room temperature. The inactivated cells were washed with PBS and the final pellet is resuspended in 100 µl PBS. The cells are then prepared for measuring Mean fluorescence intensity (MFI) using Flow cytometry. Flow cytometry was performed on BD LSRFortessa™ cell analyzer. MFI data was collected for 50,000 cells for each sample and processed using FlowJo (Tree Star).

Proteome analysis of mycobacterial strains

Mtb strains were grown in 20 ml Middlebrook 7H9 medium supplemented with 0.085% NaCl, 0.2% Glucose, 0.5% Glycerol and 0.05% Tyloxapol at 37˚C. Cells were centrifuged at 4500 g, 4˚C for 10 minutes. Cells were washed with 1X PBS thrice and the final pellet was resuspended in 1/10 volume of the culture. The cells were then lysed by bead-beating using 100 µm silica-zirconium beads three times (QIAGEN TissueLyser LT). SDS was then added to the cells to a final concentration of 1%. After mixing thoroughly, the cells were incubated at 4˚C for 30 minutes to solubilize membrane proteins followed by centrifugation at 13,000 g at 4˚C for 5 minutes to obtain clear lysate. The supernatant was then collected as protein solution and filter sterilized through 0.2 µm cellulose acetate spin filter thrice. The protein concentration was measured by BCA assay. The filtered protein was pellet dried by nitrogen stream and stored at -80˚C.

Extraction and TLC analysis of Mycolic Acid Methyl Esters (MAMEs)

10 mL liquid culture of each mycobacterial strain to be analyzed were grown in 7H9 complete medium supplemented with ADS (Albumin fraction, glucose, NaCl), 0.5% (w/v) glycerol and 0.05% Tyloxapol in a square bottle until the OD600 reaches ~0.8. This was followed by centrifugation for 10 minutes at 4000 rpm at room temperature. The pellet was washed with 1XPBS twice and dried with nitrogen flow. The fatty dry mass of the pellet was weighed into Pyrex glass tube and then 7 mL $CHCl_3$: MeOH (2:1) was added to the pellet and shaken over night at room temperature. Next day, the mixture was centrifuged for 15 minutes at room temperature at 4000 rpm. The pellet was dried using nitrogen flow and the supernatant was stored for the analysis of free lipids. The pellet weight was measured again. 2 mL 15 % TBAH (tetra butyl ammonium hydroxide solution in water) was added to the pellet weighing 50 mg, in case of higher mass, volume of TBAH is increased and heated overnight at 100°C. Next day, the mixture was allowed to cool for 1-2 hours and then to the mixture following were added: 2 mL H_2O, 1 mL CH_2Cl_2 and 250 µL CH_3I (Iodo-methane). The mixture of compounds was shaken for 30 minutes at room temperature and then centrifuged at room temperature for 1 hour 4000 rpm. The upper water phase was discarded and the Organic phase was collected into an HPLC vial. After evaporating the organic solvent, Mycolic acids Methyl Esters were dissolved in 125 µL Dichloromethane. Different concentrations of MAMES were spotted onto a preheated (60°C) TLC silica 60 plate (10 µL). The mixture of 95:5 petroleum spirit: diethyl ether was used as a solvent. TLC plate was then dipped into a saturated chamber. TLC plate was stained with 5% molybdato phosphoric acid in EtOH and the plate was immersed completely into the solution so that the whole plate is stained uniformly. The TLC plate was then incubated in the heating compartment 110°C for 30 minutes.

Plasmid DNA isolation

The *E. coli* cells are resuspended in 250 µL Resuspension Buffer A1 and ensured that the cells are completely resuspended. 250 µL Lysis Buffer A2 was added to the cells and gently mixed by inverting the tube 4–6 times. The cells are then incubated for 5 minutes at room temperature. 300 µL of Neutralization Buffer A3 was added to the cell mixture and mixed thoroughly until blue samples turn white or colorless. The cells are centrifuge for 10 min at 14,000 rpm at room temperature. NucleoSpin® Plasmid Column was placed in the collection tube and the supernatant from previous step was transferred to the column followed by centrifugation at maximum speed for 1 minute. The flow through was discarded. The column was loaded with remaining volumes of supernatant and centrifuged. The column was washed with 700 µL wash buffers AW and A4 containing ethanol. The column was dried by centrifugation for 10 minutes at maximum speed.

The collection tube was then places in a 1.5 mL microcentrifuge tube and 50 - 100 µL elution Buffer AE or distilled water was added to the column. The microcentrifuge tube was then incubated for 5 minutes at room temperature and centrifuged for 1 min at 14,000 rpm. The flow through was collected and the concentration was measured using NanoDrop.

Protein expression

The Rosetta strains expressing our genes of interest (in pET vector) was inoculated into 5 mL of LB liquid medium containing the selection antibiotic and placed in shaking incubator at 37°C until the OD at 600 nm reaches 0.5 to 0.8. Once the OD reached 0.8, 2 ml of the culture was collected in a 2-mL microfuge tube. The cells were centrifuged and the supernatant was discarded. The cells are labelled as un-induced samples and stored at -20 ºC. 3 µL of 1 M IPTG was added to the culture and continued to grow them overnight at a temperature of 23 ºC. The OD was measured the next day and the pellet is collected for induced samples and stored at -20 ºC.

SDS polyacrylamide Gel electrophoresis

For each strain, 1 tube of un-induced and 1 tube of induced cells were resuspended in 100 µL of 2x SDS-PAGE sample buffer. The samples were incubated at 99 ºC for 10 minutes and cooled down to room temperature. The samples were then centrifuged for 3 minutes at 14000 rpm and 10 µL of each sample was delivered to each well of the polyacrylamide gel.

Chapter – 3

Rv3136 - PPE51 Sugar transporter

Mycobacterium tuberculosis utilizes PPE51 for transport of trehalose molecules across the mycomembrane.

1. Aim and detailed Abstract
2. Manuscript prepared
3. Figures and Supplementary materials

Percentage of contribution to the manuscript: 70%

1. Complete manuscript was written together with figures and supplementary materials
2. ΔPPE51 deletion strain – Whole genome sequencing
3. Generation of PPE51 Complemented strain
4. Metabolic labelling: Copper dependent and independent click chemistry of Δppe51
5. Concentration dependent growth of the ΔRv3136 deleted strain in the minimal medium with and without carbon sources (Trehalose and glucose)
6. Time dependent growth of the ΔRv3136 deleted strain in the minimal medium with and without carbon sources (Trehalose and glucose)
7. Proteomic profiling of the PPE51 deleted and complemented strain.

Mycobacterium tuberculosis utilizes PPE51 for transport of trehalose molecules across the mycomembrane

Mohammed Rizwan Babu Sait[1], Hendrik Koliwer-Brandl[1], Benjamin Swarts[2], Marc Jacobsen[3], Thomas R. Ioerger[4], Rainer Kalscheuer[1*]

[1] Institute of Pharmaceutical Biology and Biotechnology, Heinrich Heine University, 40225 Düsseldorf, Germany.

[3]Department of Chemistry and Biochemistry, Central Michigan University, Mount Pleasant, Michigan 48859, USA.

[3] Department of General Pediatrics, Neonatology, and Pediatric Cardiology, University Children's Hospital, Heinrich Heine University, 40225 Düsseldorf, Germany.

[4] Department of Computer Science, Texas A&M University, College Station, Texas 77843, USA.

***Correspondence:**
Prof. Dr. Rainer Kalscheuer
Rainer.Kalscheuer@hhu.de

Detailed Abstract (adapted from manuscript)

The unique cell membrane of *Mycobacterium tuberculosis (Mtb)* consists of mycolic acids, various polysaccharides, glycolipids and membrane transporter proteins. In this study, we describe one of the membrane proteins, PPE51, that transports exogenous trehalose sugars across mycomembrane. PPE51 has already been characterized for the uptake of glucose, glycerol and few other disaccharides but not trehalose. Trehalose, being one of the important compounds for the growth of *Mtb*, we were interested in understanding the route of uptake of extra cellular trehalose. 6-Azido trehalose was used as a labelling analog with an optimal concentration of about 25-150 µM. However, there have been previous studies showing that this compound inhibited the growth of fast growing mycobacterial species such as *Mycobacterium Smegmatis* and *Mycobacterium aurum* at concentrations greater than 500 µM. So we tested our laboratory virulent

strain H37Rv wildtype against this compound at various concentrations ranging from 100-2000 µM. We observed growth inhibition at a concentration of 1 mM. We also tested the wildtype strain that lacked ΔLpqY-SugC (Rv1235-1238) which codes for the transporter in the inner membrane that recycles the free trehalose, generated during the synthesis of trehalose mycolates, back to the cytoplasm. This deletion strain grew well on the medium containing 1 mM 6-Azido trehalose highlighting the fact that the 6-Azido trehalose did not enter the cytoplasm and was not converted to trehalose mycolates. We utilized the *Mtb* inhibitory concentrations of 6-Azido trehalose to derive spontaneous resistant mutants from the background wildtype merodiploid strain containing an additional copy of the ΔLpqY-SugC (Rv1235-1238) that can compensate for the lost function when generating the spontaneous resistant mutants. From whole genome sequencing, we observed that the mutations occurred in one of the proline-proline-glutamate (PPE) family, PPE51 (Rv3136). Complementation of the spontaneous resistant mutants with Rv3136 restored the growth inhibition. When the PPE51 deletion strain was cultivated with 6-Azido trehalose at optimal labelling concentration for biorthogonal labelling with AF488DIBO, they displayed lower mean fluorescence intensity when compared to that of wild type explaining that the deleted strain did not allow the intake of trehalose and thus not allowing the synthesis of modified trehalose mycolates. Also, the PPE51 deleted strain was not able to grow in the minimal medium with and without both glucose or trehalose carbon sources. Taken together, the results would provide insights into understanding the extra cellular trehalose transportation in *Mtb*.

Mycobacterium tuberculosis utilizes PPE51 for transport of trehalose molecules across the mycomembrane

Mohammed Rizwan Babu Sait[1], Hendrik Koliwer-Brandl[1], Benjamin Swarts[2], Marc Jacobsen[3], Thomas R. Ioerger[4], Rainer Kalscheuer[1*]

[1] Institute of Pharmaceutical Biology and Biotechnology, Heinrich Heine University, 40225 Düsseldorf, Germany.

[2] Department of Chemistry and Biochemistry, Central Michigan University, Mount Pleasant, Michigan 48859, USA.

[3] Department of General Pediatrics, Neonatology, and Pediatric Cardiology, University Children's Hospital, Heinrich Heine University, 40225 Düsseldorf, Germany.

[4] Department of Computer Science, Texas A&M University, College Station, Texas 77843, USA.

***Correspondence:**

Prof. Dr. Rainer Kalscheuer

Rainer.Kalscheuer@hhu.de

Abstract

The disaccharide trehalose is essential for viability of *Mycobacterium tuberculosis*, which synthesizes trehalose *de novo* but can also utilize exogenous trehalose. The mycobacterial cell wall encompasses two permeability barriers, the cytoplasmic membrane and the outer mycolic acid-containing mycomembrane. The ABC transporter LpqY-SugA-SugB-SugC has previously been demonstrated to mediate the specific uptake of trehalose across the cytoplasmic membrane. However, it is unknown how transport of trehalose across the mycomembrane is mediated. In this study, we harnessed the antibacterial activity of the analogue 6-azido trehalose to select for spontaneous resistant *M. tuberculosis* mutants in a merodiploid strain harbouring two LpqY-SugA-SugB-SugC copies. Mutations mediating resistance to 6-azido trehalose mapped to the proline-proline-glutamate (PPE) family member PPE51 (Rv3136), which has recently been shown to be an integral mycomembrane protein involved in uptake of low-molecular weight compounds. A site-specific *ppe51* gene deletion mutant of *M. tuberculosis* was unable to grow on trehalose as the sole carbon source. Furthermore, bioorthogonal labelling of cells of the *M. tuberculosis* Δ*ppe51* mutants incubated with 6-azido trehalose corroborated the impaired internalization. Taken together, the results indicate that the transport of trehalose and trehalose analogues across the mycomembrane of *M. tuberculosis* is exclusively mediated by PPE51.

Introduction

Tuberculosis (TB) is among the major infectious diseases that affects several million people every year. According to World Health Organisation TB reports 2019, there are 1.5 million deaths every year due to TB [1]. TB is caused by *Mycobacterium tuberculosis (Mtb)*, a human pathogen that belongs to the class of actinobacteria [2].

The *Mtb* cell envelope consists (from inside to outside) of the cytoplasmic membrane, the mycolyl-arabinogalactan-peptidoglycan layer (mAGP), the mycolic acid layer and a capsular layer mainly comprising α-glucan glycoconjugates. The envelope confers physical robustness and protection against physicochemical stress and is also important for virulence of the bacteria [3]. The mycolic acids are long chain α-branched β-hydroxy fatty acids that are either covalently bound to arabinogalactan, which in turn is linked to peptidoglycan, or esterified to sugars such as trehalose to give rise to the glycolipids trehalose monomycolates (TMM) or trehalose dimycolates (TDM) [4]. Many components in the biosynthetic pathways of mycolic acids represent lucrative drug targets. TDM, also known as cord factor, is essential for the growth and survival of *Mtb*. TDM provides virulence, stimulates host immune response and contributes to the interception of phagosomal maturation inside macrophages. The arabinogalactan-bound mycolates form the inner leaflet and the mycolate-containing glycolipids the outer leaflet of a lipid bilayer-like structure known as the mycomembrane with structural resemblance to the outer membrane of Gram-negative bacteria. The mycomembrane represents an efficient permeability barrier that contributes to the high intrinsic resistance of *Mtb* towards many antibiotics [5].

Trehalose is crucial for the composition of mycobacterial cell envelope. *De novo* biosynthesis of trehalose in mycobacteria occurs through the OtsA-OtsB2 and the TreY-TreZ pathway [6][7]. TMM is synthesized in the cytoplasm by 6-O-mycoloylation of trehalose catalysed by Pks13 and are then transported to the mycomembrane through the Mycobacterial Membrane Proteins Large3 (MmpL3) transporter [8]. In the mycomembrane, the mycolic acid moiety from one TMM molecule is either transferred to another TMM molecule forming TDM, or it is transferred to arabinogalactan polysaccharides forming arabinogalactan linked mycolates.

These transfers are catalysed by the Antigen 85 (Ag85A, Ag85B, and Ag85C) complex leading to the concomitant release of free trehalose. The free trehalose molecules are then recycled back to the cytoplasm through the LpqY-SugA-SugB-SugC ABC transporter located in the cytoplasmic membrane [9]. In addition to intrinsic *de novo* formation, *Mtb* can also utilize exogenous trehalose. Some flexibility regarding substrate specificity in the enzymatic machinery involved in trehalose uptake and metabolism also allows internalization of several synthetically altered trehalose analogues in a LpqY-SugA-SugB-SugC dependent manner and their subsequent metabolism and incorporation into the mycomembrane. These altered trehalose analogues might harbour structural modifications that allow conjugation with fluorescence probes for *Mtb* detection, which can be exploited for the rapid diagnosis of live mycobacteria [10]. This metabolic labelling is based on the principle of bio-conjugation, also called bioorthogonal chemistry [11]. However, while the LpqY-SugA-SugB-SugC ABC transporter exclusively mediates the uptake of trehalose across the cytoplasmic membrane, the route of trehalose transport across the mycomembrane is still unclear.

In this study, we made use of the growth inhibitory properties of 6-TreAz, which has anti-mycobacterial activity at high concentration [12], for the isolation of spontaneously resistant mutants to identify genes potentially involved in its uptake and metabolism. This led to the identification of a member of the proline-proline-glutamic acid (PPE) family proteins that is responsible for the uptake of extra cellular trehalose in *Mtb*. The *Mtb* genome contains about 7% - 10% of conserved Proline-Glutamic acid (PE) and PPE motifs at N-terminal of the proteins. There are 99 PE proteins encoding genes and 69 PPE proteins encoding genes in the genome of the laboratory strain of *Mtb* H37Rv [13]. Gey van Pittius and co-workers have reported that PE/PPE family of proteins evolved together with the ESX regions of *Mtb* [14]. PE/PPE proteins have been reported to be involved in antigen presentation, macrophage activation, interact with other bacteria and communication with members of the host immune system. It has also been shown that these proteins accumulate near the poles or localize on the surface of *Mtb* contributing to specific functions with respect to ESX5 type VII secretion system [15]. Very recently, it has been shown that PPE51 is responsible for transporter of

glucose, maltose and glycerol across mycomembrane [16][17]. In this study, we investigated the uptake of trehalose through the PPE51 mycomembrane transporter.

RESULTS

6-Azido trehalose inhibits *Mtb* growth at higher concentrations

TMM is produced by 6-O-mycolylation of trehalose in the cytoplasm and is transported to mycomembrane where it is used to generate TDM with a release of free trehalose. Differently modified trehalose analogs can also be taken up by *Mtb* and can undergo mycolylation. These modified TDMs and TMMs can be metabolically incorporated in the mycolic acid cell wall layer, the so-called mycomembrane. Modifications can occur at different positions of the trehalose molecule. 6-Azido trehalose (6-TreAz) has an azide group (N_3) at the sixth carbon position of one of the glucose moieties in trehalose and has been used to label *Mtb* species (Figure 1a). At concentrations ranging from 25-150 µM it can be used as a vital biorthogonal marker to label mycobacterial cells after conjugation with fluorescent moieties via click chemistry. However, when incubated with increased concentrations, i.e. >1 mM, we found that it inhibits growth of *Mtb* wild-type strain H37Rv on 7H10 solid medium (Figure 1b). To further analyze this growth inhibition, we also tested the *Mtb* Δ*lpqY-sugC* mutant that lacks the complete LpqY-SugA-SugB-SugC (Rv1235-1238) ABC transporter, which recycles back the free trehalose that is produced by the antigen 85 complex when using TMM as the substrate. The Δ*lpqY-sugC* deletion strain was able to grow on 7H10 solid medium containing 1 mM 6-TreAz (Figure 1b). This highlights that the antibacterial effect of 6-TreAz is uptake-dependent and that LpqY-SugA-SugB-SugC not only tolerates trehalose but also 6-TreAz as a substrate. The growth inhibition of wild-type strain H37Rv by 6-TreAz could result from the lack of TDM in the mycomembrane as *Mtb* could not conjugate the additional mycolic acid to TMM because the 6´ position is occupied by the azide group.

Spontaneous resistant mutants reveal a candidate responsible for extra cellular trehalose uptake in *Mtb*

In order to identify genes potentially involved in transport and metabolism of trehalose in *Mtb*, we isolated spontaneous resistant mutants after growth on 6-TreAz containing solid medium. In order to avoid isolating clones with loss-of-function mutations in the LpqY-SugA-SugB-SugC ABC transporter, which we have already shown to mediate 6-TreAz resistance, we employed a merodiploid strain that contains an additional copy of the *lpqY-sugC* gene cluster (Rv1235-1238) in its genome, which was generated by electroporating the integrative plasmid pMV306(Kan)::Rv1235-1238 into wild-type H37Rv (Supplementary figure 1). This additional copy of the gene cluster would compensate for any loss of function mutations in the endogenous locus and will minimize the chance of resistant mutants occurring from mutations in this gene cluster. After four weeks of incubation, 6-TreAz spontaneous resistant mutants were obtained at a frequency of 10^{-7} (Figure 2 a-b). Whole genome sequencing of five selected clones revealed that independent non-synonymous mutations in *ppe51* (Rv3136) have occurred in three 6-TreAz-resistant mutants (nucleotide 661 T→C, Leu204Pro; 41 G→C, Arg14Pro; 280 G→A, Ala94Thr) (Table 1). The two other spontaneous resistant clones harboured a non-synonymous mutation in the *eccC5* gene (Rv1783) (nucleotide 3278 C→A, Pro1093Gln). All clones except one *ppe51* mutant harboured additional mutations in different genes involved in phthiocerol dimycocerosate (PDIM) biosynthesis (*ppsA*, *ppsB*, *fadD26*; Table 1). We also generated complemented strains for these spontaneous resistant mutants recombinantly expressing wild-type copies of *eccC5* or *ppe51*, to check for their resistance on medium containing 6-TreAz and we observed that the growth of the resistant mutants was at least partially impaired (Supplementary Figure 2 a-b). These results indicate that the observed resistance phenotype could be clearly attributed to *ecc5* or *ppe51*. PPE protein family members have been shown to participate in uptake of nutrients through *Mtb* cell envelope, and PPE51 has been referred to as a mycomembrane-associated protein [18]. From previous studies it has been shown that $EccC_5$, an ATP-binding protein belonging to the FtsK/SpoIIIE-like protein family, is required for secretion of ESX-5 specific substrates [19]. Further, it was shown that numerous PE and PPE proteins are secreted in an ESX-5-dependent manner in *Mycobacterium marinum* [20]. These findings suggest that PPE51 could be a potential

gateway for the uptake of exogenous trehalose across the mycomembrane. The observed mutation in EccC5 might impair the ESX-5-mediated secretion of PPE51 and/or its proper translocation and insertion into the mycomembrane.

To further analyze the function of PPE51 in trehalose uptake, we generated a site-specific gene deletion mutant in *ppe51* (Rv3136) using the specialized transduction method as described previously [21][22]. The Δ*ppe51* deletion strain was subjected to whole genome sequencing to confirm its genotype. In addition to the *ppe51* gene deletion, the sequencing also revealed a second-site non-synonymous mutation in the hypothetical gene Rv2662 (C81Y) and a base insertion in the mycocerosic acid synthase gene *mas* causing a frame shift (Figure 3a-3b). This *mas* gene is responsible for the synthesis of multi-methyl branched mycocerosic acids, which form a segment of the phthiocerol dimycocerosate (PDIM) structure. PDIM loss is very common during *in vitro* culturing of *Mtb* strains and is also more spontaneously occurring when coupled with other mutations [23]. In addition to the Δ*ppe51* deletion strain, we also generated a corresponding complemented strain Δ*ppe51*::PPE51 that constitutively expresses wild-type *ppe51* gene from an integrative single-copy plasmid and could therefore compensate for the loss of transporter function.

Growth on minimal medium with glucose and trehalose supplementation

We analyzed the growth of Δ*ppe51*, Δ*ppe51*::PPE51 and the wild-type strain in minimal medium supplemented with increasing concentrations (0 mM - 5 mM) of trehalose or glucose to study the effect on growth of *Mtb*. The wild-type and the Δ*ppe51*::PPE51 complement strain showed a gradual increase in growth with increase in the concentrations of carbon sources provided. The Δ*ppe51* deletion strain was not able to grow on the minimal medium with or without supplementation of glucose or trehalose, which strongly suggests a proposed function of PPE51 as a transporter for both sugars (Figure 4 a-b). In addition to these strains, the *lpqY-sugC* merodiploid strain exhibited normal growth patterns on glucose and trehalose as carbon sources as expected. In contrast, the Δ*lpqY-sugC* deletion was able to grow in presence of glucose but not trehalose, which is accordance with a previous report demonstrating that the

LpqY-SugC ABC transporter is a trehalose-specific uptake system (Supplementary figure 3). In addition to these concentration-dependent growth assays, we also measured the time-dependent growth kinetics of H37Rv wild-type, the Δ*ppe51* deletion strain and the Δ*ppe51*::PPE51 complemented mutant in both minimal medium and 7H9+0.05% tyloxapol containing 10 mM glucose or trehalose. Cultures grown in 7H9 supplemented with ADS, 0.5% glycerol and 0.05% tyloxapol were used as positive control. The Δ*ppe51* deletion strain did not grow in both limited media with glucose or trehalose but displayed normal growth in 7H9 complete medium containing glycerol. Complementation of this mutant restored growth similar to the wild-type strain (Figure 5 a-c), demonstrating that the growth defect of the mutant was unequivocally attributed to the loss of *ppe51*. Previous studies have shown that a *ppe51* deletion strain was unable to utilize glycerol as a carbon source [16]. In contrast, we observed that our Δ*ppe51* mutant was able to utilize glycerol as the carbon source when cultivated in 7H9 medium containing 0.5% glycerol and 0.05% tyloxapol without ADS (Figure 6 a-c). This could result from an impaired formation or complete loss of PDIM due the observed spontaneous second-site frame shift mutation in the *mas* gene that might allow the Δ*ppe51* deletion mutant to use glycerol for the growth in a PPE51-independent manner. However, no growth of the Δ*ppe51* deletion mutant was observed with trehalose as the carbon source under these conditions, indicating that trehalose was unable to enter the cells in a PPE51-independent manner despite the defect in PDIM biosynthesis.

The Δ*ppe51* deletion mutant shows reduced fluorescence intensity when labelled with 6-TreAz and AF488 DIBO.

Mtb strains have been labelled with various trehalose analogs employing click chemistry to study the roles of different glycoproteins, membrane lipids and glycan molecules in the cellular envelope [24][25]. Copper-free click chemistry is based on the principle of biorthogonal labelling which involves alkyne-azide cycloaddition. *Mtb* cells cultivated with azide-functionalized metabolic substrates can be conjugated to a cyclooctyne-functionalized probe such as dibenzocyclooctynes (DIBO). In this study, *Mtb* wild-type (positive control), the Δ*lpqY*

(Rv1235) gene deletion mutant (negative control) and the Δ*ppe51* gene deletion mutant were grown in 7H9 medium containing 100 μM 6-TreAz and were subsequently labelled with Alexa Fluor 488 DIBO Alkyne. Mean fluorescence intensity (MFI) was measured for 50,000 cells. It was observed that the Δ*ppe51* mutant had reduced MFI compared to wild-type and almost similar MFI when compared to that of the Δ*lpqY* deletion strain indicating that uptake of 6-TreAz in wild-type is dependent both on PPE51 and LpqY-SugABC transporters (Figure 7). In the absence of PPE51, 6-TreAz was not taken up by *Mtb* and hence AF488 DIBO Alkyne could not conjugate with any azide molecules. Similarly, in the absence of LpqY-SugABC, 6-TreAz cannot enter the cytoplasm and is retained in the cellular envelope. The antigen 85 complex working in reverse with 6-TreAz and TDM as substrates, however, can produce some 6-TreAz-containing TMM extracellularly in the cell wall compartment. This 6-TreAz-containing TMM are incorporated into the cell wall and be conjugated with AF488 DBO Alkyne, thus resulting in background labeling even in the absence of uptake.

Discussion

Although the complete genome sequence of the *Mtb* wild-type strain H37Rv was revealed in 1998, many of its genes have not been functionally characterized yet. One such group of genes are the PE/PPE family of proteins. Initially, a set of PE/PPE proteins were known to contribute to the evasion of host immunity and replication in human macrophages [13]. It is very recently that these proteins gained attention in relevance to uptake of various molecules across the mycomembrane. In our study, we investigated the *Mtb* growth inhibition against the azide-functionalized sugar 6-TreAz. The growth inhibition by 6-TreAz was previously observed with *Mycobacterium aurum* by Belisle et al [12]. It was shown that this compound inhibited the bacterial growth at 200 μg/ml on solid medium and also suppressed mycolyltransferase activity of the antigen 85 complex by 60% at a concentration of 100 μg/ml. It also resulted in lesser synthesis of TMMs and TDMs. In this paper, we examined the anti-mycobacterial activity of the compound against *Mycobacterium tuberculosis* H37Rv wild type strain and found the growth inhibition at 1 mM. This compound was also tested against *Mycobacterium*

smegmatis in another study and it caused growth inhibition at higher concentrations (500 µM). Interestingly, it displayed a significant anti-biofilm activity at 50 µM [27]. They also shown a high anti-mycobacterial activity of 2-TreAz against *Mycobacterium smegmatis*. So, we grew our spontaneous resistant mutants on 7H10 solid medium containing 0, 1, 2 mM concentrations of 2-Azido Trehalose (2-TreAz) but however we observed only partial growth inhibition (Supplementary Figure 4). Very recently, *Mtb* was shown to be inhibited by agrichemical compounds such as 3,3-bis-di(methyl sulfonyl) propionamide (3bMP1) and carbohydrate derivatives with thio group such as thio-glycoside. Spontaneous resistant mutants raised against these anti-mycobacterial compounds were characterized by whole genome sequencing and revealed PPE51 as a determinant of resistance. Subsequent biochemical characterisation of PPE51 in these studies demonstrated that PPE51 is required for transport of low-molecular weight molecules such as the studied anti-mycobacterial compounds but also for carbohydrates such as glucose, glycerol, maltose and lactose [16][17].

However, information about the role of PPE51 in transport of trehalose was missing. Given the central importance of trehalose for vitality of *Mtb*, it was important to understand the uptake of exogenous trehalose across the mycomembrane. Hence, spontaneous resistant mutants were isolated using 6-TreAz as an anti-mycobacterial surrogate and sequenced to identify the cause of resistance. Mutations occurred in *ppe51* and in genes involved in PDIM biosynthesis. The role of PDIM biosynthesis in relation to essentiality of PPE51 was observed by Wang et al during their effort to make a *ppe51* gene deletion in *Mtb*. They have shown that function of PPE51 is strictly essential for viability of *Mtb* during growth on carbohydrates unless loss of PDIM biosynthesis apparently enables the PPE51-independent uptake of glycerol and glucose across the mycomembrane [16]. We observed that our Δ*ppe51* mutant could not utilize trehalose and glucose as the carbon sources during growth in minimal media despite having a second-site frame shift mutation in the *mas* gene. However, in Wang et al. and in our study, there were different mutations (*fadD26* and *mas* respectively) that might have affected PDIM biosynthesis to different degrees. We speculate that the frame shift mutation did not abolish *mas* gene function completely in our Δ*ppe51* mutant leading to at least some residual

PDIM formation that rendered the barrier function of the mycomembrane largely intact towards carbohydrates under the tested culture conditions. Korycka-Machała et al. reported that the uptake of other disaccharides such as maltose and lactose is also mediated through PPE51, and they also noticed that some isolated resistant mutants had mutations in *eccC5* similar to our findings. The observed mutations in *eccC5* might impair secretion of protein substrates including PPE51 by the ESX-5 secretion apparatus, thus leading to the uptake defect that confers resistance towards 6-TreAz or thioglycosides [17]. When our resistant mutants were cultivated with 6-TreAz and labelled with AF488DIBO to determine uptake-dependent fluorescence, the spontaneous resistant mutants exhibited a reduced fluorescence close to that of the Δ*ppe51* mutant. A similar phenotype was observed with Δ*lpqY-sugC* deletion strain in one of the recent studies that aimed at investigating the metabolism of asymmetric trehalose by mycobacteria [25]. Taken together, in this study, we suggest that PPE51 is responsible for uptake of trehalose and trehalose analogues in addition to glucose, glycerol, maltose and lactose across the mycomembrane (Figure 8).

MATERIALS AND METHODS

Bacterial strains and growth conditions

All *Mtb* strains were grown at 37˚C either in Middlebrook 7H9 complete medium supplemented with ADS (bovine serum albumin fraction V, glucose, NaCl), 0.5% glycerol and 0.05% tyloxapol or in 7H10 agar medium supplemented with ADS and 0.5% glycerol unless otherwise stated. For the selection of appropriate strains, hygromycin (50 mg/l), apramycin (40 mg/l) and kanamycin (40 mg/l) were added. List of strains used for this study is provided in Supplementary table 1A. *Mtb* strains were also grown in minimal medium containing 0.15 g L-Asparagine×H_2O, 0.5 g $(NaH_4)_2SO_4$, 1 g KH_2PO_4, 2.5 g Na_2HPO_4, 50 mg ferric ammonium citrate, 0.5 g $MgSO_4$×7 H_2O, 0.5 mg $CaCl_2$, 0.05% (v/v) tyloxapol and 0.1 mg $ZnSO_4$, dissolved in 1 L H_2O (pH 7.0). The 7H9 minimal medium contains only Middlebrook 7H9 and 0.05% tyloxapol.

Construction of merodiploid strain and generation of targeted gene deletion in *Mtb*

A merodiploid strain with an additional copy of the trehalose recycling transporter LpqY-SugC (Rv1235-1238) in the *Mtb* genome was generated by electroporating the integrative plasmid pMV306(Kan)::Rv1235-1238 (1000 Ω, 25 µF, 2500 V) into *Mtb* H37Rv wild-type strain. This additional copy of the gene cluster compensates for any loss of Rv1235-1238 gene functions in spontaneous resistant mutants. *Mtb* mutants were generated by allelic exchange using specialized transduction as described in Bardarov et al. [21] and Jain et al. [22]. Briefly, the regions flanking Rv3136 were amplified using Phusion DNA polymerase (New England Biolabs) and cloned into a vector containing hygromycin selection marker. The *Pac*I digested vector was cloned into shuttle phasmid phAE159 and electroporated into *M. smegmatis* (1000 Ω, 25 µF, 2500 V). The shuttle phasmid is able to produce phages containing recombinant DNA in *M. smegmatis* only at 30˚C permissible temperature. These phages are multiplied and delivered as high titer phage lysates to the *Mtb* cells through transduction. The selection plates are incubated for 3-4 weeks at 37˚C. List of primers used for generation of mutant and the merodiploid strain are provided in Supplementary table 1B.

***Mtb* genomic DNA extraction and whole genome sequencing**

Spontaneous resistant mutants were cultured in 7H9 complete medium and the genomic DNA was extracted using CTAB-lysozyme method. Briefly, the cultures were pelleted and incubated with 9:1 mixture of GTE (50 mM glucose, 25 mM Tris-HCl, 10 mM EDTA) and lysozyme solution (10 mg/ml) overnight at 37˚C. Next day, 150 µl of 2:1 solution of 10% SDS and 10 mg/ml proteinase K was added and incubated for 30 minutes at 55˚C. Then, 200 µl of 5 M NaCl was added and mixed gently. 160 µl of preheated CTAB (cetrimide – hexadecyltrimethylammonium bromide in water) was added and mixed gently followed by incubation for 10 minutes at 65˚C. Then an equal volume of 24:1 (v/v) chloroform/isoamyl alcohol was added and mixed vigorously and then centrifuged for 5 min. The aqueous layer was then transferred to fresh microcentrifuge tube and the previous step was repeated again to get rid of residual organic phase. 560 µl of 70% isopropanol was then added to the aqueous

layer for precipitating the genomic DNA. This step was followed by incubation for 5 minutes and then centrifugation for 10 minutes. The pellet was then washed with 70% ethanol, air dried and resuspended in water. The concentration of the genomic DNA was measured using AccuClear® Ultra High Sensitivity dsDNA Quantitation kit. 50 ng of genomic DNA was used for whole genome sequencing. Whole genome sequencing was performed using Illumina MiSeq Next Generation Sequencer. The DNA was sequenced with genome coverage of approximately 60 – 80-fold with a read length of 2 x 250 bp using MiSeq Reagent kit v2 (500 cycles) from Illumina.

Resazurin microplate assay (REMA) for growth quantification

Trehalose and glucose dependent growth of *Mtb* strains was quantified using the phenoxazine dye resazurin. Cells were grown in the minimal medium containing concentrations ranging from 0 mM to 5 mM of trehalose or glucose in a total volume of 100 µl and incubated at 37˚C for 5 days. After 5 days, resazurin solution (10 µl/well from 100 µg/ml, Sigma-Aldrich) was added to the cells and incubated overnight at room temperature for reduction of resazurin to resorufin by aerobic respiration of metabolically active cells. Next day, *Mtb* cells were inactivated by incubating with 10% formalin for 30 minutes at room temperature. The fluorescence (excitation 560 nm, emission 590 nm) was measured using a microplate reader (TECAN).

Metabolic labelling of Mycobacteria

All *Mtb* strains were grown in Middlebrook 7H9 complete medium supplemented with ADS, 0.5% (w/v) glycerol and 0.05% Tyloxapol in a square bottle until the $OD_{600\ nm}$ reached ~0.8. 50 µl from the stock culture was added to 950 µl Middlebrook 7H9 complete medium containing 100 µM 6-TreAz in a 1.5 ml screw cap tube and incubated for 3 days at 37˚C. After 3 days, the cells were centrifuged at 13,000 rpm for 5 minutes and the supernatant was discarded. The cells were then washed twice with PBS containing 0.5% bovine serum albumin (PBSB) by centrifugation. After the washing step, the cells were incubated with 1 ml from 1:500 dilution

of 1 mM Alexa Fluor 488 DIBO Alkyne stock solution in DMSO (ThermoFisher Scientific) at room temperature for 45 minutes in dark. Then, cells were washed again with PBSB twice and inactivated with 4% paraformaldehyde for 60 minutes at room temperature. The inactivated cells were washed with PBS and the final pellet was resuspended in 100 µl PBS. The cells were then prepared for measuring Mean fluorescence intensity (MFI) using flow cytometry. Flow cytometry was performed on BD LSRFortessa™ cell analyzer. MFI data was collected for 50,000 cells for each sample and processed using FlowJo (Tree Star).

References

[1] G. Churchyard *et al.*, "What We Know about Tuberculosis Transmission: An Overview," *J. Infect. Dis.*, vol. 216, no. Suppl 6, pp. S629–S635, 2017, doi: 10.1093/infdis/jix362.

[2] A. Koch and V. Mizrahi, "Mycobacterium tuberculosis," *Trends Microbiol.*, vol. 26, no. 6, pp. 555–556, 2018, doi: 10.1016/j.tim.2018.02.012.

[3] L. Chiaradia *et al.*, "Dissecting the mycobacterial cell envelope and defining the composition of the native mycomembrane," *Sci. Rep.*, vol. 7, p. 12807, 2017, doi: 10.1038/s41598-017-12718-4.

[4] M. Jankute, J. A. G. Cox, J. Harrison, and G. S. Besra, "Assembly of the Mycobacterial Cell Wall," *Annu. Rev. Microbiol.*, vol. 69, no. 1, pp. 405–423, 2015, doi: 10.1146/annurev-micro-091014-104121.

[5] C. L. Dulberger, E. J. Rubin, and C. C. Boutte, "The mycobacterial cell envelope — a moving target," *Nat. Rev. Microbiol.*, vol. 18, no. January, pp. 47–59, 2020, doi: 10.1038/s41579-019-0273-7.

[6] M. Tropis *et al.*, "The crucial role of trehalose and structurally related oligosaccharides in the biosynthesis and transfer of mycolic acids in corynebacterineae," *J. Biol. Chem.*, vol. 280, no. 28, pp. 26573–26585, 2005, doi: 10.1074/jbc.M502104200.

[7] M. K. O'Neill, B. F. Piligian, C. D. Olson, P. J. Woodruff, and B. M. Swarts, "Tailoring trehalose for biomedical and biotechnological applications," *Pure Appl. Chem.*, vol. 89, no. 9, pp. 1223–1249, 2017, doi: 10.1515/pac-2016-1025.

[8] J. M. Belardinelli *et al.*, "The MmpL3 interactome reveals a complex crosstalk between cell envelope biosynthesis and cell elongation and division in mycobacteria," *Sci. Rep.*, vol. 9, no. 1, pp. 1–14, 2019, doi: 10.1038/s41598-019-47159-8.

[9] R. Kalscheuer, B. Weinrick, U. Veeraraghavan, G. S. Besra, and W. R. Jacobs, "Trehalose-recycling ABC transporter LpqY-SugA-SugB-SugC is essential for virulence

of Mycobacterium tuberculosis," *Proc. Natl. Acad. Sci. U. S. A.*, vol. 107, pp. 21761–21766, 2010, doi: 10.1073/pnas.1014642108.

[10] S. B. O'Neill MK, Piligian BF, Olson CD, Woodruff PJ, "Tailoring Trehalose for Biomedical and Biotechnological Applications," *Pure Appl Chem.*, vol. 89(9), pp. 1223–1249, 2017, doi: 10.1016/j.physbeh.2017.03.040.

[11] B. M. Swarts *et al.*, "Probing the mycobacterial trehalome with bioorthogonal chemistry," *J. Am. Chem. Soc.*, vol. 134, pp. 16123–16126, 2012, doi: 10.1021/ja3062419.

[12] J. T. Belisle, V. D. Vissa, T. Sievert, K. Takayama, P. J. Brennan, and G. S. Besra, "Role of the major antigen of Mycobacterium tuberculosis in cell wall biogenesis," *Science (80-.).*, vol. 276, no. 5317, pp. 1420–1422, 1997, doi: 10.1126/science.276.5317.1420.

[13] M. J. Brennan, "The Enigmatic PE / PPE Multigene Family Vaccination," *Infect. Immun.*, vol. 85, no. 6, pp. 1–8, 2017.

[14] N. C. Gey Van Pittius, S. L. Sampson, H. Lee, Y. Kim, P. D. Van Helden, and R. M. Warren, *Evolution and expansion of the Mycobacterium tuberculosis PE and PPE multigene families and their association with the duplication of the ESAT-6 (esx) gene cluster regions*, vol. 6. 2006.

[15] P. Singh *et al.*, "PE11, a PE/PPE family protein of Mycobacterium tuberculosis is involved in cell wall remodeling and virulence," *Sci. Rep.*, vol. 6, no. January, pp. 1–16, 2016, doi: 10.1038/srep21624.

[16] Q. Wang *et al.*, "PE/PPE proteins mediate nutrient transport across the outer membrane of Mycobacterium tuberculosis," *Science (80-.).*, vol. 367, no. 6482, pp. 1147–1151, 2020, doi: 10.1126/science.aax3072.

[17] M. Korycka-Machała *et al.*, "PPE51 Is Involved in the Uptake of Disaccharides by Mycobacterium tuberculosis," *Cells*, vol. 9, no. 3, p. 603, 2020, doi: 10.3390/cells9030603.

[18] J. J. Baker and R. B. Abramovitch, "Genetic and metabolic regulation of Mycobacterium tuberculosis acid growth arrest," *Sci. Rep.*, vol. 8, no. 1, pp. 1–16, 2018, doi: 10.1038/s41598-018-22343-4.

[19] M. Di Luca *et al.*, "The ESX-5 Associated eccB5-eccC5 Locus Is Essential for Mycobacterium tuberculosis Viability," *PLoS One*, vol. 7, no. 12, p. e52059, 2012, doi: 10.1371/journal.pone.0052059.

[20] L. S. Ates *et al.*, "Essential Role of the ESX-5 Secretion System in Outer Membrane Permeability of Pathogenic Mycobacteria," *PLoS Genet.*, 2015, doi: 10.1371/journal.pgen.1005190.

[21] S. Bardarov *et al.*, "Specialized transduction: An efficient method for generating marked and unmarked targeted gene disruptions in Mycobacterium tuberculosis, M. bovis BCG

and M. smegmatis," *Microbiology*, vol. 148, no. 10, pp. 3007–3017, 2002, doi: 10.1099/00221287-148-10-3007.

[22] P. Jain *et al.*, "Specialized Transduction Designed for Precise High-Throughput," *Methods Mol. Biol.*, vol. 5, no. 3, pp. e01245-14, 2014, doi: 10.1128/mBio.01245-14.Editor.

[23] P. Domenech and M. B. Reed, "Rapid and spontaneous loss of phthiocerol dimycocerosate (PDIM) from Mycobacterium tuberculosis grown in vitro: Implications for virulence studies," *Microbiology*, vol. 155, no. 11, pp. 3532–3543, 2009, doi: 10.1099/mic.0.029199-0.

[24] D. B. Backus KM, Boshoff HI, Barry CS, Boutureira O, Patel MK, D'Hooge F, Lee SS, Via LE, Tahlan K, Barry CE 3rd, "Uptake of unnatural trehalose analogs as a reporter for Mycobacterium tuberculosis," *Nat Chem Biol*, vol. 7(4), pp. 228–235, 2011, doi: 10.1161/CIRCULATIONAHA.110.956839.

[25] H. L. Parker, R. M. F. Tomás, C. M. Furze, C. S. Guy, and E. Fullam, "Asymmetric trehalose analogues to probe disaccharide processing pathways in mycobacteria," *Org. Biomol. Chem.*, vol. 18, no. 18, pp. 3607–3612, 2020, doi: 10.1039/d0ob00253d.

[26] K. M. Backus *et al.*, "Uptake of unnatural trehalose analogs as a reporter for Mycobacterium tuberculosis," *Nat. Chem. Biol.*, vol. 7, pp. 228–235, 2011, doi: 10.1038/nchembio.539.

[27] J. M. Wolber *et al.*, "The trehalose-specific transporter LpqY-SugABC is required for antimicrobial and anti-biofilm activity of trehalose analogues in Mycobacterium smegmatis," *Carbohydr. Res.*, vol. 450, pp. 60–66, 2017, doi: 10.1016/j.carres.2017.08.003.

[28] M. Korycka-Machala *et al.*, "Evaluation of the mycobactericidal effect of thio-functionalized carbohydrate derivatives," *Molecules*, vol. 22, no. 5, 2017, doi: 10.3390/molecules22050812.

Author contributions

M.R.B.S. performed most of the experiments and wrote the manuscript. R.K designed and supervised the study. H.K.B performed the growth inhibition assay and generated the spontaneous resistant mutants. B.S provided 6-Azido Trehalose. M.J processed data from flow cytometry analysis.

Acknowledgments

We would like to thank the Jürgen Manchot foundation and the MOI graduate school for funding.

Conflict of interest

The authors declare that the research was conducted in the absence of any commercial or financial relationships that could be construed as a potential conflict of interest.

Data Availability Statement

All data generated or analysed during this study are included in this published article and its Supplementary information files.

Figure Legends

Figure 1

6-Azido trehalose inhibits *Mtb* growth at higher concentrations. (1a) Structure of trehalose and 6-azido trehalose. (1b) Growth inhibition of wild-type, Δ*lpqY-sugC* and *ΔlpqY-sugC*::pMV306(Kan)::Rv1235-1238 on 7H10 medium containing 1 mM 6-azido trehalose (6-TreAz). Δ*lpqY-sugC* allows for the growth as 6-TreAz was not taken up into the cytoplasm and did not interfere with normal metabolism to generate trehalose dimycolates.

Figure 2

Spontaneous resistant mutants against 6-azido trehalose. Growth of *Mtb* H37Rv, *Mtb* H37Rv::pMV306(Kan)::Rv1235-1238 (merodiploid strain), Δ*lpqY-sugC*, Δ*lpqY-sugC*::pMV306(Kan)::Rv1235-1238 and spontaneous resistant mutant clones on Middlebrook 7H10 medium containing without (2a) and with 6-azido trehalose (2b).

Figure 3

Growth inhibition of *Mtb* H37Rv, Δ*lpqY-sugC* and Δ*ppe51* on 7H10 + 6-TreAz (1 mM). Growth inhibition of wild-type, Δ*lpqY-sugC* and Δ*ppe51* on 7H10 medium containing 1 mM 6-azido trehalose (3a) .Whole genome sequencing information of the Δ*ppe51* deletion mutant (3b).

Figure 4

Growth of *Mtb* strains on minimal medium supplemented with different carbon sources. Concentration dependent growth of wild-type, Δ*ppe51* deletion mutant, Δ*ppe51*::PPE51 complement strain in minimal medium containing increasing concentrations (0 mM to 5 mM) of trehalose (4a) and glucose (4b). Experiment was repeated thrice and data shown here is representative of the three independent experiments. Error bars represent SD.

Figure 5

Growth of *Mtb* strains on minimal medium supplemented with different carbon sources. Time-dependent growth of wild-type H37Rv (5a), Δ*ppe51* deletion strain (5b) and Δ*ppe51*::PPE51 complement strain (5c) in both minimal medium and 7H9 + 0.05% tyloxapol with glucose or trehalose supplementation (10 mM). Strains grown in 7H9 complete medium were treated as positive control. Experiment was repeated thrice and data shown here is representative of the three independent experiments. Each experiment contained triplicates of every sample. Error bars represent SD.

Figure 6

Growth of Δ*ppe51* in 7H9 medium containing glycerol.

Growth of *Mtb* wild type H37Rv (6a), Δ*ppe51* deletion (6b) and Δ*ppe51*::PPE51 complement (6c) strains in 7H9 (containing 0.05% tyloxapol) supplemented with 0.5% glycerol or trehalose (10 mM). Strains grown in 7H9 complete medium (7H9 + ADS + 0.5% glycerol + 0.05% tyloxapol) and in 7H9 + 0.05% tyloxapol only were treated as positive and negative controls,

respectively. Experiment was repeated thrice and data shown here is representative of the three independent experiments. Each experiment contained triplicates of every sample. Error bars represent SD.

Figure 7

Metabolic labelling of *Mtb* strains by click chemistry. *Mtb* strains were grown with labelling concentrations (100 μM) of 6-azido trehalose and later conjugated with AF488 DIBO alkyne. Mean fluorescence intensity (MFI) was measured for 50,000 cells. Data are representative of three independent experiments and error bars represent SD. The two-tailed P value equals 0.0014 and 0.0039 for wild-type/Δ*ppe51* and wild-type/Δ*lpqY* comparison, respectively, and these differences are considered to be very statistically significant. (P<0.005***).

Figure 8

Trehalose transport mechanism in *Mycobacterium tuberculosis*. The figure shows the flow of uptake of trehalose compounds through PPE51 transporter and synthesis of trehalose mycolates. LpqY-SugC transporter allows the flow of the exogenous trehalose through the cytoplasm membrane and also recycles the free trehalose released after synthesis of trehalose dimycolates.

526 **Table 1**

527 List of Spontaneous resistant mutants and their gene mutations.

Spontaneous Resistant Mutants	**Mutated gene**	**Nucleotide change**	**Amino acid change**	**Other mutations**
Clone 1	Rv1783c	3278 C→A;	Pro1093Gln	ppsA (3882 G→A; Trp1294Stop); 1876 aa
Clone 2	Rv1783c	3278 C→A;	Pro1093Gln	ppsA (3882 G→A; Trp1294Stop); 1876 aa
Clone 3	Rv3136 (ppe51)	661 T→C	Leu204Pro	-
Clone 4	Rv3136 (ppe51)	41 G→C	Arg14Pro	fadD26 (154 delC; Pro52fs); 583 aa
Clone 5	no mutations detected	-	-	fadD26 (154 delC; Pro52fs); 583 aa
Clone 6	Rv3136 (ppe51)	280 G→A	Ala94Thr	ppsB (38 delC; Thr13fs); 1538 aa
Parental reference strain		**Mtb Wild Type H37Rv + pMV306::Rv1235-1238 (merodiploid)**		

Supplementary Information

Mycobacterium tuberculosis utilizes PPE51 for transport of trehalose molecules across the mycomembrane

Mohammed Rizwan Babu Sait[1], Hendrik Koliwer-Brandl[1], Benjamin Swarts[2], Marc Jacobsen[3], Thomas R. Ioerger[4], Rainer Kalscheuer[1*]

[1] Institute of Pharmaceutical Biology and Biotechnology, Heinrich Heine University, 40225 Düsseldorf, Germany.

[2] Department of Chemistry and Biochemistry, Central Michigan University, Mount Pleasant, Michigan 48859, USA.

[3] Department of General Pediatrics, Neonatology, and Pediatric Cardiology, University Children's Hospital, Heinrich Heine University, 40225 Düsseldorf, Germany.

[4] Department of Computer Science, Texas A&M University, College Station, Texas 77843, USA.

***Correspondence:**

Prof. Dr. Rainer Kalscheuer

Rainer.Kalscheuer@hhu.de

Supplementary Figure 1

(a) Construction of integrating plasmid pMV306 (Kanamycin resistance) containing the additional copy of LpY-SugC gene for the Wild type H37Rv. (b) Gene structure of *Mtb* H37Rv BamHI/ClaI fragment (8475bps). (c) Southern blot showing the differences in *Mtb* H37Rv wild type cut with BamHI/ClaI (8475 bps) and the merodiploid strain that contains additional band (5252 bps) (Probe: SmaI/HindIII fragment).

Supplementary Figure 2

The complemented spontaneous resistant strains (that were complemented with the gene that caused the mutation) were serially diluted and plated on Middlebrook 7H10 agar without (a) and with (b) 6-Azido trehalose at 1mM concentration. The complemented strains were able to undergo certain level of growth inhibition under the pressure of 6-Azio trehalose which is comparable to that of wild type

Supplementary Figure 3

Mtb Wild type H37Rv (a), Merodiploid strain (b), and ΔLpqY-SugC deletion strain (c) were grown in minimal medium with increasing concentrations of glucose and trehalose carbon sources. Wild type and merodiploid strain grows gradually with increasing concentrations of carbon sources whereas the ΔLpqY-SugC deletion strain does not grow with trehalose supplementation as the trehalose intake is blocked but grows normally with glucose supply.

Supplementary Figure 4

2-TreAz resistance of 6-TreAz spontaneous resistant mutants. Earlier studies have also shown that there is a high anti-mycobacterial activity of 2-TreAz against *Mycobacterium smegmatis*. To test this, we grew our spontaneous resistant mutants on 7H10 solid medium containing 0, 1, 2 mM concentrations of 2-Azido Trehalose (2-TreAz). We observed partial growth inhibition although not fully in this case.

Supplementary Table 1

List of *Mtb* strains (1A) and Primers (1B) used in the study**.**

No	*Mycobacterium tuberculosis* (MTB) strains	Antibiotic Resistance	Source /Reference
1	MTB H37Rv WT	-	Parent strain
2	MTB ∆LpqY - Rv1235	Hygromycin (50 µg/ml)	Kalscheuer et al., 2010
3	MTB ∆SugC - Rv1238	Hygromycin (50 µg/ml)	Kalscheuer et al., 2010
4	MTB ∆LpqY-SugC - Rv1235-1238	Hygromycin (50 µg/ml)	Kalscheuer et al., 2010
5	MTB ∆LpqY - pMV306::1235-1238	Hygromycin (50 µg/ml) Kanamycin (40 µg/ml)	Kalscheuer et al., 2010
6	MTB ∆SugC - pMV306::1235-1238	Hygromycin (50 µg/ml) Kanamycin (40 µg/ml)	Kalscheuer et al., 2010
7	MTB ∆LpqY-SugC- pMV306::1235-1238	Hygromycin (50 µg/ml) Kanamycin (40 µg/ml)	Kalscheuer et al., 2010
8	MTB H37Rv WT - pMV306::Rv1235-1238	Kanamycin (40 µg/ml)	This study
9	MTB H37Rv WT 6-TreAz resistant - pMV306::Rv1235-1238 C1	Kanamycin (40 µg/ml)	This study
10	MTB H37Rv WT 6-TreAz resistant - pMV306::Rv1235-1238 C2	Kanamycin (40 µg/ml)	This study
11	MTB H37Rv WT 6-TreAz resistant - pMV306::Rv1235-1238 C3	Kanamycin (40 µg/ml)	This study
12	MTB H37Rv WT 6-TreAz resistant - pMV306::Rv1235-1238 C4	Kanamycin (40 µg/ml)	This study
13	MTB H37Rv WT 6-TreAz resistant - pMV306::Rv1235-1238 C6	Kanamycin (40 µg/ml)	This study
14	MTB 6-TreAz-res. C1 pMV361::Rv1783-84	Apramycin (40 µg/ml)	This study
15	MTB 6-TreAz-res. C2 pMV361::Rv1783-84	Apramycin (40 µg/ml)	This study
16	MTB 6-TreAz-res. C3 pMV361::ppe51	Apramycin (40 µg/ml)	This study
17	MTB 6-TreAz-res. C4 pMV361::ppe51	Apramycin (40 µg/ml)	This study
18	MTB 6-TreAz-res. C6 pMV361::ppe51	Apramycin (40 µg/ml)	This study
19	MTB ∆Rv3136c (PPE51)	Hygromycin (50 µg/ml)	This study
20	MTB ∆Rv3136c (PPE51) pMV361::ppe51	Hygromycin (50 µg/ml) Apramycin (40 µg/ml)	This study

583

584

585

586

587

588

589

590

591

592

Figure 1a

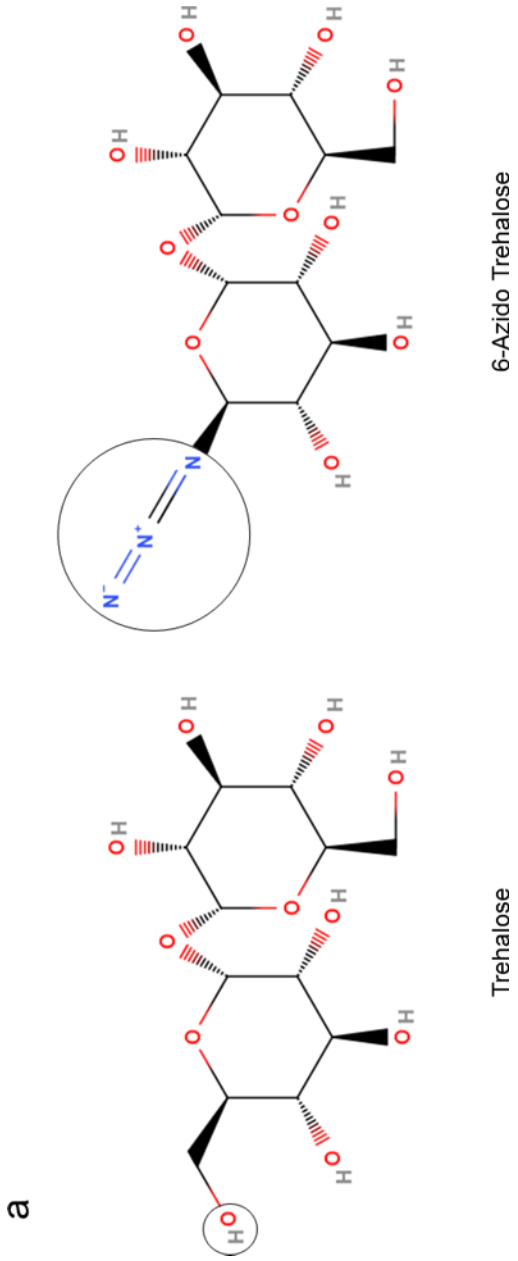

603 Figure 1b

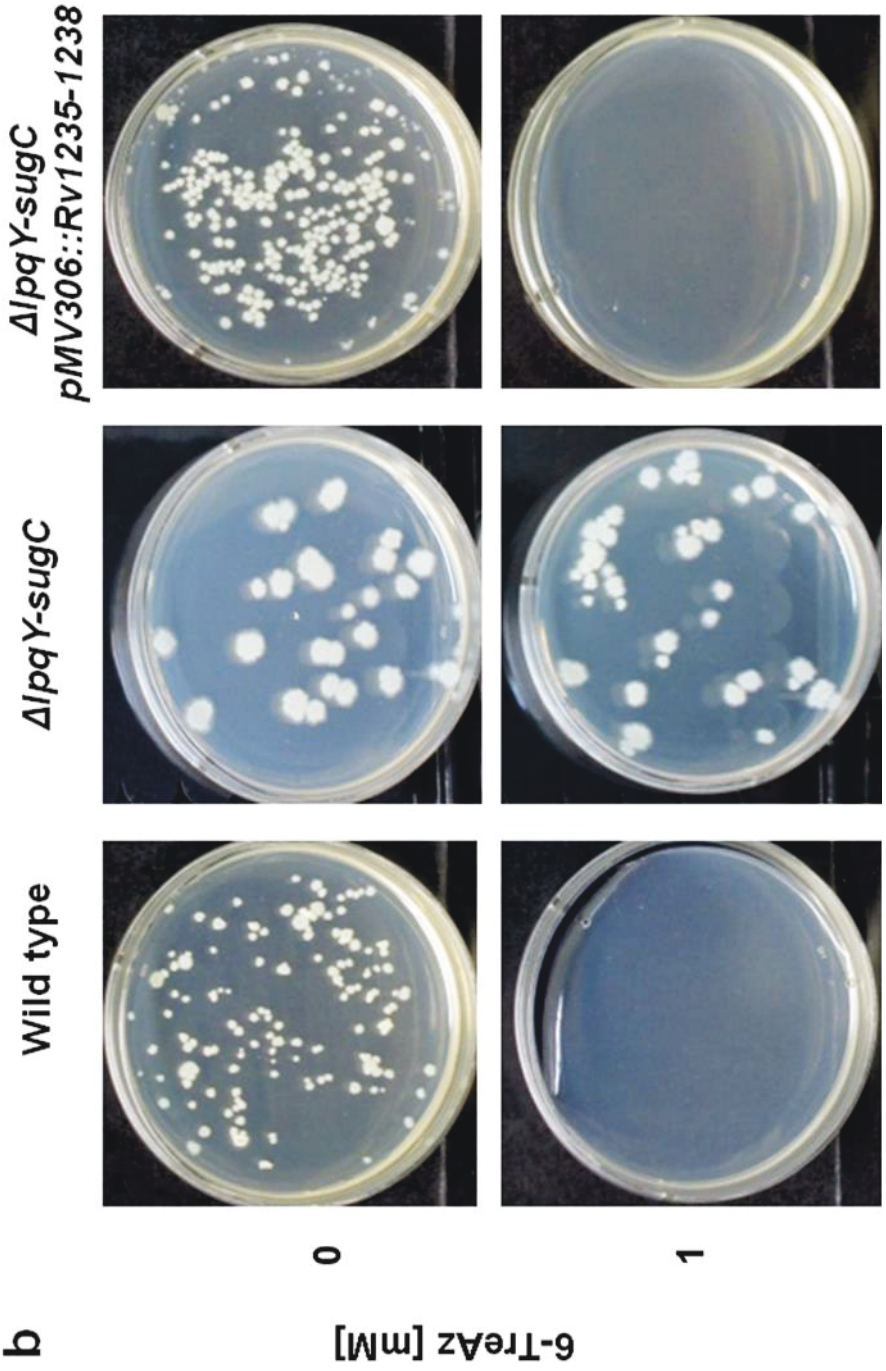

604

605

606

607

608

609

610

Figure 2a

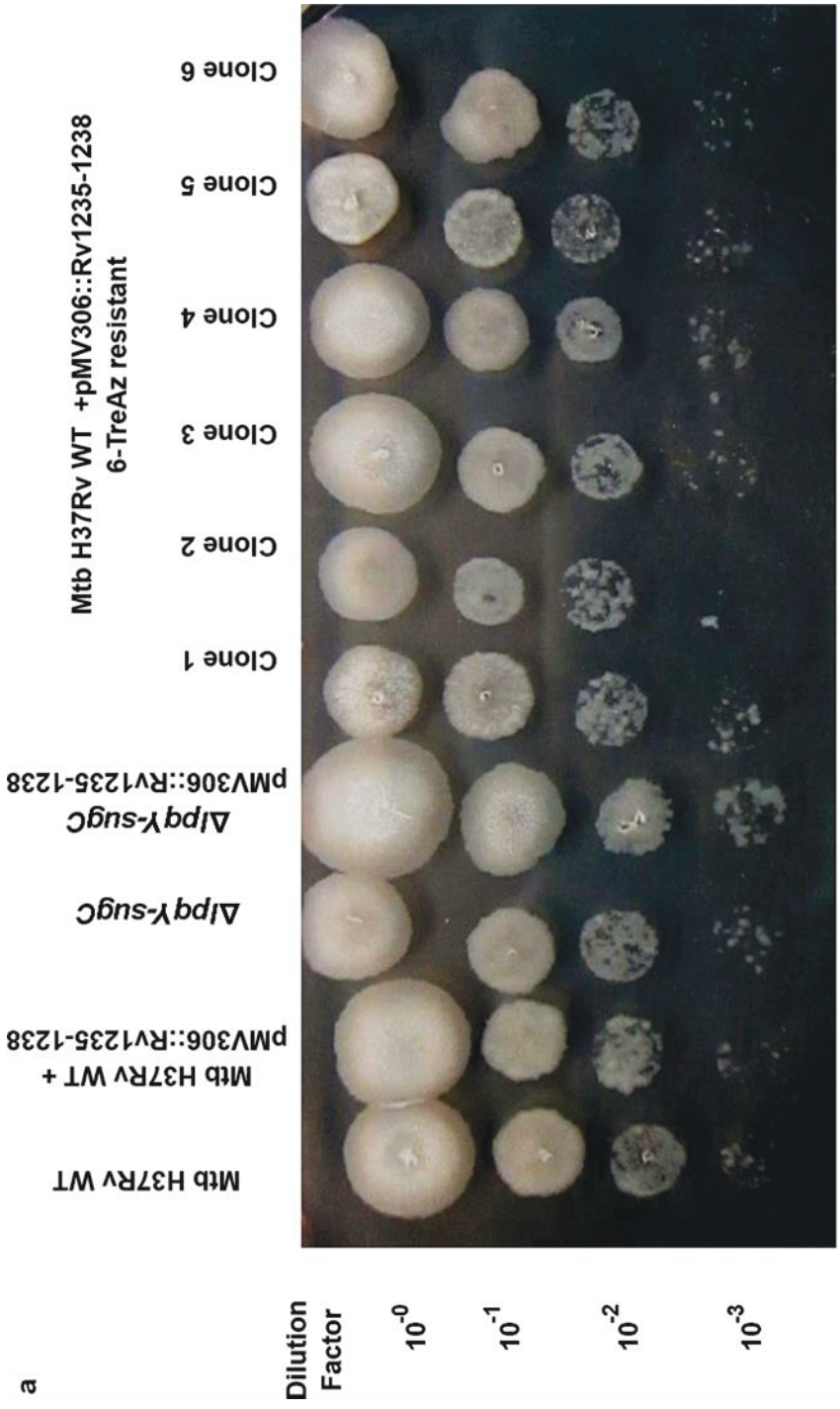
a
Dilution Factor
10-0
10-1
10-2
10-3
Mtb H37Rv WT
Mtb H37Rv WT + pMV306::Rv1235-1238
ΔlpqY-sugC
ΔlpqY-sugC pMV306::Rv1235-1238
Clone 1
Clone 2
Clone 3
Clone 4
Clone 5
Clone 6
Mtb H37Rv WT +pMV306::Rv1235-1238
6-TreAz resistant

Figure 2b

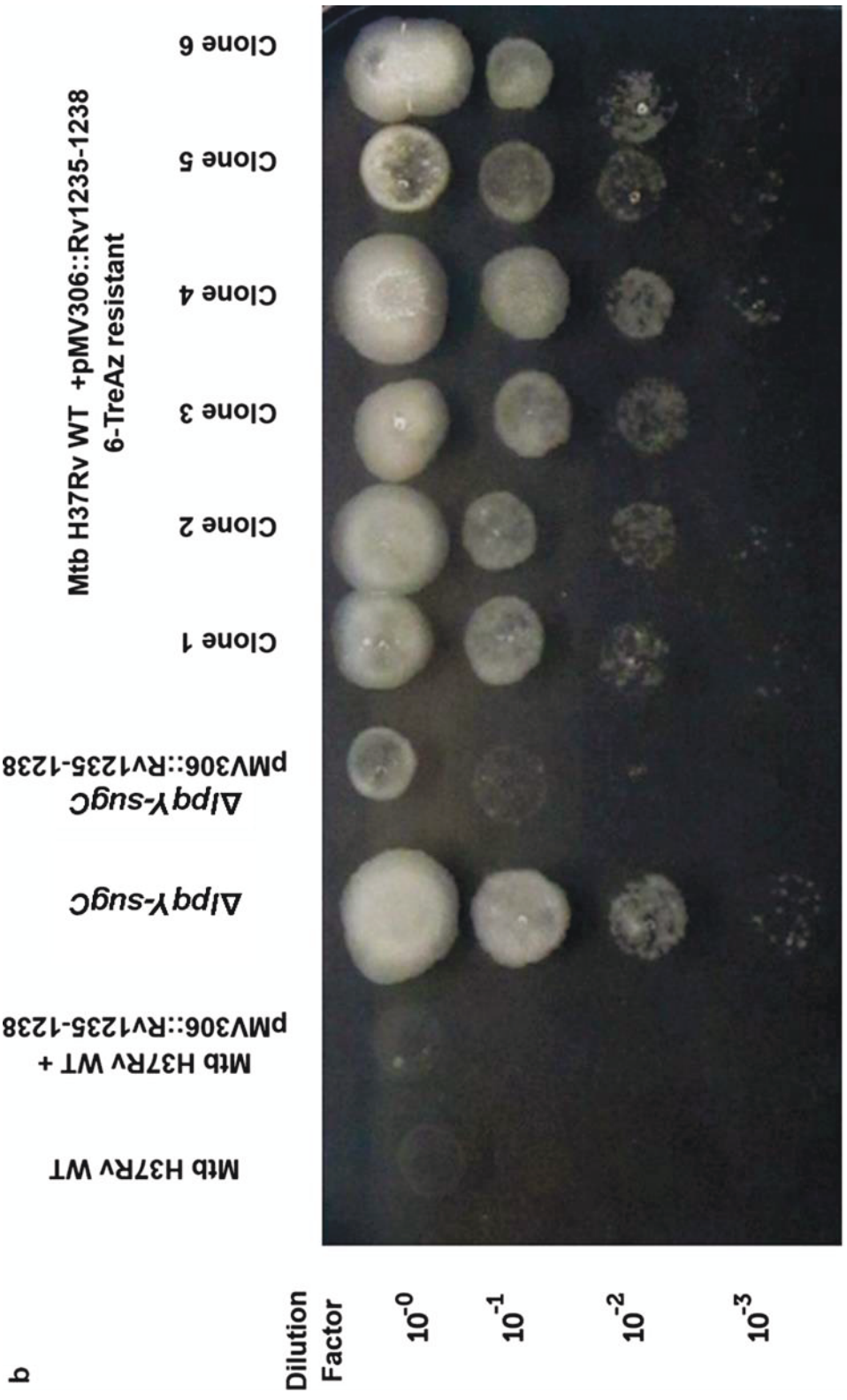
b
Dilution Factor
10^{-0}
10^{-1}
10^{-2}
10^{-3}
Mtb H37Rv WT
Mtb H37Rv WT + pMV306::Rv1235-1238
Δlpqγ-sugC
Δlpqγ-sugC pMV306::Rv1235-1238
Mtb H37Rv WT +pMV306::Rv1235-1238 6-TreAz resistant
Clone 1
Clone 2
Clone 3
Clone 4
Clone 5
Clone 6

623 Figure 3

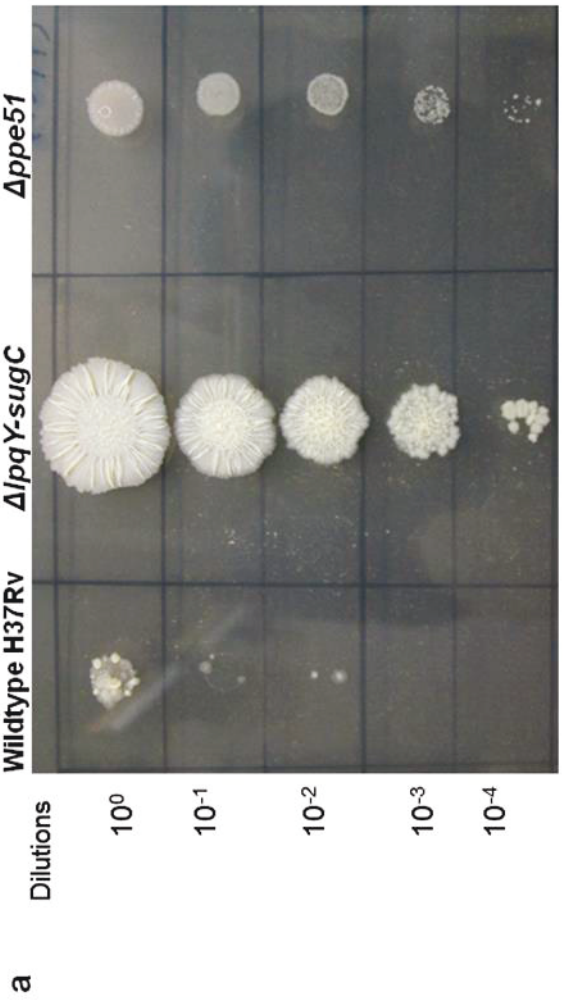

b

Strain	Parental reference strain	Mutation	Other mutations
ΔRv3136 (ppe51)	**MtbH37Rv**	**del (3501215-1999); ins 3693 bp**	**Rv2662:C81Y; mas:+a (1bp ins)**

624
625
626
627
628
629
630
631
632

633 Figure 4

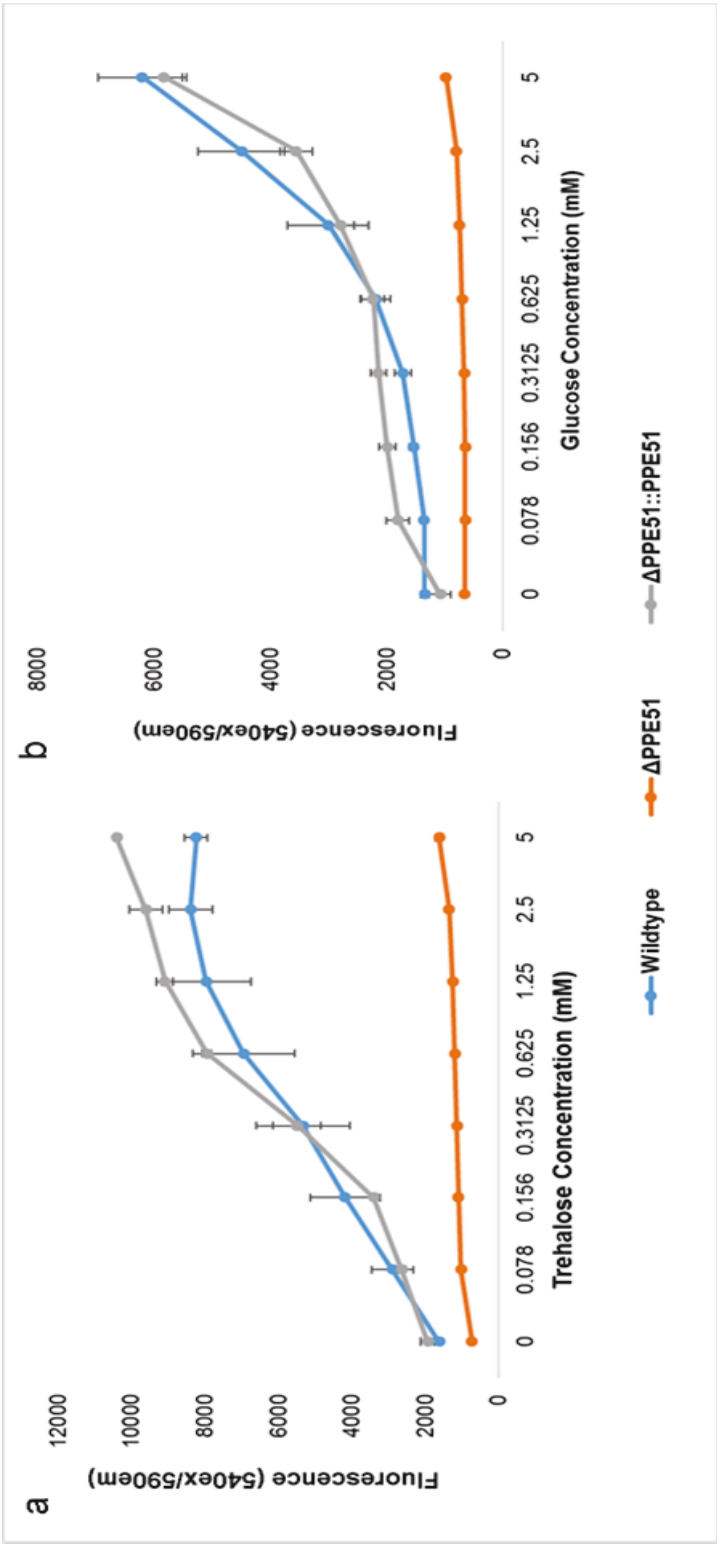

634

635

636

637

638 Figure 5

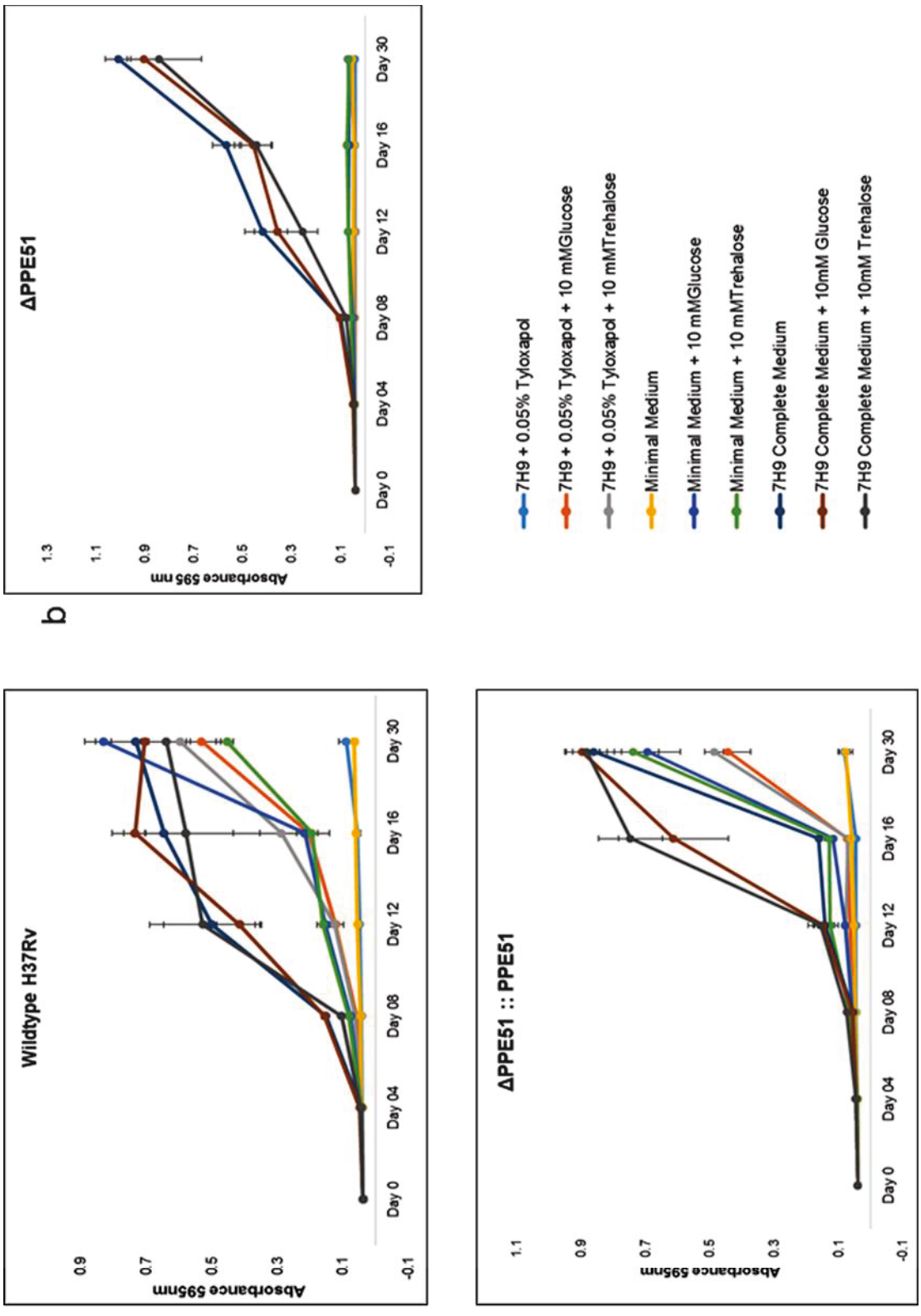

639

640

641

Figure 6

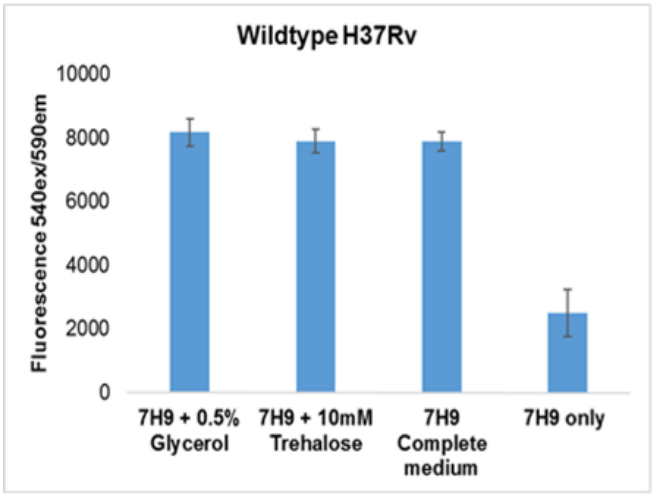
Wildtype H37Rv
Fluorescence 540ex/590em
10000
8000
6000
4000
2000
0
7H9 + 0.5% Glycerol
7H9 + 10mM Trehalose
7H9 Complete medium
7H9 only

a

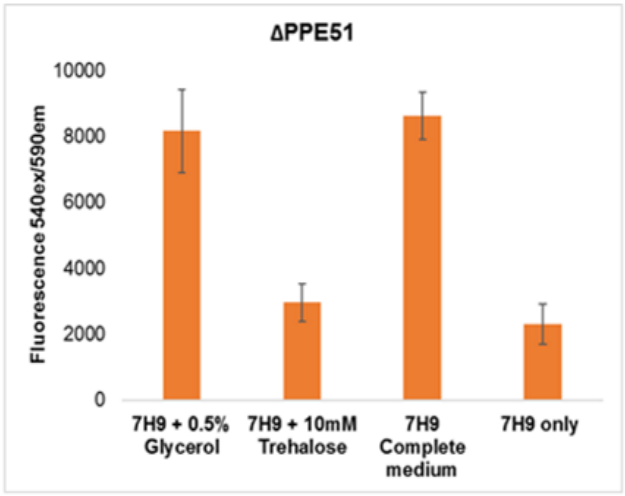
ΔPPE51
Fluorescence 540ex/590em
10000
8000
6000
4000
2000
0
7H9 + 0.5% Glycerol
7H9 + 10mM Trehalose
7H9 Complete medium
7H9 only

b

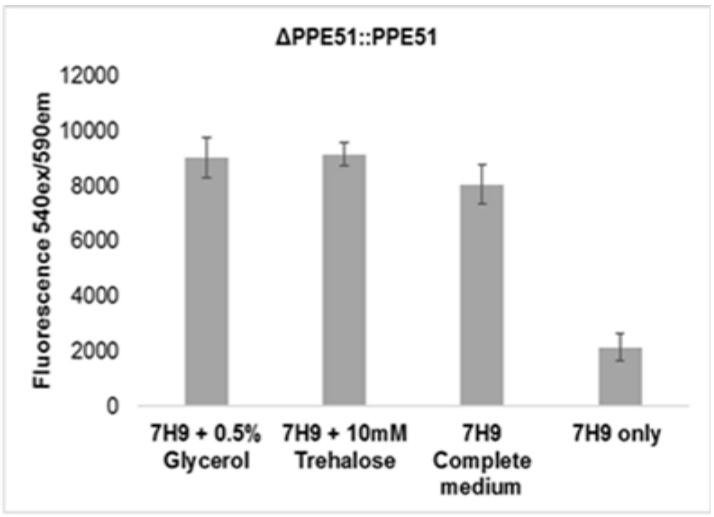
ΔPPE51::PPE51
Fluorescence 540ex/590em
12000
10000
8000
6000
4000
2000
0
7H9 + 0.5% Glycerol
7H9 + 10mM Trehalose
7H9 Complete medium
7H9 only

c

Figure 7

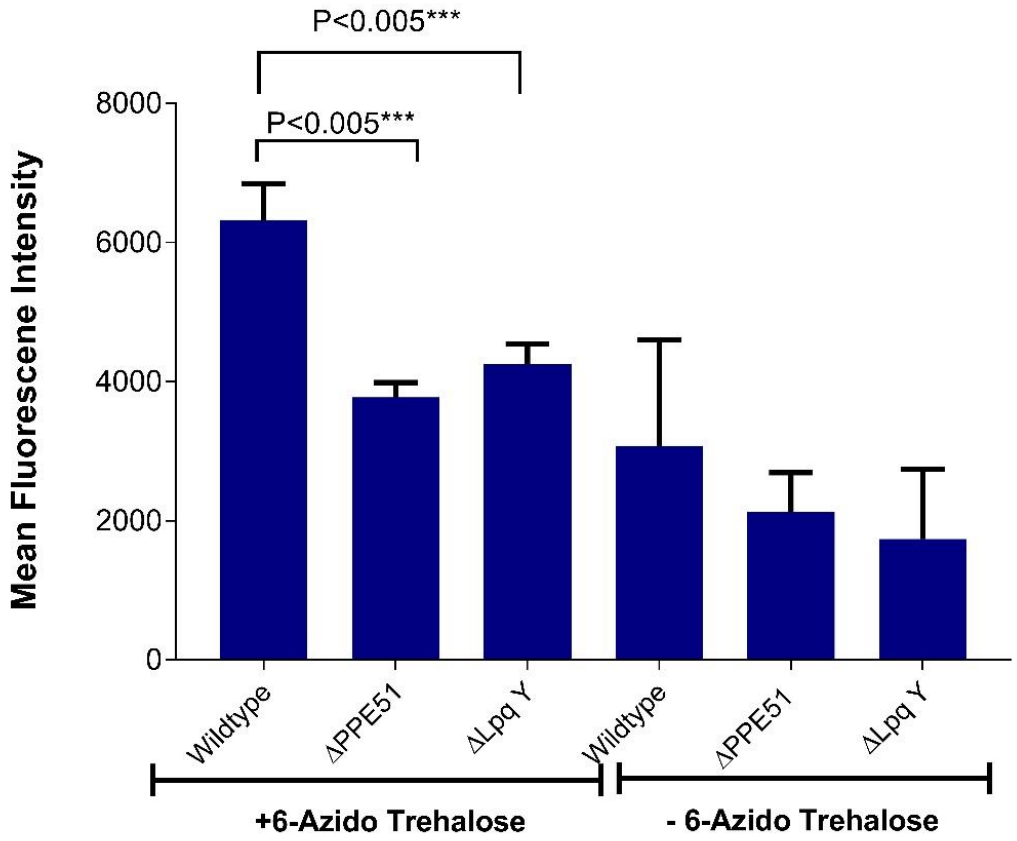
P<0.005***
P<0.005***
8000
6000
4000
2000
0
Mean Fluorescene Intensity
Wildtype
ΔPPE51
ΔLpq Y
Wildtype
ΔPPE51
ΔLpq Y
+6-Azido Trehalose
- 6-Azido Trehalose

670 Figure 8

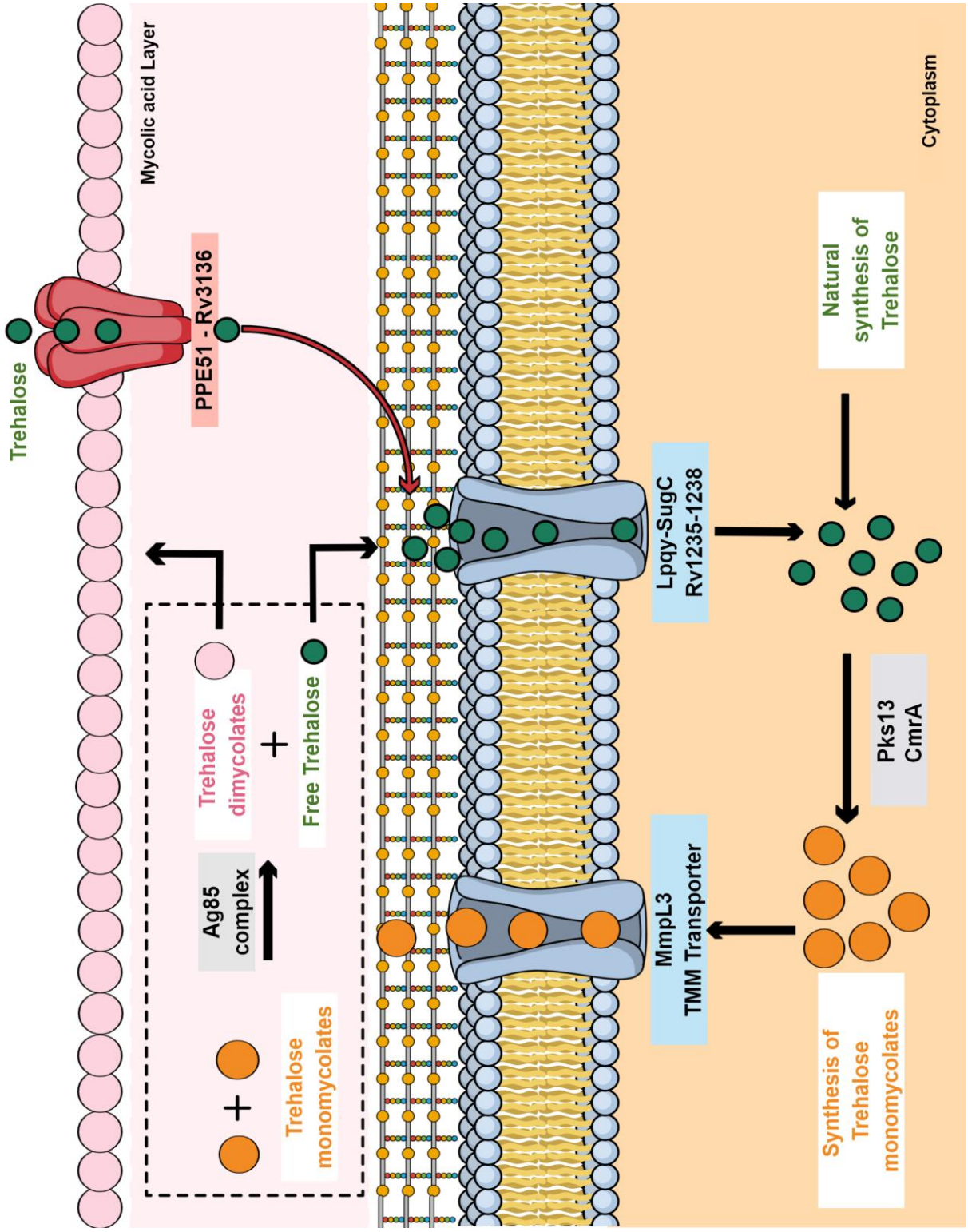

671

672

673

674

675 Supplementary figure 1

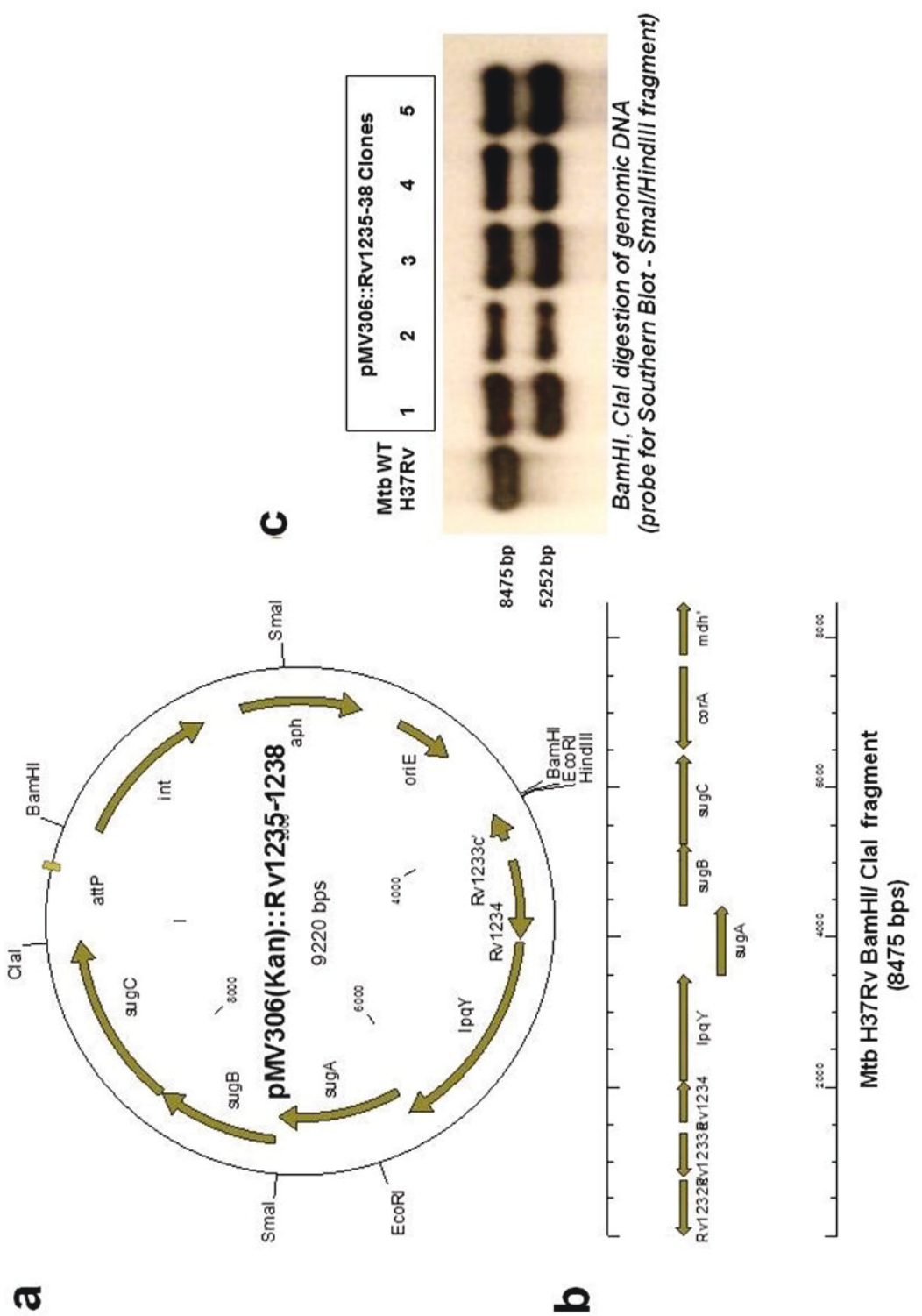

676

677

678

679

680 Supplementary Figure 2a

681

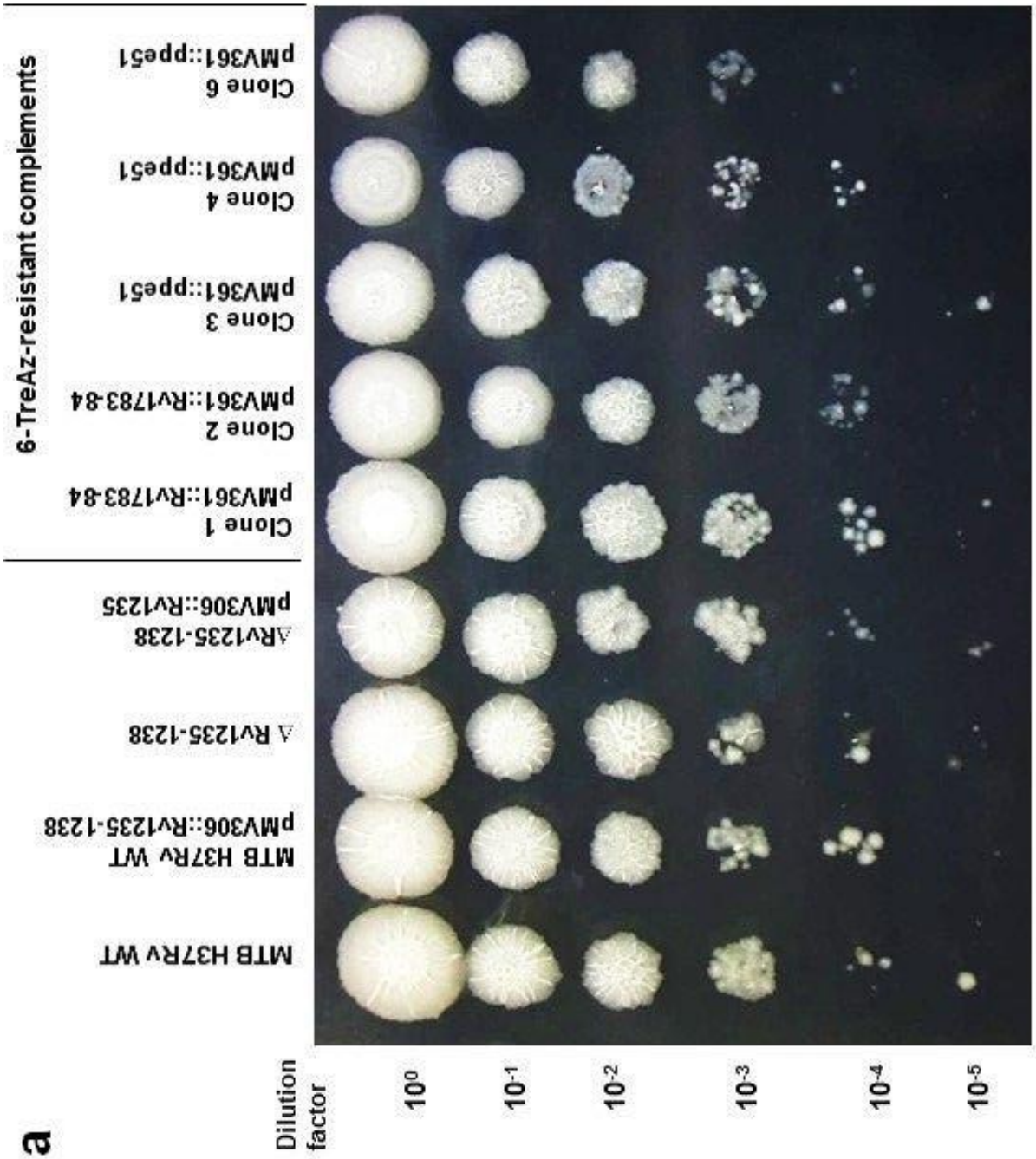

682

683

684

685

686

687

Supplementary figure 2b

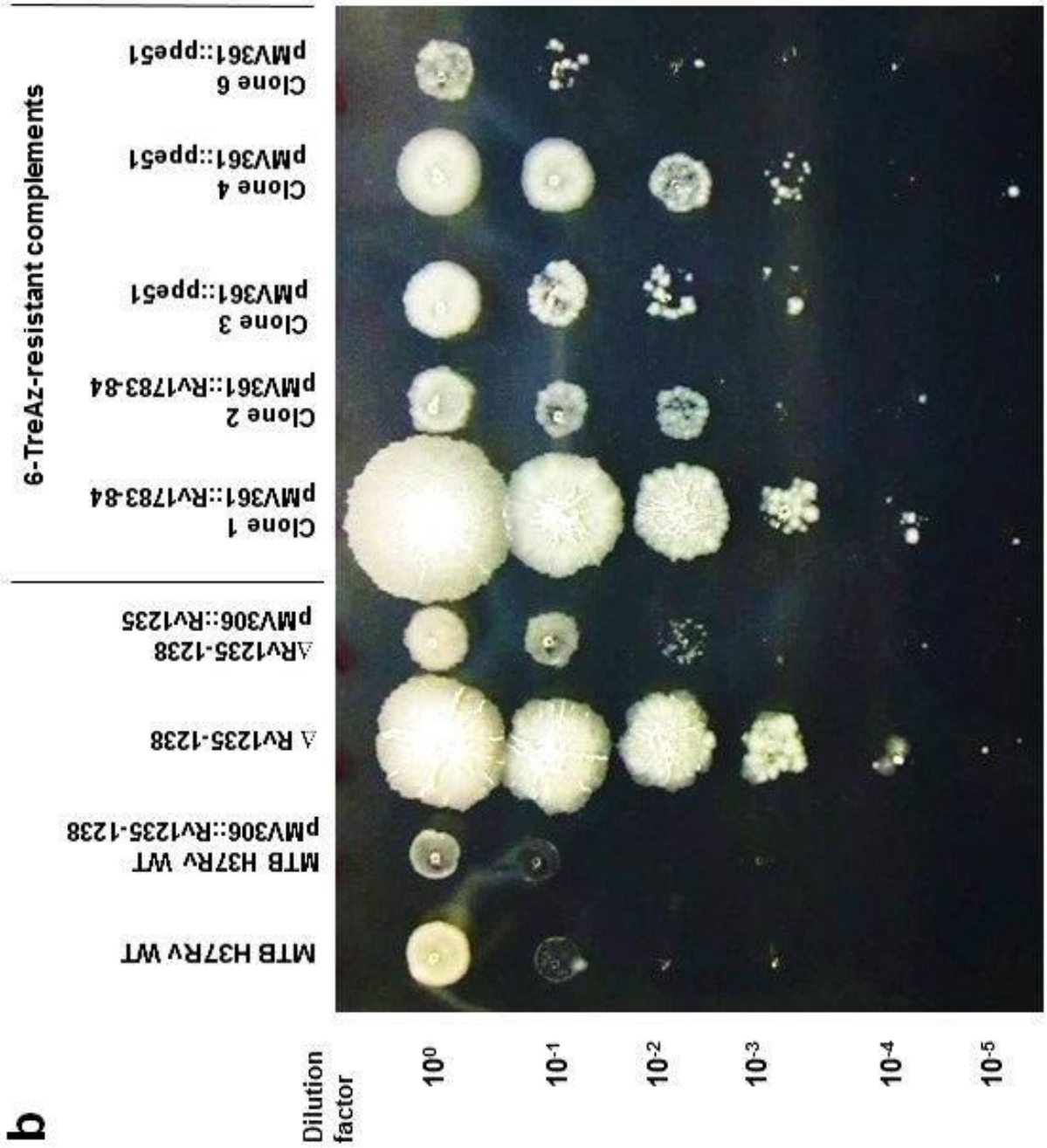

Supplementary Figure 3

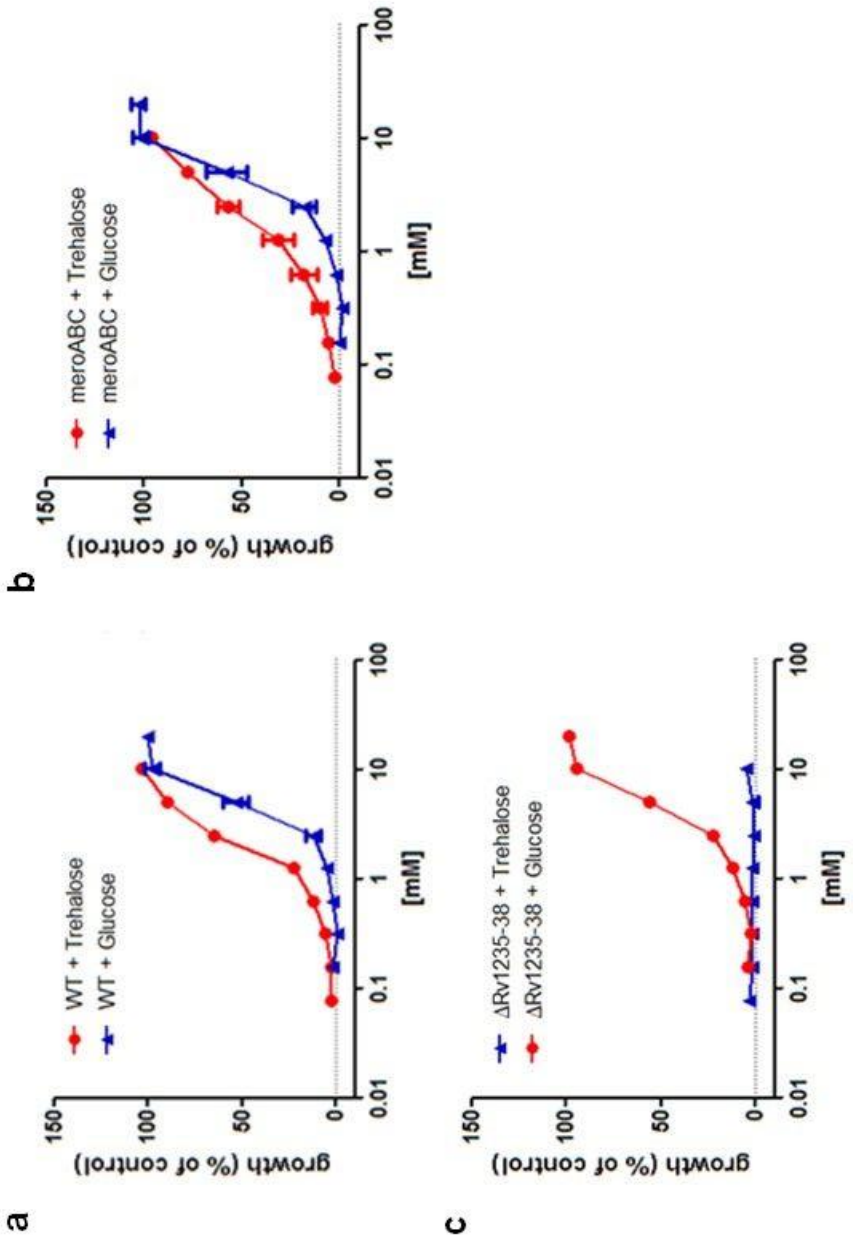

Supplementary figure 4

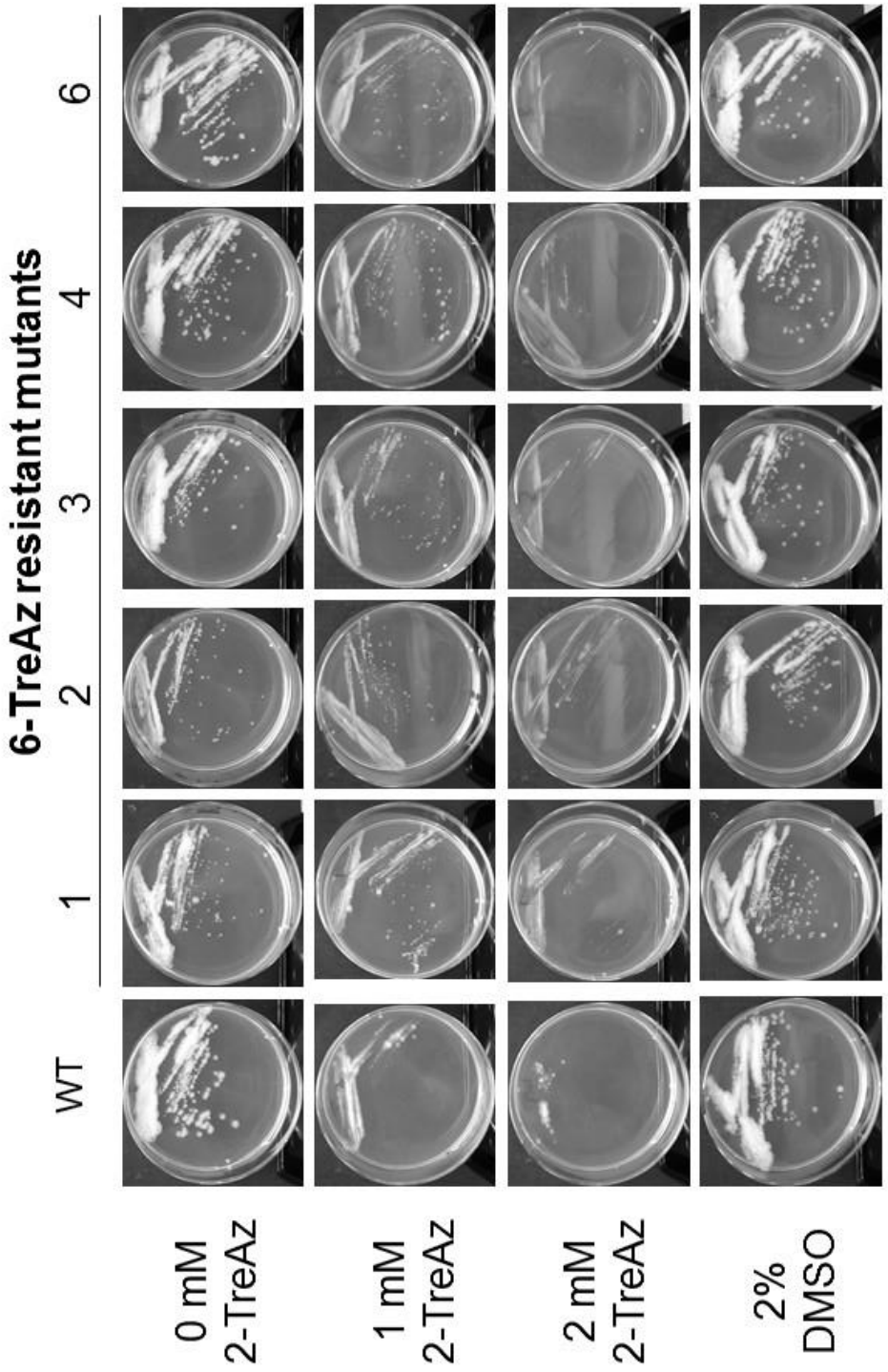

Chapter - 4

Rv3031 – a putative branching enzyme in MGLP biosynthesis

Gene essentiality of Rv3031 – a putative 1,6 branching enzyme involved in the biosynthesis of MGLPs in *Mycobacterium tuberculosis*.

1. Detailed Abstract
2. Manuscript prepared
3. Figures and Supplementary materials

Percentage of contribution to the data generated: 70%

1. First version of the manuscript was written together with figures and supplementary materials.
2. Generation of Rv3031 conditional mutants in *Mtb*H37Rv wildtype strain.
3. ATC dependent growth analysis of the Rv3031 conditional mutants.
4. Extraction of Mycolic acid methyl esters from the partially silenced Rv3031 mutants.
5. Proteomic profiling of the Rv3031 conditional mutants.
6. Generation of orthologous mutants in *Mycobacterium smegmatis.*
7. Generation of protein expressing plasmids for Rv3031 and expression test.

Detailed Abstract *(adapted from the manuscript)*

Mycobacterium tuberculosis (Mtb), in addition to capsular polysaccharides*,* also produces intracellular polysaccharides, such as polymethylated polysaccharides. These polysaccharides are known to be present in closely related mycobacterial species and other bacteria such as *Streptomyces griseus, Nocardia farcinica and Nocardia brasiliensis*. Two classes of polymethylated polysaccharides have been identified so far in mycobacterial species: Methyl mannose polysaccharides (MMP) and methyl glucose lipopolysaccharides (MGLP). They have been known to regulate the in vitro enzymatic activity of FAS-I and are also believed to play a vital role in the biosynthesis and maturation of mycolic acids in *Mtb*. MMP are composed of a α-(1-4) branched chain containing ten to fourteen 3-O-methylmannoses and are found to exist in only fast growing organisms such as *Mycobacterium smegmatis and Streptomyces griseus*. The slow growing mycobacteria such as *Mtb, Mycobacterium bovis and Mycobacterium xenopi* contain only MGLP. MGLPs are known to form 1:1 ratio stable complex with fatty acyl chains and acyl-CoA, thereby regulating the *in vitro* enzymatic activity of fatty acid synthase-I. MGLPs comprise 10-20 glucose or 6-O-methylglucose units with additional 3-O-methylglucose units at the non-reducing end and diglucosylglycerate (DGG) at the reducing end. The formation of DGG from glucosylglycerate is an essential step in the synthesis of MGLPs. We hypothesize that the enzyme catalyzing DGG formation is a branching enzyme encoded by the essential Rv3031 gene. We generated Rv3031 knock-in mutants in *M. tuberculosis* by inserting a tetracycline-regulatable synthetic promoter cassette immediately upstream of the start codon of Rv3031 employing specialized transduction. Heterologous expression in the knock-in strains of a Tet repressor protein (TetR) or a mutated reverse Tet repressor protein (RevTetR) resulted in Tet-ON or Tet-OFF conditional mutants, respectively, in which the Rv3031 gene could be conditionally silenced either in absence (Tet-ON) or presence (Tet-OFF) of Anhydrotetracycline, respectively. Employing these conditional mutants, strict essentiality of Rv3031 was demonstrated. We performed proteomic profiling of the conditional mutants under both fully induced and partially silenced conditions to observe different expression levels of protein related to mycolic acid biosynthesis and mycomembrane proteins. Mycolic acid methyl esters were extracted to monitor the mycolic acid content at different gene expression levels of Rv3031. Taken together, the results would provide insights into understanding the role of the putative branching enzyme Rv3031 in MGLP biosynthesis in *M. tuberculosis*.

Mycobacterium tuberculosis requires a putative branching enzyme Rv3031 for its viability

Mohammed Rizwan Babu Sait[1], Rainer Kalscheuer[1*]

[1] Institute of Pharmaceutical Biology and Biotechnology, Heinrich Heine University Düsseldorf, 40225 Düsseldorf, Germany.

*Correspondence:
Prof. Dr. Rainer Kalscheuer
Rainer.Kalscheuer@hhu.de

Abstract

Mycobacterium tuberculosis produces cytoplasmic complex oligomeric glycoconjugates such as 6-O-methylglucose lipopolysaccharides (MGLPs). MGLPs are known to form 1:1 ratio stable complex with fatty acyl chains and acyl-CoA, thereby regulating the *in vitro* enzymatic activity of fatty acid synthase-I. MGLPs comprise 10-20 glucose or 6-O-methylglucose units with additional 3-O-methylglucose units at the non-reducing end and diglucosylglycerate (DGG) at the reducing end. The formation of DGG from glucosylglycerate is an essential step in the synthesis of MGLPs. We hypothesize that the enzyme catalyzing DGG formation is a branching enzyme encoded by the essential Rv3031 gene. We generated Rv3031 knock-in mutants in *M. tuberculosis* by inserting a tetracycline-regulatable synthetic promoter cassette immediately upstream of the start codon of Rv3031 employing specialized transduction. Heterologous expression in the knock-in strains of a Tet repressor protein (TetR) or a mutated reverse Tet repressor protein (RevTetR) resulted in Tet-ON or Tet-OFF conditional mutants, respectively, in which the Rv3031 gene could be conditionally silenced either in absence (Tet-ON) or presence (Tet-OFF) of Anhydrotetracycline, respectively. Employing these conditional mutants, strict essentiality of Rv3031 was demonstrated. We performed proteomic profiling of the conditional mutants under both fully induced and partially silenced conditions to observe different expression levels of protein related to mycolic acid biosynthesis and mycomembrane proteins. Mycolic acid methyl esters were extracted to monitor the mycolic acid content at different gene expression levels of Rv3031. Taken together, the results would provide insights into understanding the role of the putative branching enzyme Rv3031 in MGLP biosynthesis in *M. tuberculosis*.

Introduction

Mycobacterium tuberculosis (*Mtb*) is a life threatening human pathogen, which is responsible for tuberculosis (TB) disease in about 10 million people annually [1]. It is the primary cause of death from a single infectious organism and also belong to worlds' top 10 causes of death. TB can exist in two forms: latent state and active state. Among two billion people who have latent TB infection, only 5-10% develop the active TB disease [2]. *Mtb* is a rod-shaped bacillus measuring 0.1 μm - 0.5 μm wide by 2 μm - 5 μm long without flagellum. The bacteria are aerobic, non-motile, non–spore-forming and slow growing so that it takes 18-24 hours for each division [3]. The cell wall comprises an inner cytoplasmic membrane, the periplasmic space, the peptidoglycan layer, the arabinogalactan, which linked to mycolic acids (mAGP complex), an outer mycomembrane and a capsular layer [4][5]. The high concentrations of lipids in the cell envelope is responsible for the mycobacterial resistance to antibiotics to lysis by acidic and alkaline compounds. They also confer resistance to osmotic lysis and lethal oxidation [6]. There are few other unbound polysaccharides in the capsular layer that play role in the host-pathogen interactions. *Mtb* also synthesizes intracellular polysaccharides, such as polymethylated polysaccharides. These polymethylated polysaccharides are known to be present in closely related mycobacterial species and other bacteria such as *Streptomyces griseus*, *Nocardia farcinica* and *Nocardia brasiliensis*. They contain multiple units of glucose or mannose molecules and have ability to form a complex with long chain fatty acids in 1:1 ratio [7]. Two classes of polymethylated polysaccharides have been identified so far in mycobacterial species: methyl mannose polysaccharides (MMPs) and methyl glucose lipopolysaccharides (MGLPs). They have been known to regulate the *in vitro* enzymatic activity of fatty acid synthase I (FAS-I) and are also believed to play a vital role in the biosynthesis and maturation of mycolic acids in *M. tuberculosis* [8] . MMPs are composed of a α-(1-4) branched chain containing ten to fourteen 3-O-methylmannoses and are found to exist in only fast growing organisms such as *Mycobacterium smegmatis* and *Streptomyces griseus* [9]. Interestingly, *M. smegmatis* contains both MMPs and MGLPs. In contrast, the slow growing mycobacteria such as *Mtb, Mycobacterium bovis* and *Mycobacterium xenopi* only produce MGLPs. MGLPs have sixteen to twenty units of glucoses and 6-O-methyl glucoses linked in an α-(1-4) linear chain with α-(1-6) branched diglucosylglycerate at the reducing end. It is to the first glucose of the diglucosylglycerate that the MGLP main chain of methyl glucoses is attached. Diglucosylglycerate is the initial precursor for the synthesis of long chain MGLPs. There are two additional glucoses linked to the first and third glucoses of the main chain in a β-(1-3) branching fashion [10][11][12].

MGLP contain propionate, acetate and isobutyrate linked to the methyl glucose units close to the non-reducing end and an octanoate moiety linked to the glyceric acid at the reducing end [13]. MGLPs are proposed to act as carriers of newly synthesized fatty acid chains and protect them from interacting with lytic enzymes. MGLPs are also known to contribute to the temperature adaptability of *M. tuberculosis* and also protect them from environmental stress. Taken together, MGLPs are considered to be one of the important components of the *M. tuberculosis* . However, the biosynthesis and the function of MGLPs have not fully characterized yet. MGLPs are critical for the viability of *M. tuberculosis* as strict essentiality of some genes involved in their biosynthesis has been suggested from genome-wide transposon mutant studies. The formation of diglucosylglycerate (DGG) from glucosylglycerate (GG) is an essential step in the synthesis of MGLPs (Figure 1). In this study, we will characterize the branching enzyme Rv3031, potentially catalyzing the DGG synthesis by employing molecular genetics to reveal insights into the essential role of MGLPs for viability of *M. tuberculosis .*

Materials and methods

Bacterial strains and growth conditions

The mycobacterial strains were grown at 37˚C in Middlebrook 7H9 medium supplemented with ADS (Bovine albumin serum fraction, glucose, NaCl), 0.5% (w/v) glycerol and 0.05% Tyloxapol. For growth on solid medium, Middlebrook 7H10 agar medium supplemented with ADS and 0.5% (w/v) glycerol is used unless otherwise stated. For antibiotic markers, Hygromycin (50 mg/l), apramycin (40 mg/l) and kanamycin (40 mg/l) were used. For proteomic profiling, mycobacterial strains were grown in Middlebrook 7H9 medium supplemented with 0.5% glycerol, 0.2% glucose, 0.085% sodium chloride, and 0.05% Tyloxapol. All 7H9 medium were sterilized by filtration through 0.22-µm membrane. *E. coli* strains were grown in LB broth containing 5 g tryptone, 2.5 g yeast extract and 5 g sodium chloride in 500ml water followed by autoclaving the medium at 121˚C. Middlebrook top agar was prepared by autoclaving the medium containing 0.47 g Middlebrook 7H9 powder and 0.75 g noble agar in 100 ml distilled water. Mycobacteriophage buffer contains 50 mM Tris-Cl, 150 mM NaCl, 10 mM $MgCl_2$, and 2 mM $CaCl_2$. Mycobacteriophage wash medium contains 5% glycerol and 10% albumin dextrose saline. A list of primers and strains used in this study are provided in supplementary table 1 and 2, respectively.

Generation of knock-in mutants in *M. tuberculosis*

The allelic exchange substrate plasmid are generated as described in [14] and [15]. The schematic representation of step by step procedure of generating the Knockin mutants are represented in supplementary figure 1. The upstream and downstream flanking regions of the Rv3031 starting codons were amplified by Polymerase Chain Reaction for 30 cycles consisting of Premix J or H (Lucigen) 25 µl, DNA (250 ng) 5 µl, Forward Primer (1 µM) 0.5 µl, Reverse Primer (1 µM) 0.5 µl, Water 18.5 µl, Phusion polymerase enzyme 0.5 µl with a total volume of 50 µl. PCR conditions: Initial denaturation at 98 ºC for 5 minutes, Denaturation at 98 ºC for 30 seconds, Annealing at 60 ºC for 30-60 seconds, Extension at 72 ºC for 15-30 seconds per kb and Final Extension at 72 ºC for 10 minutes. The PCR samples were purified using NucleoSpin® PCR Clean-up Column (MACHEREY-NAGEL). The flanking regions were digested separately with appropriate enzymes and ligated with Van91 cut vector fragments containing a *tet* operators (*4xtetO*) - Hygromycin/SacB fragment and a OriE - cos fragment using T4 DNA Ligase. The ligated plasmid was then transformed by heat shock to NEB 5-alpha Competent *E. coli* cells and plated on LB + Hygromycin (150 mg/L). The colonies were grown individually and plasmid DNA were purified using NucleoSpin® Plasmid Column. After verifying the AES plasmids, the plasmid

DNA was cloned into the shuttle vector phAE159 and packed into *E. coli* HB101 cells (grown in LB medium supplemented with 10 mM MgSO4, and 0.2% maltose) using MaxPlax packaging extract (Lucigen). The cells were then plated on LB plates containing Hygromycin (150 mg/L) and incubated overnight at 37ºC. The colonies are cultivated and the Phasmid DNA were purified using NucleoSpin® Plasmid Column. The phasmid DNA was then electroporated into *M. smegmatis* mc^2155 using GenePulser electroporator with conditions of 2500V, resistance 1000 Ω, and capacitance 25 µFD. After the electroporation, transformed cell mixture was transferred to microcentrifuge tube containing 1 ml 7H9 medium and incubated for 1-2 hours at 37°C. The transformed mc^2155 cells were mixed with actively growing mc^2155 cells in different dilutions and 400 µl of these dilutions were mixed separately with 7 ml top agar and plated onto pre-warmed 7H10 plates. The plates were incubated at 30ºC for 3 days. The plaques were cut into 200 µl MP buffer and incubated at 37°C for 4 hours then stored at 4ºC. Then, they are mixed with mc^2155 cells, resuspended in MP buffer, in different dilutions and mixed separately with 7 ml top agar and plated onto pre-warmed 7H10 plates. The plates were incubated at 30ºC for 3-4 days. The plates with the maximum number of phages were flooded with 5 ml MP buffer and incubated overnight at 4º C and the phage lysates were harvested. Later, these lysates were purified twice using 0.2 µm filters. Before phage transduction, a *Mtb* H37Rv culture (10 ml) was cultivated to an OD 0.8 to 1.0 at 600nm. The culture was centrifuged for 10 minutes at 4000 rpm at 4˚C. The supernatant was discarded and the pellet was resuspended with 10 ml Mycobacteriophage wash medium. This is followed by centrifugation for 10 minutes at 4000 rpm and the supernatant is discarded. The washing step was repeated again. The final pellet was resuspended in 1 ml MP buffer. 1 ml of phages which was previously warmed at 37˚C, was then mixed with 1 ml *M. tuberculosis* cells in MP buffer and incubated overnight at 37˚C. Next day, the cells were centrifuged for 15 minutes at 4000 rpm at 4˚C and the pellet was resuspended in 200 µl 7H9 medium which was then plated on Hygromycin selection plates (50 mg/L) and incubated for 3 to 4 weeks at 37˚C.

Generation of conditional mutants from knock-in mutants in *M. tuberculosis*

In order to generate conditional mutants, an episomal plasmid expressing Tet-repressor gene (Tet-ON condition) and another episomal plasmid expressing reverse Tet-repressor gene (Tet-OFF condition) were electroporated individually to the previously obtained Rv3031 Knockin cultures. After electroporation, the cells were divided to two microcentrifuge tube each containing 1 mL of 7H9 medium with Hygromycin (50 mg/L), Kanamycin (40 mg/L) and 1 mL of 7H9 medium with Anhydrotetracycline(ATC) (1 ug/mL), Hygromycin (50 mg/L), Kanamycin (40 mg/L) respectively. Next day, the cells were centrifuged and the supernatant was discarded. The pellet

was resuspended in the same growth medium as in the previous step and plated on to pre-warmed 7H10 plates containing the previously mentioned growth supplements. The plates were incubated for 4 weeks at 37˚C.

Resazurin microplate assay (REMA) for growth quantification

Anhydrotetracycline dependent growth of the conditional mutants were measured using a phenoxazine dye, Resazurin. The Tet-ON and Tet-OFF conditional mutants were grown in the 7H9 medium containing different concentrations of Anhydrotetracycline (ATC), from 0 µg/mL to 1 ug/mL, in a total volume of 100 µl and incubated at 37˚C for 7 days. On the eighth day, Resazurin solution (Sigma-Aldrich) of 10 µL was added to each well and incubated overnight at 37˚C. During the incubation, the resazurin reduces to resorufin (blue to pink) by aerobic respiration of the viable cells. The cells were then inactivated next day by treating with 10% formalin for 30 minutes at room temperature. The fluorescence (excitation 560 nm, emission 590 nm) was measured using a microplate reader (TECAN). The antibiotic susceptibility test for various mycobacterial strains were also determined using Resazurin assay.

Proteome analysis of mycobacterial strains

M. tuberculosis strains were grown in 20 ml Middlebrook 7H9 medium supplemented with 0.085% NaCl, 0.2% Glucose, 0.5% Glycerol and 0.05% Tyloxapol at 37˚C. Cells were centrifuged at 4000 rpm, 4˚C for 10 minutes. Cells were washed with 1X PBS thrice and the final pellet was resuspended in 1/10 volume of the culture. The cells were then lysed by bead-beating using 100 µm silica-zirconium beads three times (QIAGEN TissueLyser LT). SDS was then added to the cells to a final concentration of 1%. After mixing thoroughly, the cells were incubated at 4˚C for 30 minutes to solubilize membrane proteins followed by centrifugation at 14000 rpm at 4˚C for 10 minutes to obtain clear lysate. The supernatant was then collected as protein solution and filter sterilized through 0.2 µm cellulose acetate spin filter thrice. The protein concentration was measured by BCA assay. The filtered protein was pellet dried by nitrogen stream and stored at -80˚C.

Extraction and TLC analysis of mycolic acid methyl esters (MAMEs)

10 mL liquid culture of each mycobacterial strain to be analyzed were grown in 7H9 complete medium supplemented with ADS (Albumin fraction, glucose, NaCl), 50% (w/v) glycerol and 20% Tyloxapol in a square bottle until the OD600 reaches ~0.8. This was followed by centrifugation for 10 minutes at 4000 rpm at room temperature. The pellet was washed with 1XPBS twice and

dried with nitrogen flow. The fatty dry mass of the pellet was weighed and transferred to the Pyrex glass tube and then 7 mL of Chloroform: Methanol (2:1) mixture was added to the pellet and shaken over night at room temperature. Next day, the mixture was centrifuged for 30 minutes at room temperature at 4000 rpm. The pellet was dried using nitrogen flow and the supernatant was stored for the analysis of free lipids. The pellet weight was measured again. 2 mL of 15 % Tetra butyl ammonium hydroxide solution (TBAH) in water was added to the pellet weighing 50 mg and heated overnight at 100°C. Next day, the TBAH mixture was allowed to cool for 1-2 hours and then to the 50 mg pellet mixture following were added: 2 mL water, 1 mL Dichloromethane and 250 µL Iodomethane. This is followed by incubation for 30 minutes at room temperature on a shaking platform and then centrifuged at room temperature for 1 hour 4000 rpm. The upper water phase was discarded and the Organic phase was collected into an HPLC vial. After evaporating the organic solvent, Mycolic acids Methyl Esters were dissolved in 125 µL Dichloromethane. Different concentrations of MAMES in a volume of 20 µL were spotted onto a preheated (60°C) TLC silica 60 plate (Merckmillipore). The mixture of 95:5 petroleum spirit: diethyl ether was used as a solvent. TLC plate was then dipped into a saturated chamber. After running the samples, TLC plate was uniformly stained with 5% molybdato phosphoric acid in Ethanol and then incubated in the heating compartment at 120°C for 30 minutes.

Rv3031 protein expression

The Rosetta pLyss strains contains Rv3031 expressing plasmids (pET28 vector for N-Terminal His-Tag and pET30 vector for C-Terminal His-Tag) (Supplementary figure 2) and were inoculated into 5 mL of LB liquid medium containing kanamycin and chloramphenicol and placed in shaking incubator at 37°C until the OD at 600 nm reaches 0.5 to 0.8. Once the OD reaches 0.8, 2 ml of the culture was collected in a 2 mL microcentrifuge tube. The cells were centrifuged and the supernatant was discarded. The pelleted cells were labelled as un-induced samples and stored at -20 ºC. 3 µL of 1 M IPTG was added to the growing culture and continued to grow them overnight at a reduced temperature of 23 ºC. The OD was measured the next day and the pellet is collected for induced samples and stored at -20 ºC. For each culture, 1 tube of un-induced and 1 tube of induced cells were resuspended in 100 µL of 2x SDS-PAGE sample buffer. The samples were incubated at 99 ºC for 10 minutes and then incubated at room temperature. The samples were then centrifuged for 3 minutes at 14000 rpm and 20 µL of each sample was delivered to each well of the polyacrylamide gel and SDS PAGE is performed at 125V.

Results

Rv3031 is essential for the viability of *M. tuberculosis*

The Rv3031 gene has two potential unusual starting codons: TTG and GTG. Both these starting codons are separated by only a few bases. Therefore, we generated two Rv3031 conditional knock-in mutants by inserting a tetracycline-regulatable synthetic promoter cassette upstream of the two potential start codons of Rv3031 individually through specialized transduction. We characterized the gene essentiality of Rv3031 by conditional silencing of these mutants. The Rv3031 knock-in mutants showed an altered colony morphology when compared to wild-type indicating differential gene expression (Supplementary figure 3). Heterologous gene expression in the knock-in strains of a Tet repressor protein (TetR) resulted in Tet-ON conditional mutants that required the inducer Anhydrotetracycline (ATC) for their growth (Figure 2a). Conversely, the expression of reverse Tet repressor protein (RevTetR) in the knock-in strains resulted in Tet-OFF conditional mutants that could grow only in the absence of ATC (Figure 3a). Employing these conditional mutants, strict essentiality of Rv3031 was demonstrated. ATC dependent growth was also studied in these conditional mutants. The Tet-ON and Tet-OFF conditional mutants were grown in 7H9 medium in a 96-well plate containing a gradient dilution of different concentrations of ATC ranging from 0 µg/mL to 1 ug/mL, in a total volume of 100 µl and incubated at 37˚C for 7 days. After the resazurin reduction, the fluorescence was measured. We observed a gradual increase in the growth of Tet-ON mutants with increase in the concentration of the inducer ATC (Figure 2b - 2c). Similarly, we observed a decrease in the growth of Tet-OFF mutants with increase in the concentration of ATC (Figure 3b – 3c).

Mycolic acid methyl esters extraction from partially silenced conditional mutants

MAMEs were extracted from wild-type, knock-in mutants, as well as fully induced and partially silenced conditional mutants. There are three different types of mycolic acids present in *Mtb* H37Rv, and they are α-mycolic acids, methoxy-mycolic acids and keto-mycolic acids. α-Mycolic acids accounts to approximately 70% of the mycolic acids composition and contain about 74–80 carbon atoms. We hypothesized that the partial silencing of MGLP biosynthesis would result in the loss of mycolic acid content in *M. tuberculosis* . We extracted MAMEs from both Tet-ON and Tet-OFF conditional mutants grown in 0.25 µg/mL (partial inhibitory concentrations) of ATC, and a thin layer chromatography was run to observe the mycolic acid content in each strain. There

was no significant change in the amount of mycolic acids extracted (Figure 4). The MAMEs from wild-type and fully induced conditional mutants were treated as the positive controls and partially silenced mutants still possessed equal amounts of mycolic acid as in the wild-type strain. This denotes that the 50% inhibitory concentrations of ATC still allowed the growth of conditional mutants without affecting the overall MAME levels. However, it would be necessary to grow these mutants under 70-80% inhibitory concentrations of the inducer to see a significant effect in the mycolic acid content extracted.

Proteomic profiling of partially silenced Rv3031

We analyzed the ATC induced stress response by comparing the proteomic profiles of fully induced and partially silenced cells (70-80% inhibitory ATC concentrations) of the Tet-ON Rv3031 mutants. Three genes were found to be highly upregulated including Rv3031 in the fully induced strain when compared with the partially silenced mutant of the first starting codon. The two other gene that were highly upregulated were Rv3032A, a putative glucosyl transferase which might play a role in MGLP biosynthesis, and Rv3039c, a probable enoyl-CoA hydratase *echA17* that can contribute to lipid metabolism. There were 13 genes that were highly upregulated in the fully induced conditional mutant of the first starting codon against partially silenced mutant of the second starting codon. Some important upregulated genes include Rv3039c, Rv3825c which codes for the phthioceranic/hydroxyphthioceranic acid synthase pks2, Rv1180/Rv1181 that codes for mycolipanoate synthase, and Rv0156, which codes for proton-translocating NAD(P) (+) transhydrogenase. The Scatterplot for Rv3031 fully induced against partially silenced mutants are represented in Figure 5. The upregulated and downregulated genes from proteomic profiling are listed in table 1.

Generation of orthologous mutants in *M. smegmatis* and Rv3031 protein expressing plasmids (currently under progress)

The orthologue of Rv3031 gene in *Mycobacterium smegmatis* is Msmeg2349. This gene is 1545 bp long and considered to share the same function as Rv3031 which is to perform branching activity in the alpha glucans. It belongs to the GH57, Glycoside Hydrolase Family 57 similar to Rv3031. The essentiality of gene is not characterized yet and therefore we attempt to generate a conditional knock in mutant by placing the tetracycline regulatable operator in front of the start codon of the MSmeg2349. Also, in order to further characterize the function of Rv3031 at protein

level, we generated N-terminal and C-Terminal his tagged protein expressing plasmids (pET28 vector for N-Terminal His-Tag and pET30 vector for C-Terminal His-Tag) for both starting sites of Rv-3031 in Rosetta pLysS strain. There were about 10 frequently occurring rare codons in the Rv3031 gene and therefore expression in *E. coli* BL21 would not be optimal. Rosetta pLysS strain contains chloramphenicol-resistant plasmid that contains rare codons which is not usually expressed in *E. coli*. The IPTG was used for protein induction and from the protein expression test, we were able to observe the expression of Rv3031 in induced samples at size of 57kDa on a SDS PAGE gel (Figure 6).

Discussion

The biosynthetic pathways of many complex polysaccharides and glycolipids have been characterized in recent times due to the extensive information available about the *M. tuberculosis* genome and various metabolic regulations. MGLPs have recently drawn attention since they are known to offer many important functions for growth and cell wall metabolism of *M. tuberculosis* . This study was carried out with the goal to characterize an essential gene Rv3031, which might catalyze an important step in the initial stages of MGLP biosynthesis. MGLP clusters have been proposed in [7]. The neighboring genes, for instance, Rv3032, a putative glucosyl transferase, was characterized but later its function was known to be compensated by the other glucosyltransferase gene, Rv1212 (GlgA) and the Rv3030 was predicted as the methyl transferase gene. The other genes that are not closely located in the cluster are the Rv1208 that codes for the glucosyl-3-phosphoglycerate synthase (GpgS) and Rv2419 that codes for the glucosyl-3-phosphoglycerate phosphatase [16][11]. The gene functions of Rv3030, Rv1208, and Rv2419 were predicted based on bioinformatics and protein studies. Many orthologous genes of MGLP biosynthesis were studied in *Mycobacterium hassiacum* and *Mycobacterium smegmatis* due to the advantage of faster growth and easier genetic manipulations. Firstly, in this study, we validated the gene essentiality of Rv3031 by Tet regulation system. As described earlier, the major challenge was to predict the appropriate starting codon for the gene. We were able to regulate the gene expression with both starting codons in our conditional knock in mutants. With TetON system, the growth was completely based on the availability of ATC whereas with the TetOFF, normal growth was observed in the absence of ATC. However, we observed that the TetOFF mutants require higher concentrations of ATC in order to suppress the growth of these mutants to 70% to 80%. This might also interfere with the normal antibiotic activity of tetracycline which is used as an inducer. We then proceeded with extracting MAMEs with 50% ATC induced

expression concentrations and we observed no significant change in the mycolic acid content. In a few cases, we observed a reduced keto-mycolic acid content in the partially silenced cells when compared with the fully induced or wildtype cells, but this was only a preliminary observation and needs more evaluation. This indicates that the 50% ATC inhibitory concentrations allowed the growth of conditional mutants without affecting the MGLP biosynthesis and there by overall MAME levels. We will further reduce the gene expression to 20% - 30% and extract MAMEs to detect any significant reduction in the mycolic acids. We performed proteomic studies to identify the co-regulatory genes of Rv3031, up or downregulation of genes related to cell wall metabolism or mycolic acids. In case of the partially silenced gene with second starting codon vs. the fully induced strain, there were many upregulated and downregulated genes, which were linked to fatty acid biosynthesis, lipid or cell wall metabolism. From the gene essentiality and preliminary data of the proteomics, it is still unclear which is likely to be the correct starting codon for Rv3031. We predict the acceptor molecule to be glucosyl glycerate and there is a glucose from unknown donor substrates for the diglucosyl glycerate synthesis catalyzed by Rv3031. In order to evaluate this, we expressed this gene in the pET vectors in Rosetta strains. We would like to perform assays to identify the function and potential donor substrates of this gene and also test for the branching activity. We will also look for the accumulation of precursor molecule, glucosyl glycerate, in the silenced growth conditions of Rv3031 during in-vitro culture. Further studies on the Rv3031 gene, its regulation and function would be helpful to understand the MGLP biosynthesis and their protective role in the fatty acid metabolism and hence mycolic acid biosynthesis.

Author contributions

M.R.B.S. performed most of the experiments and wrote the manuscript. R.K designed and supervised the study.

Acknowledgments

We would like to thank Jurgen Manchot foundation for the funding.

Conflict of interest

The authors declare that the research was conducted in the absence of any commercial or financial relationships that could be construed as a potential conflict of interest.

Data Availability Statement

All data generated or analysed during this study are included in this published article and its Supplementary information files.

REFERENCES

[1] P. K. Drain *et al.*, “Incipient and subclinical tuberculosis: A clinical review of early stages and progression of infection,” *Clin. Microbiol. Rev.*, vol. 31, no. 4, pp. 1–24, 2018, doi: 10.1128/CMR.00021-18.

[2] S. Ehrt, D. Schnappinger, and K. Y. Rhee, “Metabolic principles of persistence and pathogenicity in Mycobacterium tuberculosis,” *Nat. Rev. Microbiol.*, vol. 16, no. 8, pp. 496–507, 2018, doi: 10.1038/s41579-018-0013-4.

[3] A. Koch and V. Mizrahi, “Mycobacterium tuberculosis,” *Trends Microbiol.*, vol. 26, no. 6, pp. 555–556, 2018, doi: 10.1016/j.tim.2018.02.012.

[4] C. L. Dulberger, E. J. Rubin, and C. C. Boutte, “The mycobacterial cell envelope — a moving target,” *Nat. Rev. Microbiol.*, vol. 18, no. January, pp. 47–59, 2020, doi: 10.1038/s41579-019-0273-7.

[5] A. T. Vincent, S. Nyongesa, I. Morneau, M. B. Reed, E. I. Tocheva, and F. J. Veyrier, “The mycobacterial cell envelope: A relict from the past or the result of recent evolution?,” *Front. Microbiol.*, vol. 9, no. OCT, pp. 1–9, 2018, doi: 10.3389/fmicb.2018.02341.

[6] L. Chiaradia *et al.*, “Dissecting the mycobacterial cell envelope and defining the

composition of the native mycomembrane," *Sci. Rep.*, vol. 7, p. 12807, 2017, doi: 10.1038/s41598-017-12718-4.

[7] V. Mendes, A. Maranha, S. Alarico, and N. Empadinhas, "Biosynthesis of mycobacterial methylglucose lipopolysaccharides," *Nat. Prod. Rep.*, vol. 29, no. 8, pp. 834–844, 2012, doi: 10.1039/c2np20014g.

[8] M. Jackson and P. J. Brennan, "Polymethylated polysaccharides from Mycobacterium species revisited," *J. Biol. Chem.*, vol. 284, no. 4, pp. 1949–1953, 2009, doi: 10.1074/jbc.R800047200.

[9] J. Ripoll-Rozada *et al.*, "Biosynthesis of mycobacterial methylmannose polysaccharides requires a unique 1-O-methyltransferase specific for 3-O-methylated mannosides," *Proc. Natl. Acad. Sci. U. S. A.*, vol. 116, no. 3, pp. 835–844, 2019, doi: 10.1073/pnas.1813450116.

[10] G. Stadthagen *et al.*, "Genetic basis for the biosynthesis of methylglucose lipopolysaccharides in Mycobacterium tuberculosis," *J. Biol. Chem.*, vol. 282, no. 37, pp. 27270–27276, 2007, doi: 10.1074/jbc.M702676200.

[11] V. Mendes, A. Maranha, S. Alarico, M. S. Da Costa, and N. Empadinhas, "Mycobacterium tuberculosis Rv2419c, the missing glucosyl-3-phosphoglycerate phosphatase for the second step in methylglucose lipopolysaccharide biosynthesis," *Sci. Rep.*, vol. 1, pp. 1–8, 2011, doi: 10.1038/srep00177.

[12] Q. Zheng *et al.*, "Mechanism of dephosphorylation of glucosyl-3-phosphoglycerate by a histidine phosphatase," *J. Biol. Chem.*, vol. 289, no. 31, pp. 21242–21251, 2014, doi: 10.1074/jbc.M114.569913.

[13] A. Maranha *et al.*, "Octanoylation of early intermediates of mycobacterial methylglucose lipopolysaccharides," *Sci. Rep.*, vol. 5, pp. 1–18, 2015, doi: 10.1038/srep13610.

[14] S. Bardarov *et al.*, "Specialized transduction: An efficient method for generating marked and unmarked targeted gene disruptions in Mycobacterium tuberculosis, M. bovis BCG and M. smegmatis," *Microbiology*, vol. 148, no. 10, pp. 3007–3017, 2002, doi: 10.1099/00221287-148-10-3007.

[15] P. Jain *et al.*, "Specialized Transduction Designed for Precise High-Throughput," *Methods Mol. Biol.*, vol. 5, no. 3, pp. e01245-14, 2014, doi: 10.1128/mBio.01245-14.Editor.

[16] N. Empadinhas, L. Albuquerque, V. Mendes, S. Macedo-Ribeiro, and M. S. Da Costa, "Identification of the mycobacterial glucosyl-3-phosphoglycerate synthase," *FEMS Microbiol. Lett.*, vol. 280, no. 2, pp. 195–202, 2008, doi: 10.1111/j.1574-6968.2007.01064.x.

Figure legends

Figure 1.

Schematic representation of MGLP Biosynthetic pathway and the predicted function of MGLP to preserve fatty acids from degradation by the lytic enzymes.

Figure 2.

Rv3031 Tet ON regulated gene expression. The figure 2a shows mycobacterial growth on the Anhydrotetracycline (ATC inducer) containing 7H10 plates indicating Tet ON induced expression of Rv3031 when compared to plates without the inducer molecules. On the right, the ATC dependent growth was observed for both starting sites of Rv3031 gene. With increase in ATC concentration, there was increase in the bacterial growth (2b - 2c). ATC-Anhydrotetracycline. Rv3031-1 denotes gene with first starting codon TTG and Rv3031-2 denotes gene with second starting codon GTG.

Figure 3.

Rv3031 Tet OFF regulated gene expression. The figure 3a shows mycobacterial growth on the 7H10 plates without ATC inducer indicating Tet OFF induced expression of Rv3031 when compared to plates with ATC. On the right, the ATC independent growth was observed for both starting sites of Rv3031 gene (3b-3c). ATC-Anhydrotetracycline. Rv3031-1 denotes gene with first starting codon TTG and Rv3031-2 denotes gene with second starting codon GTG.

Figure 4.

MAME profiling. Mycolic acid methyl esters (MAMEs) were extracted and run on TLC for observing changes in the amount of mycolic acids from partially silenced conditional mutants. No significant changes were observed with partial inhibitory concentration of 0.25 µg/mL ATC. ATC-Anhydrotetracycline. PS-Partially silenced, CM-conditional mutants. Rv3031-1 denotes gene with first starting codon TTG and Rv3031-2 denotes gene with second starting codon GTG.

Figure 5

Proteomic profiling. (a) Scatter plot of Rv3031-1 Fully induced vs. Rv3031 – 1 partially silenced (b) Scatter plot of Rv3031 – 1 Fully induced vs. Rv3031 – 2 partially silenced. In both cases, we

see Rv3031 (P9WQ27) has been upregulated in the fully induced strains against the partially silenced strains. (chosen threshold: $\log_2$ Difference ≥ 1 → at least 2-fold enrichment; p ≤ 0.05 → FDR max 5 %; Rv3031 marked with a red dot). Rv3031-1 denotes Rv3031 gene with first starting codon TTG and Rv3031-2 denotes Rv3031 gene with second starting codon GTG. The information on upregulated and downregulated genes are described in Table 1.

Figure 6

Protein expression profiles of Rv3031. Rv3031-1 denotes Rv3031 gene with first starting codon TTG and Rv3031-2 denotes Rv3031 gene with second starting codon GTG. kDa – Kilodalton.

Supplementary figure 1

Schematic representation of step by step generation of Rv3031 conditional Knockin mutants in *Mycobacterium tuberculosis* by specialized transduction.

Supplementary figure 2

Rv3031 protein expressing plasmids map. We used pET28 vector for generating N-Terminal His-Tagged Rv3031 protein and pET30 vector for generating C-Terminal His-Tagged Rv3031 protein.

Supplementary figure 3

Morphological changes observed with Rv3031 Knockin mutants when compared to *Mtb* wild type H37Rv strain. These morphological changes were also reported previously with mutants related to mycolic acids.

Table 1

Proteomic profiling

Supplementary table 1

List of Primers used in this study

Supplementary table 2

List of bacterial strains used in this study.

Table 1

Proteomic profiling

Protein	Gene Information	Metabolism involved
Upregulated genes (Rv3031-1 fully induced Vs Rv3031-1-partially silenced)		
P9WQ27	Rv3031 - Probable 1,4-alpha-glucan branching enzyme	MGLP Biosynthesis
I6X630	Rv3032A - Probable glucosyl transferase	MGLP Biosynthesis
P9WNN3	Rv3039c - Probable enoyl-CoA hydratase echA17	Lipid metabolism
Upregulated genes (Rv3031-1 fully induced Vs Rv3031-2-partially silenced)		
P9WQ27	Rv3031 - Probable 1,4-alpha-glucan branching enzyme	MGLP Biosynthesis
P9WNN3	Rv3039c - Probable enoyl-CoA hydratase echA17	Lipid metabolism
P9WQE9	Rv3825 – Phthioceranic / hydroxyphthioceranic acid synthase pks2	Biosynthesis and metabolism of fatty acids and Lipids.
P96833	Rv0156 - Proton-translocating NAD(P)(+) transhydrogenase	Membrane proton pumps
P9WK85	Rv3084 - Putative acetyl-hydrolase LipR	Mycolic acid composition and membrane permeability.
P9WQB7	Rv2428 - Alkyl hydroperoxide reductase C	Bacterial Virulence and detoxification
O06342	Rv3479 - Uncharacterized membrane protein	Cell wall metabolism
O50435	Rv1179 - Helicase ATP-binding domain-containing protein	Triacylglycerol synthesis
O50440	Rv1184 - Diacyltrehalose acyltransferase Chp2	Polyacyltrehalose (PAT) biosynthesis
P9WIK5	Rv1182 - Acyltransferase PapA3	Polyacyltrehalose (PAT) biosynthesis
P9WQB5	Rv2429 - Alkyl hydroperoxide reductase AhpD	Bacterial protection
P9WIK9	Rv3824 - 2'-acyl-2-O-sulfo-trehalose (hydroxy)phthioceranyltransferase PapA1	Sulfolipid-1 (SL-1) – biosynthesis

A0A089QRB9	Rv1180/Rv1181 - Mycolipanoate synthase	Fatty acid biosynthesis, Lipid metabolism.
Downregulated genes (Rv3031-1 fully induced Vs Rv3031-2-partially silenced)		
O06582	Rv1130 - 2-methylcitrate dehydratase	Tricarboxylic acid cycle and propanoate degradation
I6Y9Q3	Rv1131 - 2-methylcitrate synthase	Tricarboxylic acid cycle
P9WJ97	Rv0341 - Isoniazid-induced protein IniB	Cell wall metabolism
O53673	Rv0251 - Heat shock protein Hsp	Bacterial adaptation and virulence
O07423	Rv0179 - Probable lipoprotein LprO	Cell wall metabolism
L0T7Y7	Rv1807 - PPE family protein PPE31	Nutrient intake
P9WN55	Rv1826 - Glycine cleavage system H protein	Mediator in respiration metabolism
P9WLS3	Rv1738 - Probable membrane protein	Probable membrane metabolism
P9WJA3	Rv2626 - Hypoxic response protein 1	Host immune response
P9WHR1	Rv2625 - Putative zinc metalloprotease Rip3	Cell wall metabolism
P9WNE7	Rv2007 - Ferredoxin	Respiration metabolism, electron transfer chain
P9WMK1	Rv2031 - Alpha-crystallin	Chaperone

Supplementary table 1 - List of Primers used in this study

No	Primer Name	Primer Sequence	Source
1	cRv3031-RR-BstAPI	5' TTTTTGCATCTTTTGC-GGCCGTCGACCATGAAGTGACTG 3'	This study
2	cRv3031-RL-BstAPI	5'TTTTTGCATAGATTGCATGAACACGTCCGCAAGCCCGGTG 3'	This study
3	cRv3031-RL2-BstAPI	5' TTTTTGCATAGATTGC-GTGCCCGGCCTGTTCACGCTTGT 3'	This study
4	cRv3031-LR-BstAPI	5' TTTTTGCATTTCTTGC-TCAAGGCCGCACCGCGATCGCGATC 3'	This study
5	cRv3031-LR2-BstAPI	5' TTTTTGCATTTCTTGC-CGGGCTTGCGGACGTGTTCAAGG 3'	This study
6	cRv3031-LL	5' TTTTTGCATAAATTGC-CGGGTTAGCCTGCCTTAACAATG 3'	This study
7	MSmeg2349-LL	5' GGTTTCACAAAGTG-ATGAGCGCAATCGTGGGCGATCC 3'	This study
8	MSmeg2349-LR	5' GGTTTCACTTCGTGTCA-CCGCACTGCTATCGCCACGAG 3'	This study
9	MSmeg2349-RL	5' CCTTTCACAGAGTG-ATGACGGACGCGAGCGCAGAAC 3'	This study
10	MSmeg2349-RR	5' GGTTTCACCTTGTG-TCATCGCGGGAGCC 3'	This study
11	N Terminal His Tag Rv3031-1 Forward	5' TATCCATATGAACACGTCCGCAAGCCC 3’	This study
12	N Terminal His Tag Rv3031-2 Forward	5' TATCCATATGCCCGGCCTGTTCACGCTTGTTC 3'	This study
13	N Terminal His Tag Rv3031 Reverse	5' TATCCTCGAGTCACTTGGGCAGCCTCC 3'	This study
14	C Terminal His Tag Rv3031-1 Forward	5' TATCCATATGAACACGTCCGCAAGCCC 3’	This study
15	C Terminal His Tag Rv3031-2 Forward	5' TATCCATATGCCCGGCCTGTTCACGCTTGTTC 3'	This study
16	C Terminal His Tag Rv3031 Reverse	5' TATCCTCGAGCTTGGGCAGCCTCCGAGCGTCCAG 3'	This study

Supplementary table 2

List of bacterial strains used in this study

No	*E. coli* and Rosetta Strains	Antibiotic Resistance	Reference	RKSC no
1	NEB 5-alpha F´Iq : Rv3031-1 4xtetO Knockin Plasmid	Hygromycin (150 µg/ml)	This study	646
2	NEB 5-alpha F´Iq : Rv3031-2 4xtetO Knockin Plasmid	Hygromycin (150 µg/ml)	This study	647
3	NEB 5-alpha F´Iq : MSmeg 2349 4xtetO Knockin Plasmid	Hygromycin (150 µg/ml)	This study	650
4	NEB 5-alpha F´Iq : Rv3031-1 4xtetO Knockin shuttle Phasmid	Hygromycin (150 µg/ml)	This study	648
5	NEB 5-alpha F´Iq : Rv3031-2 4xtetO Knockin shuttle Phasmid	Hygromycin (150 µg/ml)	This study	649
6	NEB 5-alpha F´Iq : MSmeg 2349 4xtetO Knockin shuttle Phasmid	Hygromycin (150 µg/ml)	This study	651
7	*Rosetta*(DE3)pLysS - pET28a::Rv3031-1-6xHis (N-Terminal)	Kanamycin (40 µg/ml) Chloramphenicol(40 µg/ml)	This study	652
8	*Rosetta*(DE3)pLysS - pET28a::Rv3031-2-6xHis (N-Terminal)	Kanamycin (40 µg/ml) Chloramphenicol(40 µg/ml)	This study	653
9	*Rosetta*(DE3)pLysS - pET28a::Rv0225-6xHis (N-Terminal)	Kanamycin (40 µg/ml) Chloramphenicol(40 µg/ml)	This study	654
10	*Rosetta*(DE3)pLysS – pET30a::Rv3031-1-6xHis (C-Terminal)	Kanamycin (40 µg/ml) Chloramphenicol(40 µg/ml)	This study	655
11	*Rosetta*(DE3)pLysS – pET30a::Rv0225-6xHis (C-Terminal)	Kanamycin (40 µg/ml) Chloramphenicol(40 µg/ml)	This study	656
12	NEB 5-alpha F´Iq : pMV261::tetR_RBS-Mut.D	Kanamycin (40 µg/ml)	This study	201
13	NEB 5-alpha F´Iq : pMV261::tetR_RBS-Mut.E	Kanamycin (40 µg/ml)	This study	202
14	NEB 5-alpha F´Iq : pMV261::revtetR_RBS-Mut.D	Kanamycin (40 µg/ml)	This study	414

15	NEB 5-alpha F´Iq : pMV261::revtetR_RBS-Mut.E	Kanamycin (40 µg/ml)	This study	415

No	**RKSC No.**	***Mycobacterium tuberculosis* (*Mtb*) strains**	**Antibiotic Resistance**	**Source /Reference**
1	1	*Mtb* H37Rv WT	-	Parent strain
2	405	*Mtb* Rv3031 - 1 Knockin (4xtetO)	Hygromycin (50 µg/ml)	This study
3	406	*Mtb* Rv3031 - 2 Knockin (4xtetO)	Hygromycin (50 µg/ml)	This study
4	407	*Mtb* CM TetON Rv3031- 1 D ::pMV261::tetR_RBS-Mut. D	Hygromycin (50 µg/ml) Kanamycin (40 µg/ml)	This study
5	408	*Mtb* CM TetON Rv3031- 1 E ::pMV261::tetR_RBS-Mut. E	Hygromycin (50 µg/ml) Kanamycin (40 µg/ml)	This study
6	409	*Mtb* CM TetON Rv3031- 2 D ::pMV261::tetR_RBS-Mut. D	Hygromycin (50 µg/ml) Kanamycin (40 µg/ml)	This study
8	410	*Mtb* CM TetON Rv3031- 2 E ::pMV261::tetR_RBS-Mut. E	Hygromycin (50 µg/ml) Kanamycin (40 µg/ml)	This study
9	411	*Mtb* CM TetOFF Rv3031- 1 D ::pMV261::RevtetR_RBS-Mut. D	Hygromycin (50 µg/ml) Kanamycin (40 µg/ml)	This study
10	412	*Mtb* CM TetOFF Rv3031- 1 E ::pMV261::RevtetR_RBS-Mut. E	Hygromycin (50 µg/ml) Kanamycin (40 µg/ml)	This study
11	413	*Mtb* CM TetOFF Rv3031- 2 D ::pMV261::RevtetR_RBS-Mut. D	Hygromycin (50 µg/ml) Kanamycin (40 µg/ml)	This study
12	414	*Mtb* CM TetOFF Rv3031- 2 E ::pMV261::RevtetR_RBS-Mut. E	Hygromycin (50 µg/ml) Kanamycin (40 µg/ml)	This study

Figure 1

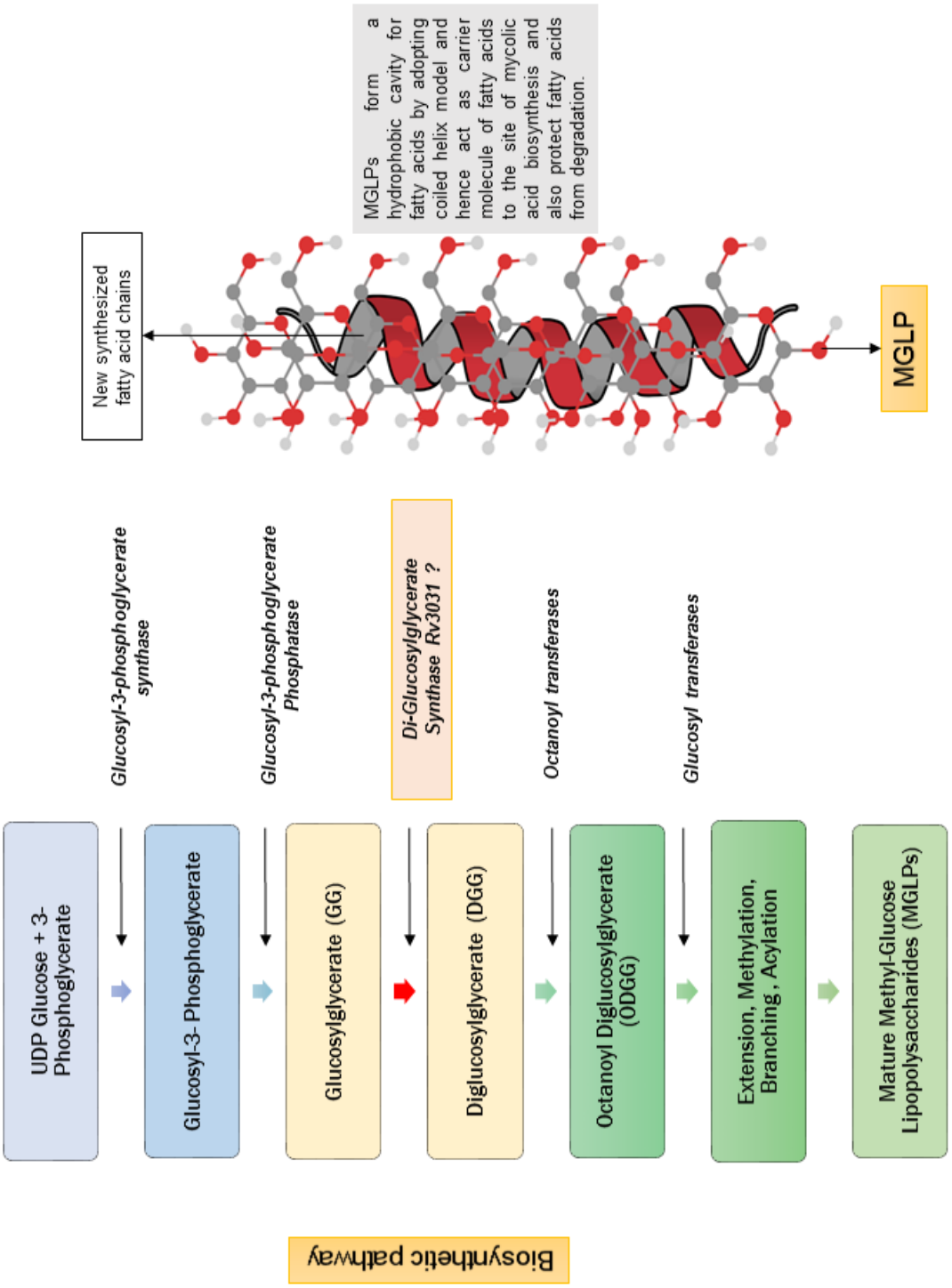
MGLPs form a hydrophobic cavity for fatty acids by adopting coiled helix model and hence act as carrier molecule of fatty acids to the site of mycolic acid biosynthesis and also protect fatty acids from degradation.
New synthesized fatty acid chains
MGLP
Glucosyl-3-phosphoglycerate synthase
Glucosyl-3-phosphoglycerate Phosphatase
Di-Glucosylglycerate Synthase Rv3031 ?
Octanoyl transferases
Glucosyl transferases
UDP Glucose + 3-Phosphoglycerate
Glucosyl-3- Phosphoglycerate
Glucosylglycerate (GG)
Diglucosylglycerate (DGG)
Octanoyl Diglucosylglycerate (ODGG)
Extension, Methylation, Branching, Acylation
Mature Methyl-Glucose Lipopolysaccharides (MGLPs)
Biosynthetic pathway

Figure 2

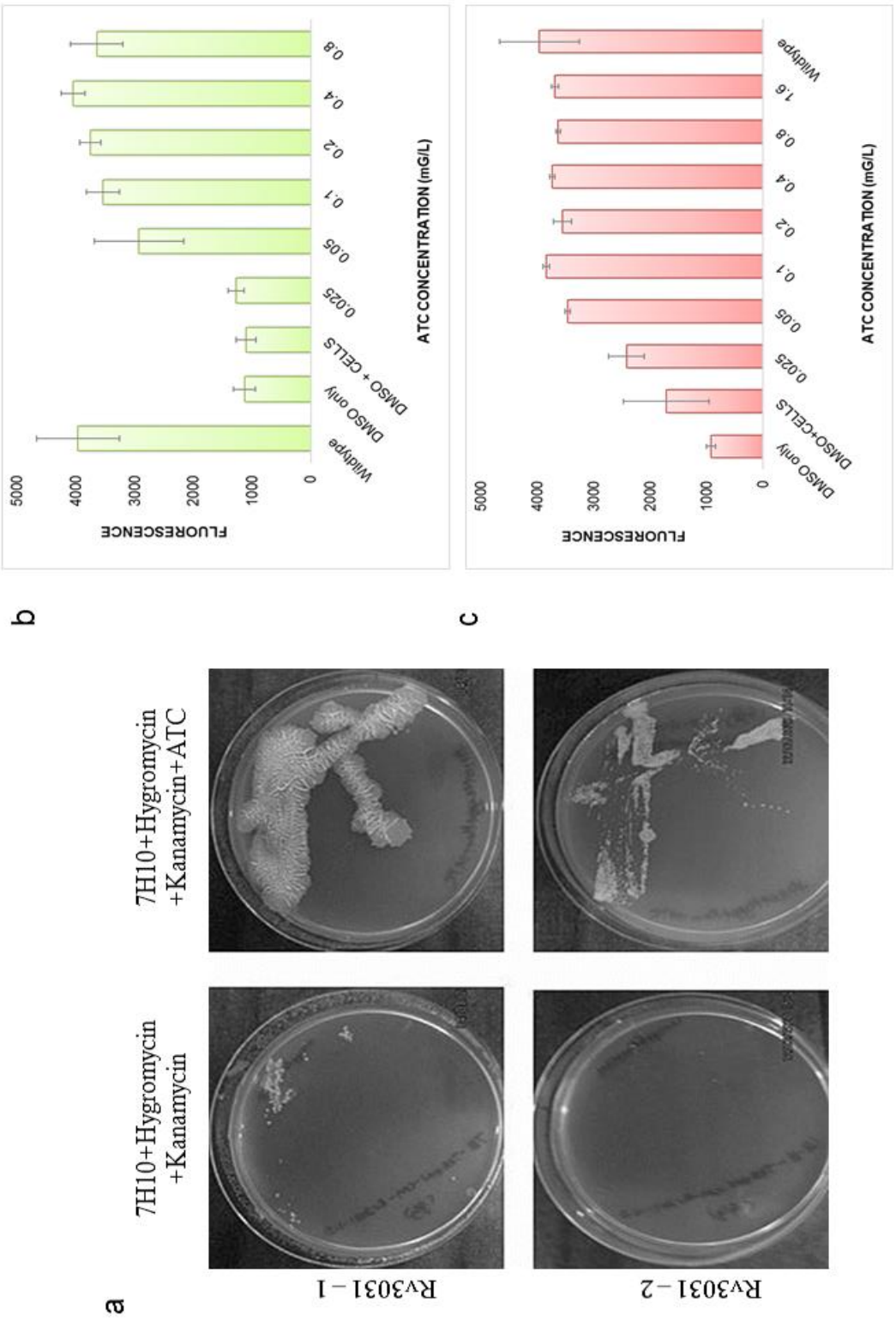
a
7H10+Hygromycin +Kanamycin
7H10+Hygromycin +Kanamycin+ATC
Rv3031 – 1
Rv3031 – 2
b
FLUORESCENCE
ATC CONCENTRATION (mG/L)
Wildtype
DMSO only
DMSO + CELLS
0,025
0,05
0,1
0,2
0,4
0,8
c
FLUORESCENCE
ATC CONCENTRATION (mG/L)
DMSO only
DMSO+CELLS
0,025
0,05
0,1
0,2
0,4
0,8
1,6
Wildtype

Figure 3

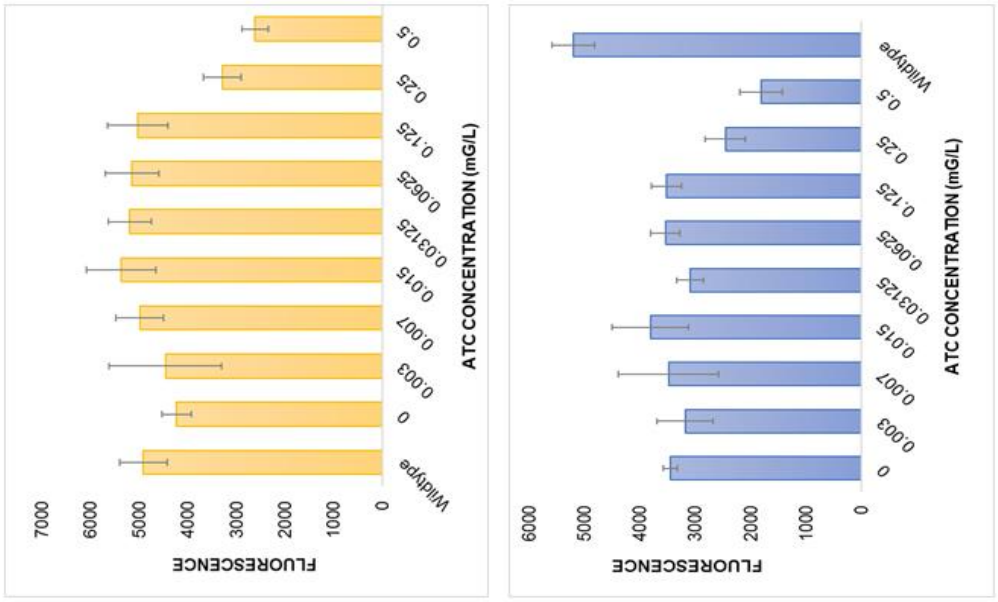
b
FLUORESCENCE
ATC CONCENTRATION (mG/L)
Wildtype
0
0.003
0.007
0.015
0.03125
0.0625
0.125
0.25
0.5
c
FLUORESCENCE
ATC CONCENTRATION (mG/L)
Wildtype
0
0.003
0.007
0.015
0.03125
0.0625
0.125
0.25
0.5

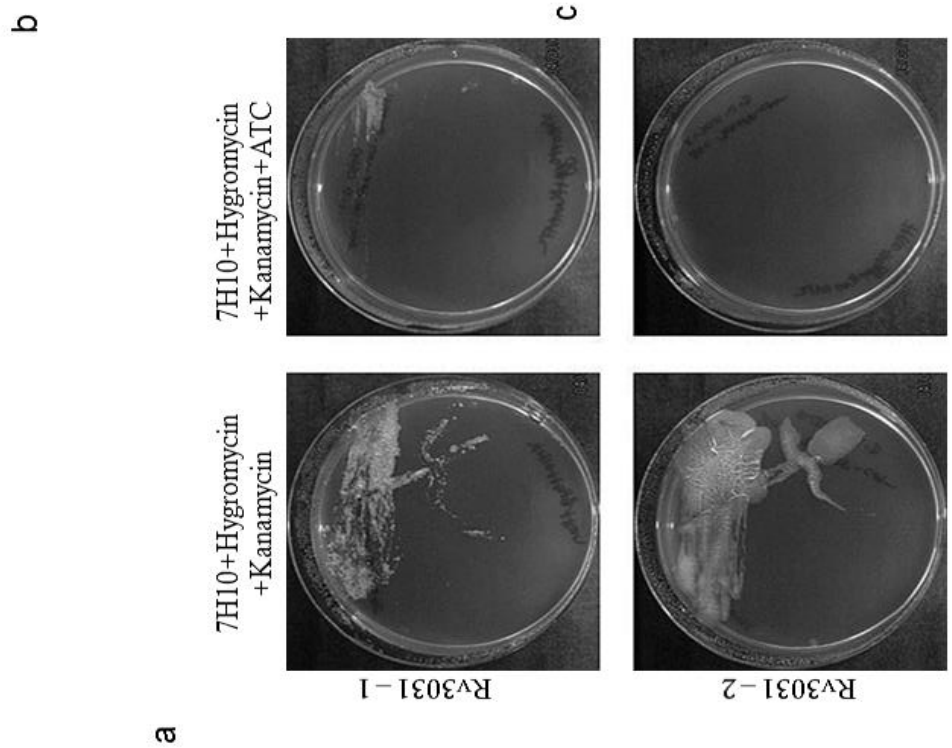
a
Rv3031 – 1
Rv3031 – 2
7H10+Hygromycin +Kanamycin
7H10+Hygromycin +Kanamycin+ATC

Figure 4

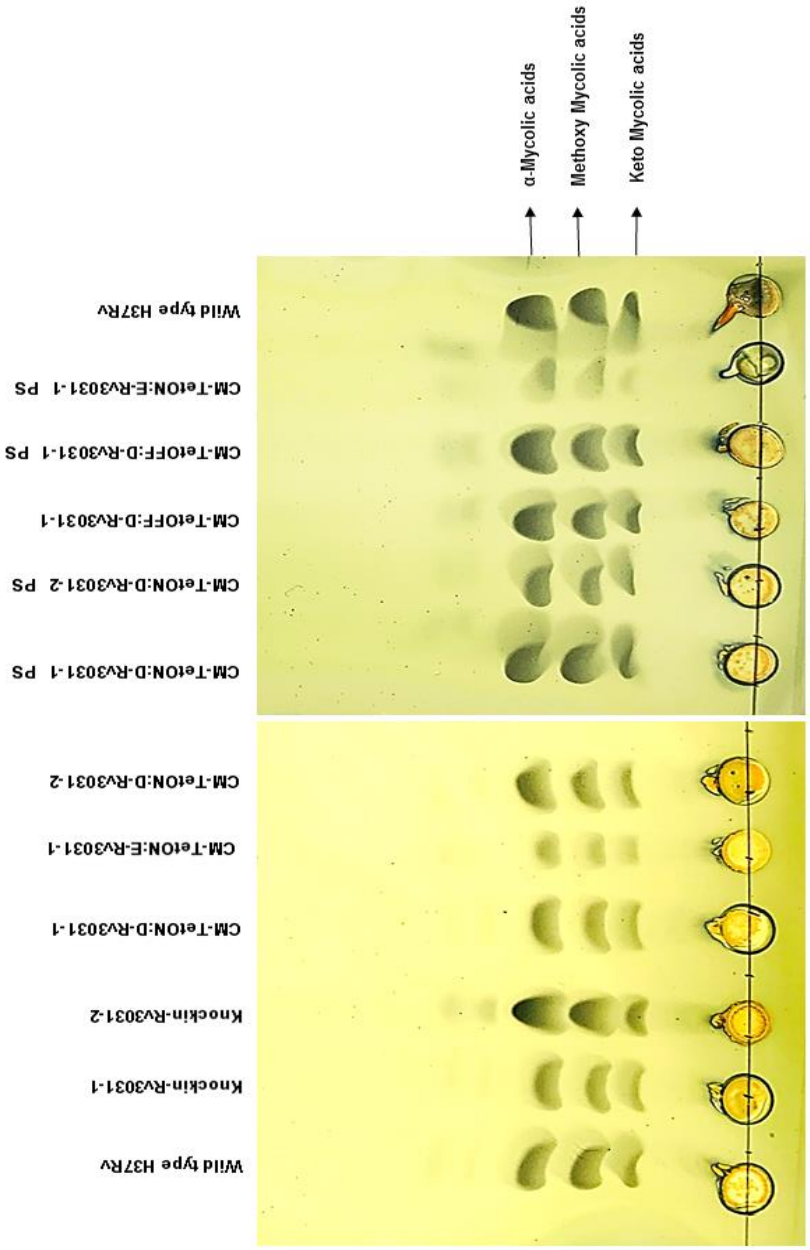
α-Mycolic acids
Methoxy Mycolic acids
Keto Mycolic acids
Wild type H37Rv
CM-TetON:E-Rv3031-1 PS
CM-TetOFF:D-Rv3031-1 PS
CM-TetOFF:D-Rv3031-1
CM-TetON:D-Rv3031-2 PS
CM-TetON:D-Rv3031-1 PS
CM-TetON:D-Rv3031-2
CM-TetON:E-Rv3031-1
CM-TetON:D-Rv3031-1
Knockin-Rv3031-2
Knockin-Rv3031-1
Wild type H37Rv

Figure 5

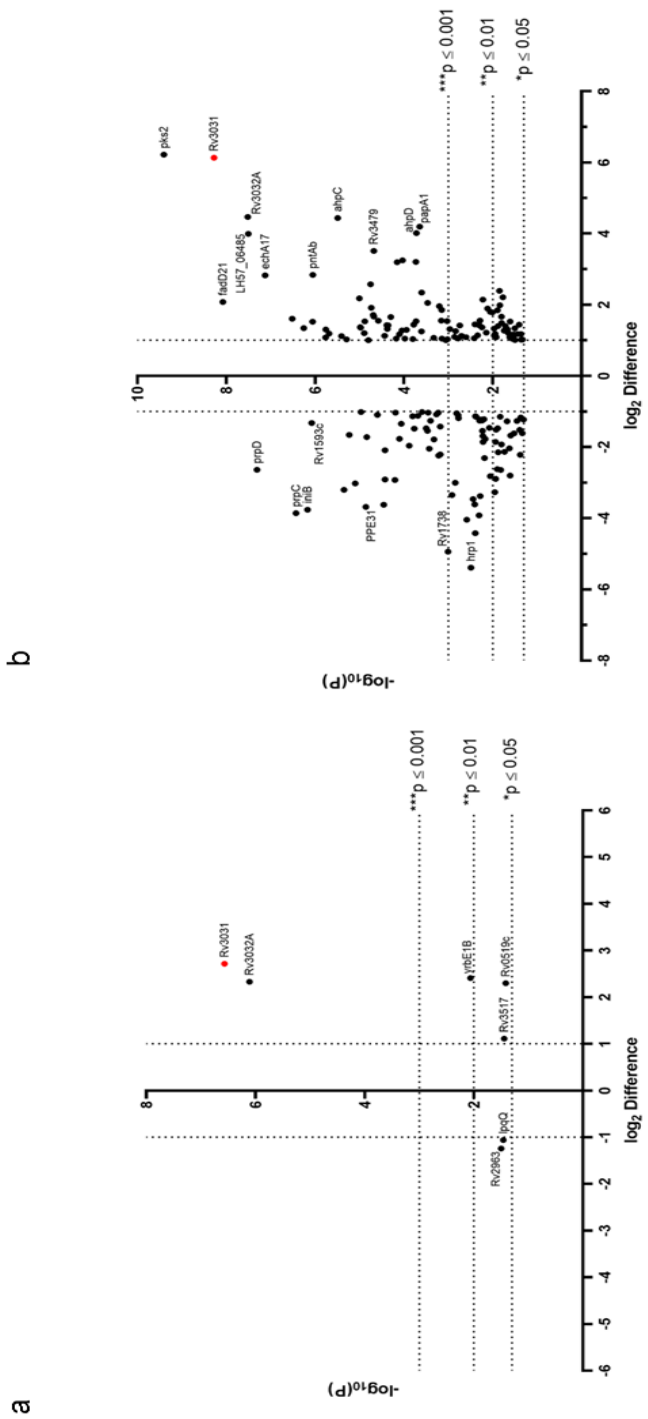
a
b
-log10(P)
log2 Difference
***p ≤ 0.001
**p ≤ 0.01
*p ≤ 0.05
Rv3031
Rv3032A
ytbE1B
Rv0518c
Rv3517
Rv2963
ppsQ
pks2
fadD21
LH57_06485
echA17
pntAb
ahpC
Rv3479
ahpD
papA1
Rv1593c
prpD
prpC
mlB
PPE31
Rv1738
hrp1

Figure 6

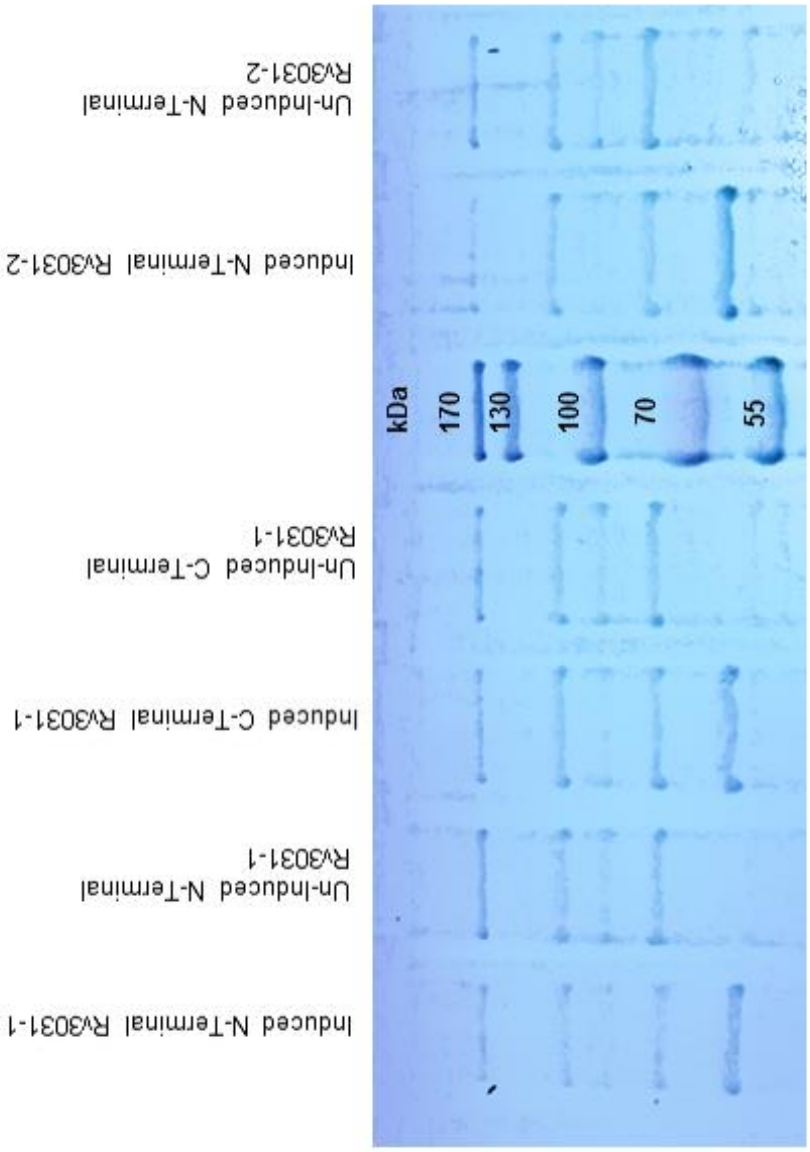
Induced N-Terminal RV3031-1
Un-Induced N-Terminal RV3031-1
Induced C-Terminal RV3031-1
Un-Induced C-Terminal RV3031-1
Induced N-Terminal RV3031-2
Un-Induced N-Terminal RV3031-2
kDa
170
130
100
70
55

Supplementary figure 1

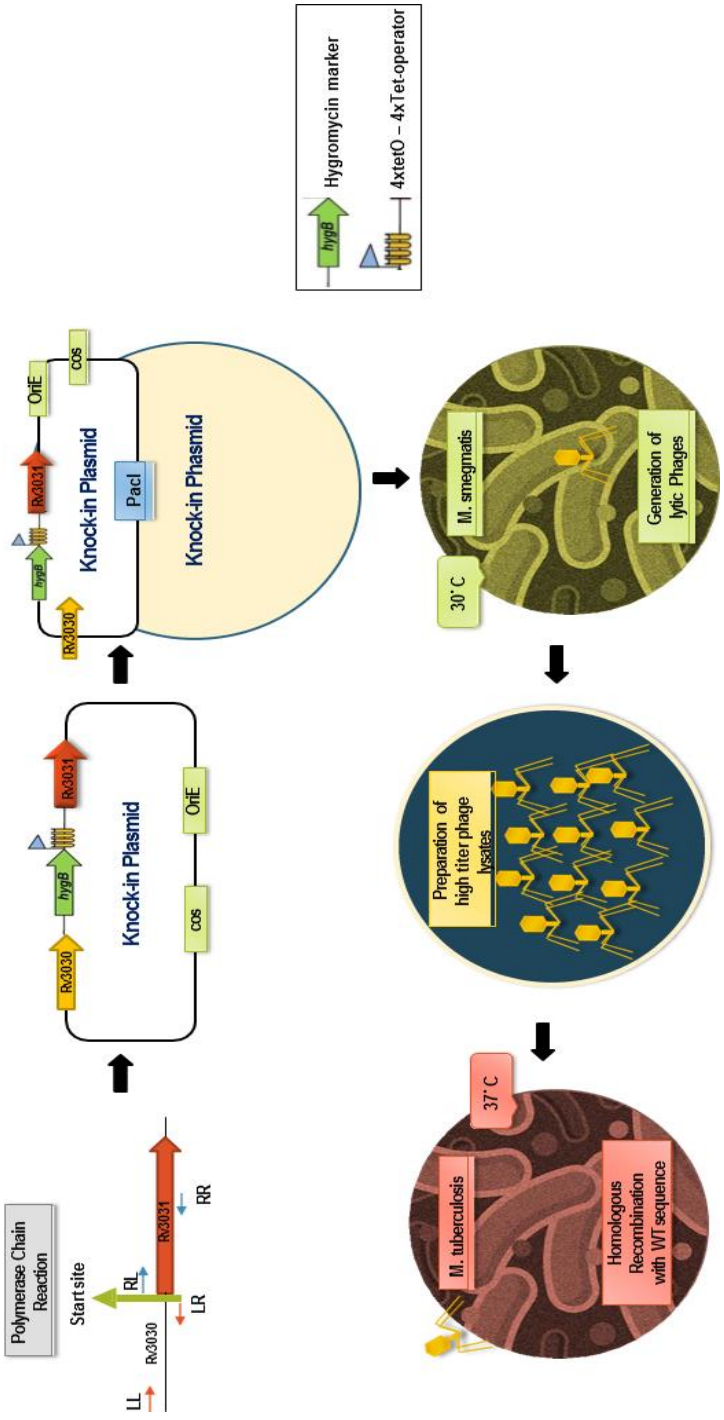

Supplementary figure 2

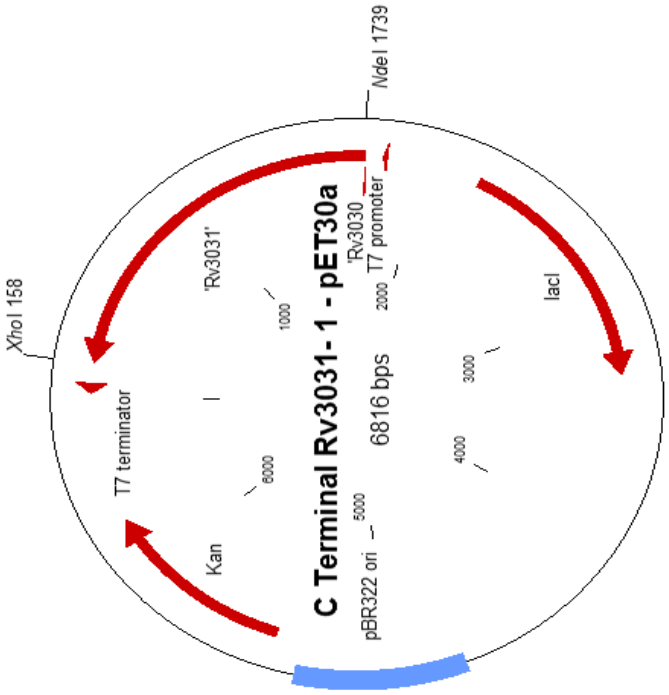

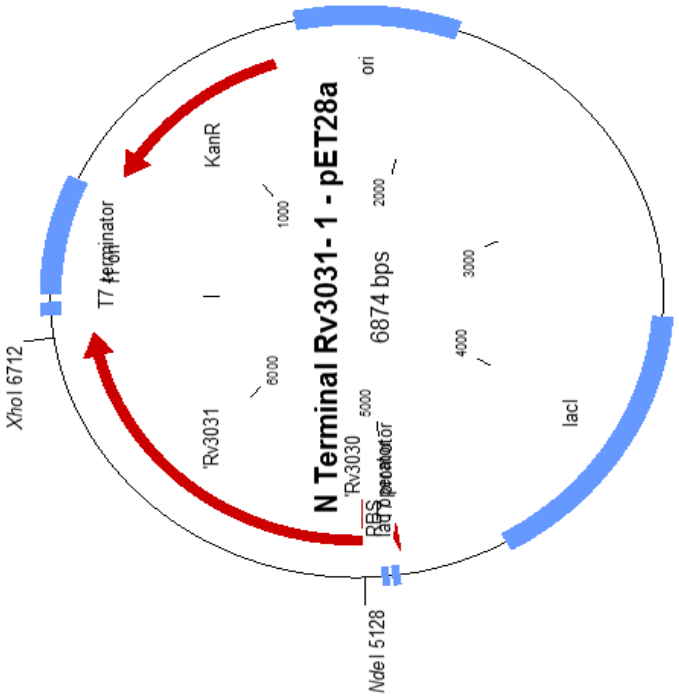

Supplementary figure 3

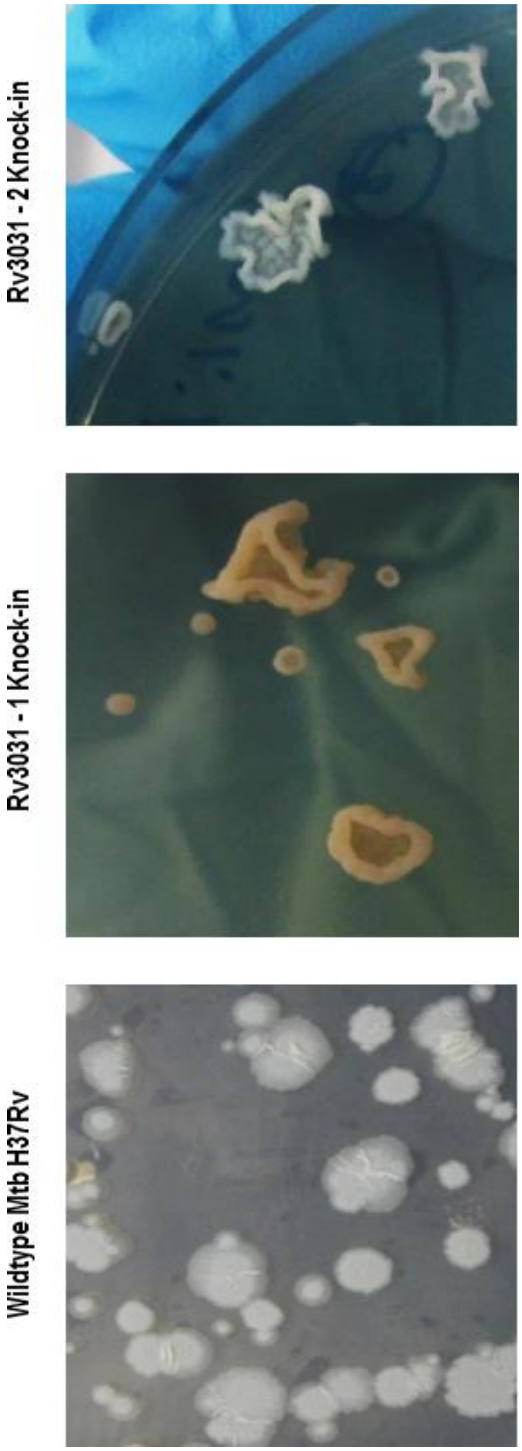

Chapter 5

TB diagnosis using DMN-Tre, a modified trehalose analog

Rapid detection of *Mycobacterium tuberculosis* in sputum with a solvatochromic trehalose probe

Authors: Mireille Kamariza[1†], Peyton Shieh[2†], Christopher S. Ealand[3], Julian S. Peters[3], Brian Chu[2], Frances P. Rodriguez-Rivera[2], Mohammed R. Babu Sait[4], William V. Treuren[5], Neil Martinson[3,6], Rainer Kalscheuer[4], Bavesh D. Kana[3,7], Carolyn R. Bertozzi[2,8*]

Published in Science Translational Medicine on 28 Feb 2018

Vol. 10, Issue 430, eaam6310

DOI : 10.1126/scitranslmed.aam6310

Impact factor : 16

Percentage of contribution to the paper: 10%

1. Generation of Knockout mutants Δ6396-6399 in *Mycobacterium smegmatis*. (6396-6399 codes for the antigen85 complex of *Mycobacterium smegmatis.*)
2. Generation of complementation mutants Δ6396-6399::Pmv306-6396-6399 in *Mycobacterium smegmatis*.
3. Morphological analysis between the knockout and complementation mutants.

Rapid detection of *Mycobacterium tuberculosis* in sputum with a solvatochromic trehalose probe

Mireille Kamariza[1†], Peyton Shieh[2†], Christopher S. Ealand[3], Julian S. Peters[3], Brian Chu[2], Frances P. Rodriguez-Rivera[2], **Mohammed R. Babu Sait[4]**, William V. Treuren[5], Neil Martinson[3,6], **Rainer Kalscheuer[4]**, Bavesh D. Kana[3,7], Carolyn R. Bertozzi[2,8*]

Aim and Detailed Abstract (adapted from the published manuscript)

Tuberculosis (TB) is the leading cause of death from an infectious bacterium. Poor diagnostic tools to detect active disease plague TB control programs and affect patient care. Accurate detection of live *Mycobacterium tuberculosis* (*Mtb*), the causative agent of TB, could improve TB diagnosis and patient treatment. Some of the non-sputum based TB diagnostic methods include Mantoux tuberculin skin test (TST) and Interferon gamma release assays (IGRA). One of the conventional approaches for rapid TB diagnosis in the regions containing high TB infections is the Ziehl-Neelsen (ZN) test that involves identification of *Mtb* in sputum or extra-pulmonary sites. This stain was commonly used for the identification of acid fast organisms. The procedure involves application of carbol fuchsin to stain the cells well followed by acid-alcohol solution for destaining. Then the counter strain such as methylene blue or malachite green are utilized. The Non-acid fast bacteria are destained and take up the counterstain whereas the acid fast organisms retain the carbol fuchsin. The other commonly used diagnosis test includes fluorescent Auramine-based Truant stain which was outlined in 1938. Both Ziehl-Neelsen and Auramine-Rhodamine stain are based on the ability of mycomembrane to retain these stains but however these tests cannot differentiate live cells from the dead cells. Hence there is urgent need for the advanced sputum based TB diagnostic methods.

There have been reports on various trehalose analogs that can be naturally incorporated into the mycobacterial cell membrane and could be useful as diagnostic tools. For instance, fluorinated trehalose analogs have been used to diagnose TB by imaging through Positron Emission Tomography (PET). These modified trehalose mycolates are integrated into the membrane by the action of Antigen 85 complex. We report that mycobacteria and other corynebacteria can be specifically detected with a fluorogenic trehalose analog. We designed a 4-*N,N*-dimethylamino-1,8-naphthalimide-trehalose (DMN-Tre) conjugate that undergoes > 700-fold increase in fluorescence intensity when transitioned from aqueous to hydrophobic environments. This

enhancement occurs upon metabolic conversion of DMN-Tre to trehalose monomycolates and incorporation into the mycomembrane of Actinobacteria. DMN-Tre labeling enabled the rapid, no-wash visualization of mycobacterial and corynebacterial species without nonspecific labeling of gram-positive or gram–negative bacteria. DMN-Tre labeling was detected within minutes and was inhibited by heat-killing of mycobacteria. Furthermore, DMN-Tre labeling was reduced by treatment with TB drugs, unlike the clinically-used Auramine stain. Lastly, DMN-Tre labelling of *Mtb* is an operationally simple method that may be deployable for TB diagnosis.

Supplementary – 2

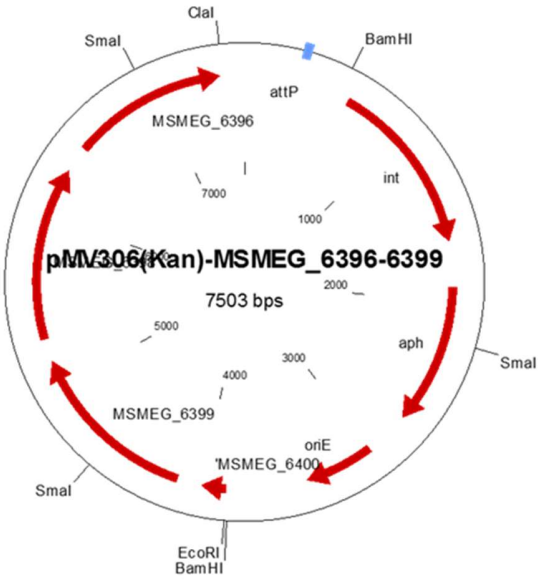

Vector molecule: pMV306
Fragment ends: ClaI and EcoRI
Fragment size: 3981
Insert molecule: MSMEG_6396-6399
Fragment ends: EcoRI and ClaI
Fragment size: 3522

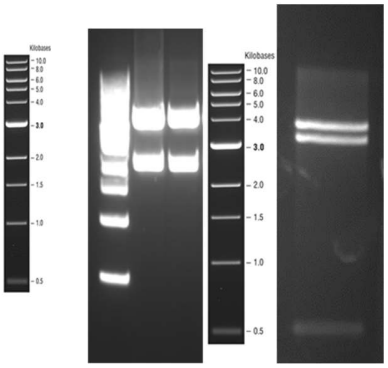

Mutant - Δ6396-6399

Complement
Δ6396-6399::pMV306-6396-6399

Chapter 6

Discussion and Conclusion

(adapted from the manuscripts)

The entire genome of the *Mtb* wild type strain H37Rv was revealed couple of decades ago but some of its important genes responsible for cell wall biosynthesis, virulence mechanism, pathogenesis and host-immune response have not been functionally characterized yet. In this study, we focused on three major areas of Tuberculosis pathogen. (1) Identification of a sugar transporter responsible for the uptake of extra cellular trehalose (2) Gene essentiality of Rv3031 which plays a vital role in MGLP biosynthesis and could be a potential drug target and (3) DMN-Tre labelling for rapid TB diagnosis.

Few genes belonging to PE/PPE family of proteins have been proposed to participate in the nutrient intake in *Mtb* and a few other were proposed to contribute to the host-immune response and replication in human macrophages. In our study, we investigated one such protein, PPE51 which is responsible for the uptake of extra cellular trehalose sugar. Earlier, this protein was also characterized for the uptake of glucose, glycerol, maltose and lactose. 6-Azido trehalose, the *Mtb* labelling analog, was used as the growth inhibitory molecule at higher concentration to identify the resistant mutants and the potential genes responsible for trehalose uptake was analyzed by whole genome sequencing. 6-Azido trehalose have also been reported earlier for growth inhibition of *Mycobacterium smegmatis* and *Mycobacterium aurum* [48][49].

From previous studies, *Mtb* Wild type had growth inhibition also against 3,3-bis-di (methyl sulfonyl) propionamide (3bMP1) [50] and thio-glycoside [51] from which the spontaneous resistant mutants were obtained and the mutation in PPE51 was found to be cause for the resistance. They reported that the PPE51 deletion mutant was unable to grow in the minimal medium supplemented with or without glucose or glycerol. However, the trehalose uptake was not reported in those studies. Also, the ability to grow on the defined carbon sources also depends upon the mutations in the PDIM biosynthesis. PDIM mutations are very common during in-vitro culturing of *Mtb* [52][53]. We observed growth inhibition of wildtype H37Rv strain against 6-Azido trehalose at a concentration of 1mM. The mutations in the spontaneous resistant strains against 6-TreAz occurred in ppe51 gene. In our study, the PPE51 deletion mutant did not utilize trehalose and glucose as the carbon sources during their growth in different minimal media. The whole genome sequencing of this deletion mutant also revealed mutation in the *mas* gene but this mutation did

not cause any functional defect as the PPE51 did block the uptake of trehalose and glucose. Wang et al., have shown that a ppe51 deletion strain was unable to utilize glycerol as a carbon source. In contrast, we observed that our Δppe51 mutant was able to utilize glycerol as the carbon source when cultivated in 7H9 medium containing 0.5% glycerol and 0.05% tyloxapol without ADS. This could result from an impaired formation of PDIM due to the observed spontaneous second-site frame shift mutation in the *mas* gene that might allow the Δppe51 deletion mutant to use glycerol for the growth in a PPE51-independent manner. However, no growth of the Δppe51 deletion mutant was observed with trehalose as the carbon source under these conditions, indicating that trehalose was unable to enter the cells in a PPE51-independent manner despite the defect in PDIM biosynthesis. Our deletion mutants were also cultivated with 6-Azido trehalose and clicked with cyclooctyne molecule, AF488DIBO, to determine uptake dependent fluorescence, where the PPE51 deleted mutant displayed lesser MFI than that of wild type strain. Considering all these findings, we suggest that PPE51 protein could be a possible transporter of extracellular trehalose in addition to other sugars such as glucose and lactose.

In addition to 6-Azido trehalose, there also have been many modified trehalose analogs in use for diagnostic labelling purposes. Tuberculosis control programs are limited due to poor diagnostic tools to detect active disease and accurate detection of live *Mtb* could improve tuberculosis diagnosis and patient treatment. Our collaborators from Stanford university were working on new sputum tests for rapid TB diagnosis. They developed a 4-N,N-dimethylamino-1,8-naphthalimide–conjugated trehalose (DMN-Tre) probe that undergoes >700-fold increase in fluorescence intensity when moving from aqueous to hydrophobic environments. DMN-Tre combines the function of DMN to produce increased fluorescence when moving from the aqueous phase to the hydrophobic phase and the function of trehalose to integrate into the mycomembrane as trehalose mycolates. Utilizing these properties, the conjugated molecule can detect the viable *Mtb* in sputum samples. The enzyme catalyzing the trehalose mycolates incorporation is the Antigen85 complex. Disruption of this gene resulted in the lower incorporation of the mycolates in the mycomembrane and therefore lower MFI with DMN-Tre. DMN-Tre labeling allows for the rapid, no-wash visualization of mycobacterial and corynebacterial species without nonspecific labeling of Gram-positive or Gram-negative bacteria. DMN-Tre labeling was detected within minutes and was inhibited by heat killing of mycobacteria. Furthermore, DMN-Tre labeling was reduced by treatment with TB drugs, unlike the clinically used Auramine stain. Lastly, DMN-Tre labelling of *Mtb* is an operationally simple method that may be deployable for tuberculosis diagnosis. However, additional evidences are needed to differentiate the latent *Mtb* cells which are non-replicating from the actively replicating cells. DMN-Tre labelling still offers a great advantage for

TB diagnosis in the low to middle income countries with higher rates of TB incidence and low testing resources.

In addition to the diagnosis and transport mechanisms in *Mtb*, we were also interested in identifying potential drug targets related to mycolic acid biosynthesis. The biosynthetic pathways of many complex polysaccharides and glycolipids have been characterized in recent times due to the extensive information available about the *Mtb* genome and various metabolic regulations. MGLPs have recently drawn attention since they are known to offer many important functions for growth and cell wall metabolism of *Mtb*. This study was carried out with the goal to characterize an essential gene Rv3031, which might catalyze an important step in the initial stages of MGLP biosynthesis. MGLP clusters have been proposed in [37]. The neighboring genes, for instance, Rv3032, a putative glucosyl transferase, was characterized but later its function was known to be compensated by the other glucosyltransferase gene, Rv1212 (GlgA) and the Rv3030 was predicted as the methyl transferase gene. The other genes that are not closely located in the cluster are the Rv1208 that codes for the glucosyl-3-phosphoglycerate synthase (GpgS) and Rv2419 that codes for the glucosyl-3-phosphoglycerate phosphatase [54][55][56]. The gene functions of Rv3030, Rv1208, and Rv2419 were predicted based on bioinformatics and protein studies. Many orthologous genes of MGLP biosynthesis were studied in *Mycobacterium hassiacum* and *Mycobacterium smegmatis* due to the advantage of faster growth and easier genetic manipulations [39].

Firstly, in this study, we validated the gene essentiality of Rv3031 by Tet regulation system. As described earlier, the major challenge was to predict the appropriate starting codon for the gene. We were able to regulate the gene expression with both starting codons in our conditional knock in mutants. With TetON system, the growth was completely based on the availability of ATC whereas with the TetOFF, normal growth was observed in the absence of ATC. However, we observed that the TetOFF mutants require higher concentrations of ATC in order to suppress the growth of these mutants to 70% to 80%. This might also interfere with the normal antibiotic activity of tetracycline which is used as an inducer. We then proceeded with extracting MAMEs with 50% ATC induced expression concentrations and we observed no significant change in the mycolic acid content. In a few cases, we observed a reduced keto-mycolic acid content in the partially silenced cells when compared with the fully induced or wildtype cells, but this was only a preliminary observation and needs more evaluation. This indicates that the 50% ATC inhibitory concentrations allowed the growth of conditional mutants without affecting the MGLP biosynthesis and there by overall MAME levels. We will further reduce the gene expression to 20% - 30% and

extract MAMEs to detect any significant reduction in the mycolic acids. We performed proteomic studies to identify the co-regulatory genes of Rv3031, up or downregulation of genes related to cell wall metabolism or mycolic acids. In case of the partially silenced gene with second starting codon vs. the fully induced strain, there were many upregulated and downregulated genes, which were linked to fatty acid biosynthesis, lipid or cell wall metabolism. From the gene essentiality and preliminary data of the proteomics, it is still unclear which is likely to be the correct starting codon for Rv3031. We predict the acceptor molecule to be glucosyl glycerate and there is a glucose from unknown donor substrates for the diglucosyl glycerate synthesis catalyzed by Rv3031. In order to evaluate this, we expressed this gene in the pET vectors in Rosetta strains. We would like to perform assays to identify the function and potential donor substrates of this gene and also test for the branching activity. We will also look for the accumulation of precursor molecule, glucosyl glycerate, in the silenced growth conditions of Rv3031 during in-vitro culture. Further studies on the Rv3031 gene, its regulation and function would be helpful to understand the MGLP biosynthesis and their protective role in the fatty acid metabolism and hence mycolic acid biosynthesis.

CHAPTER – 7 –REFERENCES

(for Chapter 1, 2, 6)

[1] N. Dookie, S. Rambaran, N. Padayatchi, S. Mahomed, and K. Naidoo, “Evolution of drug resistance in Mycobacterium tuberculosis: A review on the molecular determinants of resistance and implications for personalized care,” *J. Antimicrob. Chemother.*, vol. 73, no. 5, pp. 1138–1151, 2018, doi: 10.1093/jac/dkx506.

[2] A. Koch and V. Mizrahi, “Mycobacterium tuberculosis,” *Trends Microbiol.*, vol. 26, no. 6, pp. 555–556, 2018, doi: 10.1016/j.tim.2018.02.012.

[3] T. J. Scriba, A. K. Coussens, and H. A. Fletcher, “Human Immunology of Tuberculosis,” *Microbiol. Spectr.*, vol. 5, pp. TBTB2-0016–2016, 2017, doi: 10.1128/microbiolspec.TBTB2-0016-2016.Correspondence.

[4] P. K. Drain *et al.*, “Incipient and subclinical tuberculosis: A clinical review of early stages and progression of infection,” *Clin. Microbiol. Rev.*, vol. 31, no. 4, pp. 1–24, 2018, doi: 10.1128/CMR.00021-18.

[5] T. H. Boyles, L. Lynen, and J. A. Seddon, “Decision-making in the diagnosis of tuberculous meningitis,” *Wellcome Open Res.*, vol. 5, pp. 1–14, 2020, doi: 10.12688/wellcomeopenres.15611.1.

[6] C. Carranza, S. Pedraza-Sanchez, E. de Oyarzabal-Mendez, and M. Torres, “Diagnosis for Latent Tuberculosis Infection: New Alternatives,” *Front. Immunol.*, vol. 11, no. September, pp. 1–13, 2020, doi: 10.3389/fimmu.2020.02006.

[7] M. A. Kay AW, González Fernández L, Takwoingi Y, Eisenhut M, Detjen AK, Steingart KR, “Xpert MTB/RIF and Xpert MTB/RIF Ultra assays for active tuberculosis and rifampicin resistance in children,” *Cochrane Database Syst. Rev. 2020*, no. 8, 2020, doi: 10.1002/14651858.CD013359.pub2.www.cochranelibrary.com.

[8] R. Pi, Q. Liu, Q. Jiang, and Q. Gao, “Characterization of linezolid-resistance-associated mutations in Mycobacterium tuberculosis through WGS,” *J. Antimicrob. Chemother.*, vol. 74, no. 7, pp. 1795–1798, 2019, doi: 10.1093/jac/dkz150.

[9] M. Berney and L. Berney-Meyer, “Mycobacterium tuberculosis in the Face of Host-Imposed Nutrient Limitation ,” *Tuberc. Tuber. Bacillus*, vol. 5, no. 3, pp. 699–715, 2017, doi: 10.1128/9781555819569.ch33.

[10] C. Arnold, “Molecular evolution of Mycobacterium tuberculosis,” *Clin. Microbiol. Infect.*, vol. 13, no. 2, pp. 120–128, 2007, doi: 10.1111/j.1469-0691.2006.01637.x.

[11] I. Smith, “Mycobacterium tuberculosis pathogenesis and molecular determinants of virulence,” *Clin. Microbiol. Rev.*, vol. 16, no. 3, pp. 463–496, 2003, doi: 10.1128/CMR.16.3.463-496.2003.

[12] S. Ehrt, D. Schnappinger, and K. Y. Rhee, “Metabolic principles of persistence and pathogenicity in Mycobacterium tuberculosis,” *Nat. Rev. Microbiol.*, vol. 16, no. 8, pp. 496–507, 2018, doi: 10.1038/s41579-018-0013-4.

[13] R. Wassermann *et al.*, “Mycobacterium tuberculosis Differentially Activates cGAS- and Inflammasome-Dependent Intracellular Immune Responses through ESX-1,” *Cell Host Microbe*, vol. 17, no. 6, pp. 799–810, 2015, doi: 10.1016/j.chom.2015.05.003.

[14] A. Dorhoi *et al.*, “Type I IFN signaling triggers immunopathology in tuberculosis-susceptible mice by modulating lung phagocyte dynamics,” *Eur. J. Immunol.*, vol. 44, no. 8, pp. 2380–2393, 2014, doi: 10.1002/eji.201344219.

[15] J. E. Clark-Curtiss and S. E. Haydel, “Molecular Genetics of Mycobacterium tuberculosis Pathogenesis,” *Annu. Rev. Microbiol.*, vol. 57, pp. 517–549, 2003, doi: 10.1146/annurev.micro.57.030502.090903.

[16] D. K. Parandhaman and S. Narayanan, “Cell death paradigms in the pathogenesis of Mycobacterium tuberculosis infection,” *Front. Cell. Infect. Microbiol.*, vol. 5, no. MAR, pp. 1–7, 2014, doi: 10.3389/fcimb.2014.00031.

[17] N. Dhar, J. McKinney, and G. Manina, “Phenotypic Heterogeneity in Mycobacterium tuberculosis,” *Microbiol. Spectr.*, vol. 4, no. 6, pp. 1–27, 2016, doi: 10.1128/microbiolspec.tbtb2-0021-2016.

[18] S. Cole *et al.*, “Deciphering thebiologyof Mycobacterium tuberculosis from thecompletegenomesequence,” *Nature*, vol. 393, no. NOVEMBER, pp. 537–544, 1998.

[19] N. C. Gey Van Pittius, S. L. Sampson, H. Lee, Y. Kim, P. D. Van Helden, and R. M. Warren, *Evolution and expansion of the Mycobacterium tuberculosis PE and PPE multigene*

families and their association with the duplication of the ESAT-6 (esx) gene cluster regions, vol. 6. 2006.

[20] and W. D. Mashabela GT, de Wet TJ, "Mycobacterium tuberculosis metabolism," *Microbiol. spectru*, vol. 7, no. 4, pp. 1–26, 2019, doi: 10.1101/cshperspect.a021121.

[21] L. M. Wolfe, S. B. Mahaffey, N. A. Kruh, and K. M. Dobos, "Proteomic definition of the cell wall of mycobacterium tuberculosis," *J. Proteome Res.*, vol. 9, no. 11, pp. 5816–5826, 2010, doi: 10.1021/pr1005873.

[22] C. L. Dulberger, E. J. Rubin, and C. C. Boutte, "The mycobacterial cell envelope — a moving target," *Nat. Rev. Microbiol.*, vol. 18, no. January, pp. 47–59, 2020, doi: 10.1038/s41579-019-0273-7.

[23] M. Jankute, J. A. G. Cox, J. Harrison, and G. S. Besra, "Assembly of the Mycobacterial Cell Wall," *Annu. Rev. Microbiol.*, vol. 69, no. 1, pp. 405–423, 2015, doi: 10.1146/annurev-micro-091014-104121.

[24] A. Maitra *et al.*, "Cell wall peptidoglycan in Mycobacterium tuberculosis: An Achilles' heel for the TB-causing pathogen," *FEMS Microbiol. Rev.*, vol. 43, no. 5, pp. 548–575, 2019, doi: 10.1093/femsre/fuz016.

[25] F. Squeglia, A. Ruggiero, and R. Berisio, "Chemistry of Peptidoglycan in Mycobacterium tuberculosis Life Cycle: An off-the-wall Balance of Synthesis and Degradation," *Chem. - A Eur. J.*, vol. 24, no. 11, pp. 2533–2546, 2018, doi: 10.1002/chem.201702973.

[26] L. J. Alderwick, J. Harrison, G. S. Lloyd, and H. L. Birch, "The Mycobacterial Cell Wall—Peptidoglycan and Arabinogalactan," *Cold Spring Harb Perspect Med*, vol. 5, pp. 1–15, 2015.

[27] M. Jankute, S. Grover, H. L. Birch, and G. S. Besra, "Genetics of Mycobacterial Arabinogalactan and Lipoarabinomannan Assembly," *Microbiol. Spectr.*, vol. 2, no. 4, pp. 1–21, 2014, doi: 10.1128/microbiolspec.mgm2-0013-2013.

[28] H. Marrakchi, M. A. Lanéelle, and M. Daffé, "Mycolic acids: Structures, biosynthesis, and beyond," *Chem. Biol.*, vol. 21, no. 1, pp. 67–85, 2014, doi: 10.1016/j.chembiol.2013.11.011.

[29] J. PaweŁczyk and L. Kremer, "The Molecular Genetics of Mycolic Acid Biosynthesis," *Microbiol. Spectr.*, 2014, doi: 10.1128/microbiolspec.mgm2-0003-2013.

[30] J. M. Belardinelli *et al.*, “The MmpL3 interactome reveals a complex crosstalk between cell envelope biosynthesis and cell elongation and division in mycobacteria,” *Sci. Rep.*, vol. 9, no. 1, pp. 1–14, 2019, doi: 10.1038/s41598-019-47159-8.

[31] Y. Yamaryo-Botte *et al.*, “Acetylation of trehalose mycolates is required for efficient MmpL-mediated membrane transport in corynebacterineae,” *ACS Chem. Biol.*, vol. 10, no. 3, pp. 734–746, 2015, doi: 10.1021/cb5007689.

[32] L. Nguyen, S. Chinnapapagari, and C. J. Thompson, “FbpA-dependent biosynthesis of trehalose dimycolate is required for the intrinsic multidrug resistance, cell wall structure, and colonial morphology of Mycobacterium smegmatis,” *J. Bacteriol.*, vol. 187, no. 19, pp. 6603–6611, 2005, doi: 10.1128/JB.187.19.6603-6611.2005.

[33] M. Tropis *et al.*, “The crucial role of trehalose and structurally related oligosaccharides in the biosynthesis and transfer of mycolic acids in corynebacterineae,” *J. Biol. Chem.*, vol. 280, no. 28, pp. 26573–26585, 2005, doi: 10.1074/jbc.M502104200.

[34] K. A. L. De Smet, A. Weston, I. N. Brown, D. B. Young, and B. D. Robertson, “Three pathways for trehalose biosynthesis in mycobacteria,” *Microbiology*, 2000, doi: 10.1099/00221287-146-1-199.

[35] J. Korte *et al.*, “Trehalose-6-Phosphate-Mediated Toxicity Determines Essentiality of OtsB2 in Mycobacterium tuberculosis In Vitro and in Mice,” *PLoS Pathog.*, vol. 12, no. 12, pp. 1–22, 2016, doi: 10.1371/journal.ppat.1006043.

[36] A. Nobre, S. Alarico, A. Maranha, V. Mendes, and N. Empadinhas, “The molecular biology of mycobacterial trehalose in the quest for advanced tuberculosis therapies,” *Microbiol. (United Kingdom)*, vol. 160, no. PART 8, pp. 1547–1570, 2014, doi: 10.1099/mic.0.075895-0.

[37] V. Mendes, A. Maranha, S. Alarico, and N. Empadinhas, “Biosynthesis of mycobacterial methylglucose lipopolysaccharides,” *Nat. Prod. Rep.*, vol. 29, no. 8, pp. 834–844, 2012, doi: 10.1039/c2np20014g.

[38] J. Ripoll-Rozada *et al.*, “Biosynthesis of mycobacterial methylmannose polysaccharides requires a unique 1-O-methyltransferase specific for 3-O-methylated mannosides,” *Proc. Natl. Acad. Sci. U. S. A.*, vol. 116, no. 3, pp. 835–844, 2019, doi: 10.1073/pnas.1813450116.

[39] G. Stadthagen *et al.*, “Genetic basis for the biosynthesis of methylglucose lipopolysaccharides in Mycobacterium tuberculosis,” *J. Biol. Chem.*, vol. 282, no. 37, pp. 27270–27276, 2007, doi: 10.1074/jbc.M702676200.

[40] Q. Zheng *et al.*, “Mechanism of dephosphorylation of glucosyl-3-phosphoglycerate by a histidine phosphatase,” *J. Biol. Chem.*, vol. 289, no. 31, pp. 21242–21251, 2014, doi: 10.1074/jbc.M114.569913.

[41] D. Kaur *et al.*, “Initiation of methylglucose lipopolysaccharide biosynthesis in mycobacteria,” *PLoS One*, vol. 4, no. 5, pp. 1–7, 2009, doi: 10.1371/journal.pone.0005447.

[42] D. Nunes-Costa, A. Maranha, M. Costa, S. Alarico, and N. Empadinhas, “Glucosylglycerate metabolism, bioversatility and mycobacterial survival,” *Glycobiology*, vol. 27, no. 3, pp. 213–227, 2017, doi: 10.1093/glycob/cww132.

[43] P. De *et al.*, “Structural determinants in a glucose-containing lipopolysaccharide from Mycobacterium tuberculosis critical for inducing a subset of protective T cells,” *J. Biol. Chem.*, vol. 293, no. 25, pp. 9706–9717, 2018, doi: 10.1074/jbc.RA118.002582.

[44] A. Maranha *et al.*, “Octanoylation of early intermediates of mycobacterial methylglucose lipopolysaccharides,” *Sci. Rep.*, vol. 5, pp. 1–18, 2015, doi: 10.1038/srep13610.

[45] S. Bardarov *et al.*, “Specialized transduction: An efficient method for generating marked and unmarked targeted gene disruptions in Mycobacterium tuberculosis, M. bovis BCG and M. smegmatis,” *Microbiology*, vol. 148, no. 10, pp. 3007–3017, 2002, doi: 10.1099/00221287-148-10-3007.

[46] P. Jain *et al.*, “Specialized Transduction Designed for Precise High-Throughput,” *Methods Mol. Biol.*, vol. 5, no. 3, pp. e01245-14, 2014, doi: 10.1128/mBio.01245-14.Editor.

[47] J. C. Evans and V. Mizrahi, “The application of tetracyclineregulated gene expression systems in the validation of novel drug targets in Mycobacterium tuberculosis,” *Front. Microbiol.*, vol. 6, no. AUG, pp. 1–14, 2015, doi: 10.3389/fmicb.2015.00812.

[48] J. T. Belisle, V. D. Vissa, T. Sievert, K. Takayama, P. J. Brennan, and G. S. Besra, “Role of the major antigen of Mycobacterium tuberculosis in cell wall biogenesis,” *Science (80-.).*, vol. 276, no. 5317, pp. 1420–1422, 1997, doi: 10.1126/science.276.5317.1420.

[49] S. B. O’Neill MK, Piligian BF, Olson CD, Woodruff PJ, “Tailoring Trehalose for Biomedical and Biotechnological Applications,” *Pure Appl Chem.*, vol. 89(9), pp. 1223–1249, 2017, doi:

10.1016/j.physbeh.2017.03.040.

[50] Q. Wang *et al.*, “PE/PPE proteins mediate nutrient transport across the outer membrane of Mycobacterium tuberculosis,” *Science (80-.).*, vol. 367, no. 6482, pp. 1147–1151, 2020, doi: 10.1126/science.aax3072.

[51] M. Korycka-Machała *et al.*, “PPE51 Is Involved in the Uptake of Disaccharides by Mycobacterium tuberculosis,” *Cells*, vol. 9, no. 3, p. 603, 2020, doi: 10.3390/cells9030603.

[52] P. Domenech and M. B. Reed, “Rapid and spontaneous loss of phthiocerol dimycocerosate (PDIM) from Mycobacterium tuberculosis grown in vitro: Implications for virulence studies,” *Microbiology*, vol. 155, no. 11, pp. 3532–3543, 2009, doi: 10.1099/mic.0.029199-0.

[53] S. De Majumdar *et al.*, “Genome analysis identifies a spontaneous nonsense mutation in ppsD leading to attenuation of virulence in laboratory-manipulated Mycobacterium tuberculosis,” *BMC Genomics*, vol. 20, no. 1, pp. 1–10, 2019, doi: 10.1186/s12864-019-5482-y.

[54] G. Kumar, S. Guan, and P. A. Frantom, “Biochemical characterization of the retaining glycosyltransferase glucosyl-3-phosphoglycerate synthase from Mycobacterium tuberculosis,” *Arch. Biochem. Biophys.*, vol. 564, pp. 120–127, 2014, doi: 10.1016/j.abb.2014.10.002.

[55] N. Empadinhas, L. Albuquerque, V. Mendes, S. Macedo-Ribeiro, and M. S. Da Costa, “Identification of the mycobacterial glucosyl-3-phosphoglycerate synthase,” *FEMS Microbiol. Lett.*, vol. 280, no. 2, pp. 195–202, 2008, doi: 10.1111/j.1574-6968.2007.01064.x.

[56] V. Mendes, A. Maranha, S. Alarico, M. S. Da Costa, and N. Empadinhas, “Mycobacterium tuberculosis Rv2419c, the missing glucosyl-3-phosphoglycerate phosphatase for the second step in methylglucose lipopolysaccharide biosynthesis,” *Sci. Rep.*, vol. 1, pp. 1–8, 2011, doi: 10.1038/srep00177.

Statutory Declaration

I declare under oath that I have compiled my dissertation independently and without any undue assistance by third parties under consideration of the “Principles for the Safeguarding of Good Scientific Practice at Heinrich Heine University Düsseldorf”.

I declare that I have not used sources or means without declaration in the text. All the passages taken from other works in the wording or in the meaning have been clearly indicated with sources. This thesis has not been used in the same or similar version to achieve an academic grading or is being published elsewhere.

Düsseldorf,

Mohammed Rizwan Babu Sait